0000-0029-7705-MCAR, Rev. 0
Mixed Core Analysis Report (MCAR) for Hope Creek Reload 12 Cycle 13

GNF

Global Nuclear Fuel

A Joint Venture of GE, Toshiba, & Hitachi

0000-0029-7705-MCAR
Revision 0
April 2005

0000-0029-7705-MCAR, Rev. 0

Mixed Core Analysis Report (MCAR) for Hope Creek Reload 12 Cycle 13

Approved: M. E. Harding
M. E. Harding, Manager
Fuel Engineering Services

Approved: Rick Kingston
R. E. Kingston
Customer Account Leader

PSEG Hope Creek
Mixed Core Analysis Report

Proprietary Information Notice

This document is the GNF non-proprietary version of the GNF proprietary report. From the GNF proprietary version, the information denoted as GNF proprietary (enclosed in double brackets) was deleted to generate this version.

PSEG Hope Creek
Mixed Core Analysis Report

Important Notice Regarding Contents of This Report

Please Read Carefully

This report was prepared by Global Nuclear Fuel - Americas, LLC (GNF-A) solely for PSEG Nuclear, LLC. The information contained in this report is believed by GNF-A to be an accurate and true representation of the facts known, obtained or provided to GNF-A at the time this report was prepared.

The only undertakings of GNF-A respecting information in this document are contained in the Contract between PSEG Nuclear, LLC, Global Nuclear Fuel - Americas, LLC and General Electric Company for Fuel Fabrication and Related Components and Services for Hope Creek Generating Station, and nothing contained in this document shall be construed as changing said contract. The use of this information except as defined by said contract, or for any purpose other than that for which it is intended, is not authorized; and with respect to any such unauthorized use, neither GNF-A nor any of the contributors to this document makes any representation or warranty (expressed or implied) as to the completeness, accuracy or usefulness of the information contained in this document or that such use of such information may not infringe privately owned rights; nor do they assume any responsibility for liability or damage of any kind which may result from such use of such information.

Table of Contents

Table of Contents

List Of Tables

List Of Figures

PSEG Hope Creek
Mixed Core Analysis Report

1.0 Introduction and Summary

The implementation of a new fuel design for a General Electric (GE) Boiling Water Reactor (BWR) follows a two-step process. First, the new fuel design is submitted to and approved by the Nuclear Regulatory Commission (NRC) [[{3}]] via the GESTAR II Amendment 22 process. Then, plant-specific analyses are performed to justify use of the new fuel design in an upcoming plant reload. The [[{3}]] analyses consist of one-time [[{3}]] analyses and [[{3}]] analyses. The [[{3}]] analyses have been performed to support introduction of the GE14 fuel design at Hope Creek Generating Station (HCGS) for the Current Licensed Thermal Power of 3339 MWt. The [[{3}]] analyses are performed for each reload regardless of fuel design.

HCGS will be loading GE14 fuel for Cycle 13 operation. Currently, the plant is operating with non-GE14 fuel assemblies (SVEA 96+) in the core. [[{3}]] analyses have been performed and documented in the Fuel Transition Report for Hope Creek Generating Station.[1]

This report summarizes the results of the [[{3}]] analyses and evaluations for the HCGS Cycle 13 mixed core of GE14 and SVEA 96+ fuel. The Cycle 13 mixed core will consist of approximately 20% GE14 and 80% SVEA 96+ fuel. The cycle dependent analyses are documented in the plant and cycle unique Supplemental Reload Licensing Report (SRLR), which is included in this report as Section 7.0. The following information is provided in the SRLR:

- Plant-unique Items
- Reload Fuel Bundles
- Reference Core Loading Pattern
- Calculated Core Effective Multiplication and Control System Worth
- Standby Liquid Control System Shutdown Capability
- Reload Unique GETAB Anticipated Operational Occurrences (AOO) Analysis Initial Condition Parameters
- Selected Margin Improvement Options
- Operating Flexibility Options
- Core-wide AOO Analysis Results
- Local Rod Withdrawal Error AOO Summary
- Cycle MCPR Values
- Overpressurization Analysis Summary
- Loading Error Results
- Control Rod Drop Analysis
- Stability Analysis Results
- Loss-of-Coolant Accident Results

In addition to the SRLR, this report also presents the following information that supports the analyses:

- Lattice Physics Benchmark and Results
- Cycle 13 Base Point Determination and Previous Operating Cycle Benchmark Results
- Fuel Rod Thermal-Mechanical Performance Limits for SVEA 96+ Fuel
- Cycle 13 Mixed Core Reload Bundle Design, Core Design and Performance Summary
- Cycle 13 Safety Limit Minimum Critical Power Ratio Summary

The conclusion of the lattice physics benchmark and results evaluation is that the TGBLA06/PANC11 models are acceptable to establish the design and licensing parameters for SVEA 96+.

The benchmark of previous operating cycles with GNF methods has been utilized to determine appropriate hot and cold eigenvalues and thermal limit design margins for the Cycle 13 core design work as well as resulting in the establishment of the Cycle 13 base point.

The fuel rod thermal-mechanical performance limits for SVEA 96+ have been established. Demonstration that individual bundle and core designs meet these performance limits ensures compliance with the fuel rod thermal-mechanical design and licensing limits.

Cycle 13 mixed core reload bundle and core design has been completed. As indicated by the performance summary, all core operating and design margins have been dispositioned to be acceptable based on the Cycle 13 reload bundle and core design.

The Cycle 13 SLMCPR calculations, including a comparison to the SLMCPR calculated for Cycle 12 using GNF methods, have been completed. The calculated Cycle 13 SLMCPR values of 1.06 for dual loop operation and 1.08 for single loop operation are appropriate for the Hope Creek Cycle 13 mixed core.

The results presented in the SRLR have been determined using NRC approved methods in accordance with the basis provided in *General Electric Standard Application for Reactor Fuel*, NEDE-24011-P-A-14, June 2000 and the U. S. Supplement, NEDE-24011-P-A-14-US, June 2000. The results of the analyses and evaluations contained in the SRLR support the conclusion that HCGS can safely load and operate using GE14 fuel with SVEA 96+ fuel in HCGS Cycle 13.

1.1 References

1. *Fuel Transition Report For Hope Creek Generating Station*, NEDC-33158P, Revision 4, March 2005.

2.0 Lattice Physics Comparison

GNF methods, namely TGBLA04/PANAC10 and TGBLA06/PANAC11, have been used to design and license GNF/GE bundle designs for 8x8, 9x9 and 10x10 lattices with and without water rods. Currently they are being used to license the GE12 and GE14 designs. No changes to the GNF design system have been made to adapt to the SVEA 96+ geometry. The purpose of this analysis is to document the accuracy of TGBLA06/PANAC11 for the SVEA 96+ application in Hope Creek Generating Station Cycle 13. Extensive comparisons between TGBLA06 and the more accurate benchmark Monte Carlo code MCNP show that the accuracy of TGBLA06/PANAC11 for the SVEA 96+ designs is equivalent to the accuracy for GE12/GE14 designs. Therefore, the TGBLA06/PANAC11 models are acceptable to establish the design and licensing parameters for the SVEA 96+ fuel designs in Hope Creek Generating Station Cycle 13 and for all future Hope Creek Generating Station cycles that exhibit design characteristics consistent with the benchmark bases in which these SVEA 96+ fuel designs are utilized.

2.1 TGBLA Lattice Physics to Monte Carlo Comparison

2.1.1 Water-Cross Models

[[

{3}]]

2.1.2 Qualification Method

In this study, the benchmark model is the MCNP Monte Carlo neutron transport program. The MCNP program is a Monte Carlo neutron transport code developed at Los Alamos National Laboratory. The cross sections used in MCNP are derived from the ENDF/B-V data and are represented on a continuous energy mesh. A full scattering model developed for water and other scattering material is employed in the thermal energy region. The MCNP program is widely used as a nuclear benchmark tool throughout the world. GNF/GE was instrumental in formulating the original qualification results for BWR applications. GNF/GE has qualified MCNP against critical data. For BWR applications, the most important critical data are the TRX and B&W critical experiments [1] because they consist of UO_2 fuel in water moderated fuel pins. Table 2.1 contains a summary of the critical eigenvalues obtained by MCNP for these experiments. Note that the calculated criticality for these experiments is quite uniform regardless of the fuel type, uranium metal or uranium oxide. Hence, the MCNP program can be used to determine the accuracy of the design tool TGBLA for BWR fuel applications.

Table 2.1 - Summary of MCNP Simulation of TRX and B&W Critical Experiments

Experiment	Description	Eigenvalue
TRX-1	Uranium metal in Al clad 1.3% enriched Triangular pitch lattice Pitch = 1.086 cm	1.0008 ± .0013
TRX-2	Uranium metal in Al clad 1.3% enriched Triangular pitch lattice Pitch = 2.174 cm	0.9997 ± .0013
B&W	UO_2 in Al clad Square pitch lattice 2.5% enriched Pitch =1.626 cm	0.9995± .0014

The MCNP results can be used to compare both criticality and pin power distributions. In the past, the Monte Carlo comparisons have been restricted to beginning of life configurations. In this study, the comparisons have been extended to lattices at various stages of burn-up. The TGBLA06 code is used to establish the isotopic inventory at a number of exposure points. This isotopic inventory includes the depleted values of uranium and gadolinium, as well as the amounts of plutonium and fission products generated during the burn-up process. The isotopic inventory is then input to the MCNP code and the eigenvalue and power distribution determined. These TGBLA06/MCNP comparisons have been carried out for the SVEA 96+ designs for three void values, 0%, 40% and 70%. Similar comparisons have been made for a conventional UO_2 design to determine the difference in model accuracy between GE14 fuel and SVEA 96+ fuel.

2.1.3 TGBLA06/MCNP Comparison Results

To perform a review of the ability of TGBLA06 to model a new fuel design, three figures of merit, the infinite lattice k_∞, the pin fission density, and a lattice dynamic void coefficient, have been chosen. These figures of merit provide screening functions such that the lattice average reactivity characteristics and the individual pin power generation can be assessed, and the lattice transient response to moderator density changes (voids) can be reviewed. Through a use of these global figures of merit, comparisons of the TGBLA06 analysis and MCNP analysis can be used to gain confidence in the TGBLA06 lattice physics solution.

These figures of merit and associated criteria have been applied to all fuel designs within the application range of TGBLA06. The current application range includes several geometric configurations of 8x8, 9x9 and 10x10 fuel designs.

For screening purposes, the agreement for the infinite lattice k_∞ between TGBLA06 and MCNP for uncontrolled conditions is expected to be within +/- 1% Δk. For hot controlled and cold conditions, the expected agreement is to be within +/- 1.5% Δk. The RMS (root mean square) of

the pin fission density differences of all powered pins in the hot uncontrolled condition is expected to be less than 3%. The RMS of the fission density differences for the hot controlled and cold conditions are reviewed for reasonable agreement but may exceed 3% in some lattice designs. The expected agreement of the Dynamic Void Coefficient difference between TGBLA06 and MCNP is a +2% bias and a standard deviation of 8.0%.

Comparisons between the design model TGBLA06 and the Monte Carlo model MCNP have been carried out at beginning of life configurations and at exposed configurations. A summary of the TGBLA06/MCNP k_∞ comparisons can be found in Tables 2.2 and 2.3. In these tables, the k_∞ values are compared for three void points, 0%, 40% and 70% voids. The percent difference in these tables is defined as 100*(MCNP-TGBLA)/MCNP.

Tables 2.2 and 2.3 also give comparisons for a dynamic void coefficient. Given the k_∞ differences, an estimate can be made of the accuracy of the lattice void coefficient generated by TGBLA06. The lattice dynamic void coefficient is defined as:

$$\text{dynamic void coeff} = \frac{1}{\beta_{eff}} \frac{v}{k_\infty} \frac{\partial k_\infty}{\partial v}\bigg|_{v=0.4}$$

The derivative above can be calculated by fitting k_∞ for the three void points as a second order polynomial in v, differentiating, and evaluating at v = 0.4. The result is:

$$\text{dynamic void coeff} = \frac{0.4}{\beta_{eff}}\left[-\frac{3k_\infty(0.0)}{2.8k_\infty(0.4)} - \frac{1}{1.2} + \frac{4k_\infty(0.7)}{2.1k_\infty(0.4)}\right]$$

Table 2.2 - Hot Uncontrolled Beginning of Life k_∞ and
Dynamic Void Coefficient Comparisons
SVEA 96+ and GE14 Lattices

[[

{3}]]

Table 2.2 - Hot Uncontrolled Beginning of Life k_∞ and Dynamic Void Coefficient Comparisons SVEA 96+ and GE14 Lattices

[[

{3}]]

Table 2.3 - Hot Uncontrolled k_∞ and Dynamic Void Coefficient Comparisons for Exposed Conditions SVEA 96+ Lattice 6026

[[

{3}]]

Table 2.3 - Hot Uncontrolled k_∞ and Dynamic Void Coefficient Comparisons for Exposed Conditions SVEA 96+ Lattice 6026

[[

{3}]]

The results in Tables 2.2 and 2.3 show that the agreement between the design model TGBLA06 and MCNP is consistent with this expectation. A difference of [[{3}]] at 4.0 GWd/ST is above the two-sigma level of the expected results but is similar to differences seen in previous studies for GNF fuel and for the GE14 GNF fuel presented. The maximum difference of [[{3}]] at 25.0 GWd/ST is a result of differences between small void coefficients. The analysis for SVEA 96+ Lattice 6026 in Table 2.3 shows that the dynamic void coefficient agreement between TGBLA and MCNP improves for exposures greater than 4.0 GWd/ST and is significantly within the two-sigma level at exposures greater than 8.0 GWd/ST.

In general, the Dynamic Void Coefficient comparison shows good agreement between MCNP and TGBLA06 and is within expected bounds except as described in the previous paragraph. From these results, it is concluded that TGBLA06 can be used to model the SVEA 96+ designs present in the Hope Creek Generating Station core.

Figures 2.1 through 2.8 show Beginning of Life (BOL) TGBLA06/MCNP k_∞ comparisons for cold, 0% void hot, 40% void hot, 70% void hot and borated cases for SVEA 96+ and GE14 lattice configurations.

[[

{3}]]

Figure 2.1 - SVEA 96+ Lattice 6019 TGBLA06V/MCNP k_∞ Comparison

[[

{3}]]

Figure 2.2 - SVEA 96+ Lattice 6020 TGBLA06V/MCNP k_∞ Comparison

[[

{3}]]

Figure 2.3 - SVEA 96+ Lattice 6022 TGBLA06V/MCNP k_∞ Comparison

[[

{3}]]

Figure 2.4 - SVEA 96+ Lattice 6023 TGBLA06V/MCNP k_∞ Comparison

[[

{3}]]

Figure 2.5 - SVEA 96+ Lattice 6024 TGBLA06V/MCNP k_∞ Comparison

[[

{3}]]

Figure 2.6 - SVEA 96+ Lattice 6026 TGBLA06V/MCNP k_∞ Comparison

[[

{3}]]

Figure 2.7 - GE14 Lattice 4963 Regular Zone TGBLA06V/MCNP k_∞ Comparison

[[

{3}]]

Figure 2.8 - GE14 Lattice 4966 Vanished Zone TGBLA06V/MCNP k_∞ Comparison

The accuracy of pin power distributions can also be determined from Monte Carlo comparisons. In this case the basis for comparison is the standard deviation of the difference in pin power between TGBLA06 and MCNP. The standard deviation is given by:

$$s=\sqrt{\frac{1}{N-1}\sum_{j=1}^{N}(p_{Mj}-p_{Tj})^2}$$

where p_{M_j} and p_{T_j} are the MCNP and TGBLA06 pin peaking factors for fuel rod j and the summation is taken over all fuel rods in the lattice.

In addition to the use of these comparisons as a figure of merit for TGBLA06 range of application review, the values are also utilized as the pin power uncertainty value in the SVEA 96+ GEXL correlation development. The beginning of life standard deviations, s, are summarized in Table 2.4 for the several SVEA 96+ lattices and two GE14 lattices. The standard deviations, s, for exposed condition are summarized in Table 2.5 for SVEA 96+ lattice 6026. The standard deviation in pin power is less for the SVEA 96+ lattices compared to the GE14 lattices. Plots of the standard deviation for uncontrolled, controlled, and borated states as a function of moderator density from the cold to hot, 70% void state are shown in Figures 2.9 through 2.16. The expected results should be less than a two-sigma uncertainty of 2.88%. [2] All evaluations for the SVEA 96+ fuel meet this requirement. The weighted average of 18 beginning of life state points, shown in Table 2.4, and the 21 exposed state points, shown in Table 2.5, was found to be 1.63%. This is above the one sigma value for the fleet average of 1.44% but is consistent with GNF 10x10 products. The major contributors to the higher uncertainty are the fuel rods at location (4,5), (5,4), (6,4), (4,6), (7,5), (5,7), (7,6), and (6,7). These rods typically show a negative bias of 4-5% (TGBLA is low) as a result of the approximation of the large diamond shaped water mass in the center of the lattice.

Table 2.4 - Hot Uncontrolled Beginning of Life Pin Power Comparison SVEA 96+ and GE14 Lattices

[[

{3}]]

[[

{3}]]

Figure 2.9 - SVEA 96+ Lattice 6019 TGBLA06V/MCNP Fission Density Comparison

[[

{3}]]

Figure 2.10 - SVEA 96+ Lattice 6020 TGBLA06V/MCNP Fission Density Comparison

[[

{3}]]

Figure 2.11 - SVEA 96+ Lattice 6022 TGBLA06V/MCNP Fission Density Comparison

[[

{3}]]

Figure 2.12 - SVEA 96+ Lattice 6023 TGBLA06V/MCNP Fission Density Comparison

[[

{3}]]

Figure 2.13 - SVEA 96+ Lattice 6024 TGBLA06V/MCNP Fission Density Comparison

[[

{3}]]

Figure 2.14 - SVEA 96+ Lattice 6026 TGBLA06V/MCNP Fission Density Comparison

[[

{3}]]

Figure 2.15 - GE14 Lattice 4963 TGBLA06V/MCNP Fission Density Comparison

[[

{3}]]

Figure 2.16 - GE14 Lattice 4966 TGBLA06V/MCNP Fission Density Comparison

Table 2.5 - Hot Uncontrolled Pin Power Comparison versus Exposure for SVEA 96+ Lattice 6026

[[

{3}]]

2.1.4 Boron Worth Accuracy for Standby Liquid Control Analysis

The Standby Liquid Control Analysis uses a statistical uncertainty for the worth of soluble boron in the moderator coolant derived from TGBLA06/MCNP comparisons. Table 2.6 contains the results of this comparison for SVEA 96+ lattices compared in this qualification study.

While this analysis is not used in the SVEA 96+ qualification review of TGBLA06, it is used to provide support information to the statistical uncertainty for Standby Liquid Control Analysis.

Table 2.6 - Cold (160°C) Uncontrolled Borated Beginning of Life k_∞ Comparison SVEA 96+ and GE14 Lattices

[[

{3}]]

Table 2.6 - Cold (160°C) Uncontrolled Borated Beginning of Life k_∞ Comparison SVEA 96+ and GE14 Lattices

[[

[3]]]

2.1.5 3D Simulator Accuracy

The 3D simulator PANAC11 receives the cross section input form TGBLA06, which has been shown to be equally accurate for the SVEA 96+ fuel and GE12/GE14 fuel. Therefore no changes in reactivity and power distribution accuracy are expected when SVEA 96+ bundles are introduced.

2.1.6 References

1. *MCNP: Light Water Reactor Critical Benchmarks,* NEDO-32028, March 1992.
2. *Methodology and Uncertainties for Safety Limit MCPR Evaluations,* NEDC-32601P-A, August 1999.

2.2 Lattice Physics Results

2.2.1 Description

This section provides lattice physics results for representative SVEA 96+ and GE14 lattice designs. The GE14 design is the bottom-most enriched lattice in the bundle that was developed to support the reference core loading pattern analyses for the MCAR.

Note: Table 2.7 shows a tabulation of the data that is presented for each lattice in this Section.

Table 2.7 - Representative Lattice Evaluation

Design	BWREDB Bundle #	BWREDB Lattice #	Variable	Condition	Voids	Exposures (GWd/ST)
SVEA 96+	2657	6022	k_∞	HOT, Uncontrolled	All	All
SVEA 96+	2657	6022	k_∞	COLD, Uncontrolled	All	All
SVEA 96+	2657	6022	2-D Local Peaking	HOT, Uncontrolled	40%	0, 5, 10
GE14	2695	6203	k_∞	HOT, Uncontrolled	All	All
GE14	2695	6203	k_∞	COLD, Uncontrolled	All	All
GE14	2695	6203	2-D Local Peaking	HOT, Uncontrolled	40%	0, 5, 10

The Bundle and Lattice descriptions for the SVEA 96+ design and the GE14 design used in this study are presented in Figures 2.17 and 2.19, respectively.

The SVEA 96+ Hot Uncontrolled and Cold Uncontrolled k_∞ is presented in Table 2.8. The SVEA 96+ power peaking data is shown in Figure 2.18.

The GE14 Hot Uncontrolled and Cold Uncontrolled k_∞ is presented in Table 2.9. The GE14 power peaking data is shown in Figure 2.20.

[[

{3}]]

Figure 2.17 - SVEA 96+ Bundle 2657 Configuration

Table 2.8 - SVEA 96+ Bundle 2657 k_∞

[[

{3}]]

[[

{3}]]

Figure 2.18 - SVEA 96+ Bundle 2657 2D Dominant Lattice Power Peaking

[[

{3}]]

Figure 2.19 - GE14 Bundle 2695 Configuration

Table 2.9 - GE14 Bundle 2695 k_∞

[[

{3}]]

[[

{3}]]

Figure 2.20 - GE14 Bundle 2695 2D Dominant Lattice Power Peaking

3.0 Cycle 13 Base Point Determination - Cycle 9-12 Simulation

The operating history of the Hope Creek reactor has been tracked by the 3D simulator (PANAC11). The results of this tracking are used to determine appropriate hot and cold eigenvalues for core design work as well as to evaluate thermal margin biases, which may exist between the simulator and the process computer. The tracking simulations also provide the base point (starting point) for core design work for Cycle 13.

3.1 Cycle 9-12 Performance Tracking

This section contains several figures summarizing the results of the core tracking for Cycle 9, which was the last full loading of GE fuel, and Cycles 10, 11 and 12 where SVEA 96+ fuel was loaded. Figures 3.1 and 3.2 summarize the hot and cold eigenvalues for all these cycles. Also included are eigenvalues used for the reference fuel cycle (RFC) design of Cycle 13. Figures 3.3, 3.7 and 3.11 show hot eigenvalues for the individual cycles.

The hot eigenvalue selected as Cycle 13 design basis is based on a combination of the data for previous cycles at Hope Creek as well as GNF's methods experience with similar size and power BWRs. The eigenvalue data for Cycles 9 through 12 is well behaved and relatively tightly packed. GNF would expect the eigenvalue to behave as shown by the "GE14 Equilibrium" curve as the fraction of GE14 fuel is increased in future cycles.

The cold eigenvalue selected as the Cycle 13 design basis is again based on a combination of cold critical measurements in the previous cycles as well as GNF's method experience with its BWR fleet. Generally the cold eigenvalue basis is selected so as to conservatively bound the measured data rather than fit through the data as with the hot eigenvalue.

Figures 3.4, 3.8 and 3.12 show the evaluation of MFLCPR for each of the cycles. The simulated results are compared to measured results from the process computer. Figures 3.5, 3.9 and 3.13 show the evaluation of MFLPD for each of the cycles and comparison to the process computer. Figures 3.6, 3.10 and 3.14 show the evaluation of MAPRAT for each of the cycles and comparison to the process computer.

The process computer data comparisons of MFLCPR, MFLPD and MAPRAT are the basis for selecting the design margins shown in Table 5.2.

[[

{3}]]

Figure 3.1 - Cycle 9 - Cycle 12 Hot Critical Eigenvalue Tracking

[[

{3}]]

Figure 3.2 - Cycle 9 - Cycle 12 Cold Critical Eigenvalue Tracking

[[

{3}]]

Figure 3.3 - Cycle 10 Hot Critical Eigenvalue

[[

{3}]]

Figure 3.4 - Cycle 10 MFLCPR

[[

{3}]]

Figure 3.5 - Cycle 10 MFLPD

[[

{3}]]

Figure 3.6 - Cycle 10 MAPRAT

[[

{3}]]

Figure 3.7 - Cycle 11 Hot Critical Eigenvalue

[[

{3}]]

Figure 3.8 - Cycle 11 MFLCPR

[[

{3}]]

Figure 3.9 - Cycle 11 MFLPD

[[

{3}]]

Figure 3.10 - Cycle 11 MAPRAT

[[

{3}]]

Figure 3.11 - Cycle 12 Hot Critical Eigenvalue

[[

{3}]]

Figure 3.12 - Cycle 12 MFLCPR

[[

{3}]]

Figure 3.13 - Cycle 12 MFLPD

[[

{3}]]

Figure 3.14 - Cycle 12 MAPRAT

3.2 3D Process Computer Transverse In-core Probe (TIP) Comparisons

Comparisons between measured TIPs and predicted TIP responses provide a benchmark of bundle and nodal power distribution capability. A comparison of radial (bundle) TIPs are directly proportional to accuracy of bundle powers used for determination of core MCPR. A comparison of nodal TIPs are directly proportional to the accuracy of nodal powers used for determination of core MAPRAT and MFLPD.

For Hope Creek, summary statistics are presented in section 3.2.1. Section 3.2.2 contains graphical summaries of root mean square (RMS) differences between predicted and measured TIPs for both bundle average behavior and nodal (3D) performance. As further evidence, section 3.2.3 provides string-by-string performance for BOC, MOC, and near EOC for Cycle 11. These figures demonstrate that both core wide radial and axial behavior are captured as well as individual string behavior. These TIP comparisons for Hope Creek demonstrate that the GNF methodology is capable of predicting the mixed core environment well. Additionally, both the summary statistics for all cycles and trends within cycles do not present a departure from the GNF experience base.

3.2.1 Statistics Summary

The average over the cycles 9-12 for bundle RMS is [[{3}]] and nodal RMS [[{3}]] . The standard deviations are [[{3}]] and [[{3}]] , respectively. For cycle 11 specifically, the numbers are essentially the same. Overall, these numbers are not unreasonable for a gamma TIP plant. Bundle RMSs < [[{3}]] and nodal RMSs < [[{3}]] are generally exceptionally good. The Bundle RMSs shown in Table 3.1 demonstrate that the use of a [[{3}]] integrated effective TIP reading in the SLMCPR calculation (Table 6.2) is fully applicable.

A plot of the RMS values for the bundle data is provided in Figure 3.15.

Table 3.1 - RMS Values

[[{3}]]

3.2.2 Plots of Bundle and Nodal TIP Comparisons

[[

{3}]]

Figure 3.15 - Plot Of TIP Nodal RMS % Versus Cycle Exposure GWd/ST For Cycles 9-12

[[

(3)]]

Figure 3.16 - Plot Of TIP Bundle RMS % Versus Cycle Exposure GWd/ST For Cycles 9-12

3.2.3 Comparison of Axial TIP plots for Cycle 11

Axial TIP plots are shown in the following figures for three selected exposure points for Cycle 11 near BOC, MOC, and EOC, respectively. In the figures below, PCTIP is the process computer TIP readings and CALTIP is the PANAC11 calculated TIP readings. The exposure shown is in MWd/ST.

[[

{3}]]

Figure 3.17 - Plot Of Axial Tip Comparison For Cycle 11 At A Selected Exposure Point Near BOC

[[

(3)]]

Figure 3.18 - Plot Of Core Average Axial TIP Comparison For Cycle 11 At A Selected Exposure Point Near BOC

[[

{3}]]

Figure 3.19 - Plot Of Axial TIP Comparison For Cycle 11 At A Selected Exposure Point Near MOC

[[

{3}]]

Figure 3.20 - Plot Of Core Average Axial TIP Comparison For Cycle 11 At A Selected Exposure Point Near MOC

[[

{3}]]

Figure 3.21 - Plot Of Axial TIP Comparison For Cycle 11 At A Selected Exposure Point Near EOC

[[

{3}]]

Figure 3.22- Plot Of Core Average Axial TIP Comparison For Cycle 11 At A Selected Exposure Point Near EOC

4.0 Fuel Rod Thermal-Mechanical Report Description

This section of the MCAR documents the fuel rod thermal-mechanical performance limits for the SVEA 96+ fuel design for application in the Hope Creek Generating Station. The performance limits are applied in the nuclear bundle and core design process. Demonstration that individual bundle and core designs meet these performance limits ensures compliance with the fuel rod thermal-mechanical design and licensing limits. The steady-state LHGR performance limits for SVEA 96+ have been supplied by PSEG Nuclear LLC as part of the transfer of information for the SVEA 96+ bases. The steady-state limits are not being replaced with steady-state limits based on GNF thermal-mechanical methodology. The SVEA 96+ steady-state LHGR performance limits are being used to define the initial conditions for the subsequent Anticipated Operational Occurrence (AOO) evaluations. These initial conditions are described in Section 4.1. The AOO limits for the SVEA 96+ fuel design, as specified in Section 4.2, have been determined using the GNF thermal-mechanical methodology using the limits provided in Section 4.1 as starting points for the AOO limit evaluation. The GNF thermal-mechanical methodology has been applied to determine the allowable overpowers during an AOO that assure pellet centerline melting will not occur and the cladding strain will not exceed the 1% circumferential plastic strain criterion.

The fuel rod thermal-mechanical performance limits for GE14C are documented in the GNF Design Basis documents.

4.1 Fuel Rod Thermal-Mechanical Performance Limits for Steady-State Operation

- Maximum Steady-State Linear Heat Generation Rate [[{3}]]
- Maximum Peak Pellet Exposure [[{3}]]
- Maximum Operating Time [[{3}]]

4.1.1 UO_2 Fuel Rod Steady-State Limit versus Exposure

The maximum peak pellet power allowable for a UO_2 fuel rod at a given UO_2 rod peak pellet exposure can be calculated from Table 4.1.

4.1.2 Gd_2O_3 Fuel Rod Steady-State Limit versus Exposure

For the purposes of the AOO evaluations described in Section 4.2, gadolinia bearing fuel rods are assumed to have the same steady-state allowable limits as the UO_2 fuel rods (see Tables 4.2 and 4.3). This is a conservative assumption for the initial condition relative to AOO evaluations.

4.2 Fuel Rod Thermal-Mechanical Limits for Anticipated Operational Occurrences

The purpose of this section is to present the criteria to be applied in the core design process to ensure consistency with the General Electric fuel rod thermal-mechanical design and licensing basis with respect to Anticipated Operational Occurrences (AOOs).

4.2.1 Design and Licensing Limits

4.2.1.1 Overheating of Fuel Pellets

The fuel rod is evaluated to ensure that fuel rod failure due to fuel melting will not occur. Evaluations are performed for whole core AOOs to ensure that fuel melting does not occur. For local AOOs, such as the Rod Withdrawal Error, a small amount of calculated fuel pellet centerline melting may occur, but the event is limited by the 1% cladding circumferential plastic strain criterion.

4.2.1.2 Pellet Cladding Interaction

The fuel rod is evaluated to ensure that fuel rod failure due to pellet-cladding mechanical interaction will not occur. Evaluations are performed for the limiting AOOs to ensure that the circumferential cladding plastic strain during the event does not exceed 1%.

4.2.1.3 Cumulative Performance Limits

Other fuel performance considerations are included in fuel rod design and licensing analyses to address the cumulative effects (e.g., fatigue) of AOOs and other reactor operational behavior. No specific constraints on core design are required to ensure consistency with this cumulative effects design and licensing basis, because the input to these evaluations are based on periodically updated actual operational experience of all General Electric BWR/2-6 reactors.

4.2.2 Thermal and Mechanical Overpowers

4.2.2.1 Thermal Overpower

The thermal overpower is used to evaluate the potential for the fuel entering the molten state at the fuel centerline. Temperature at the fuel centerline is proportional to either the fuel rod linear power or the fuel rod surface heat flux, so the magnitude of these quantities reached during the AOO are the parameters of interest. The measurement of an AOO and its approach to fuel centerline melting also depends on the nuclear methods used for evaluation of the transient. Three methods are used. They are:

1. Point model. The core is represented by a point model and all changes in power are assumed to be the same percentage at all locations in the core. The current point model used by General Electric is the REDY model.
2. 1–D model. The core is represented through a one-dimensional model in the axial dimension. The core power distribution in the radial or r–θ plane is collapsed at each axial node. All fuel bundles are therefore assumed to experience the same percentage change in power at the same axial elevation. The current 1–D model used by General Electric is the ODYN model.
3. 3–D model. The core is represented by a model of each fuel bundle, which are all represented with a number of axial nodes. Changes in power are calculated for each

axial node of each individual fuel bundle throughout the core. The current 3–D model used by General Electric is the PANACEA model.

For use with the point model or the 1–D model, the thermal overpower is defined as:

$$OP^{Th} = \left[\frac{P_1^{Th} - P_0^{Th}}{P_0^{Th}}\right] \times 100 \qquad (4.1)$$

where:

OP^{Th} = The thermal overpower for a particular fuel design during an AOO, %. A fuel design is the quantity loaded in the core that has the same fuel rod thermal-mechanical limits for both steady-state operation and AOOs .

P_0^{Th} = The maximum steady-state heat flux in the fuel bundle of a particular fuel design prior to the event.

P_1^{Th} = The maximum heat flux in a fuel bundle of the same fuel design during the event. This may occur at a different axial node than P_0^{Th} when evaluated based on the 1–D model results.

A graph of this thermal overpower is shown in Figure 4.1.

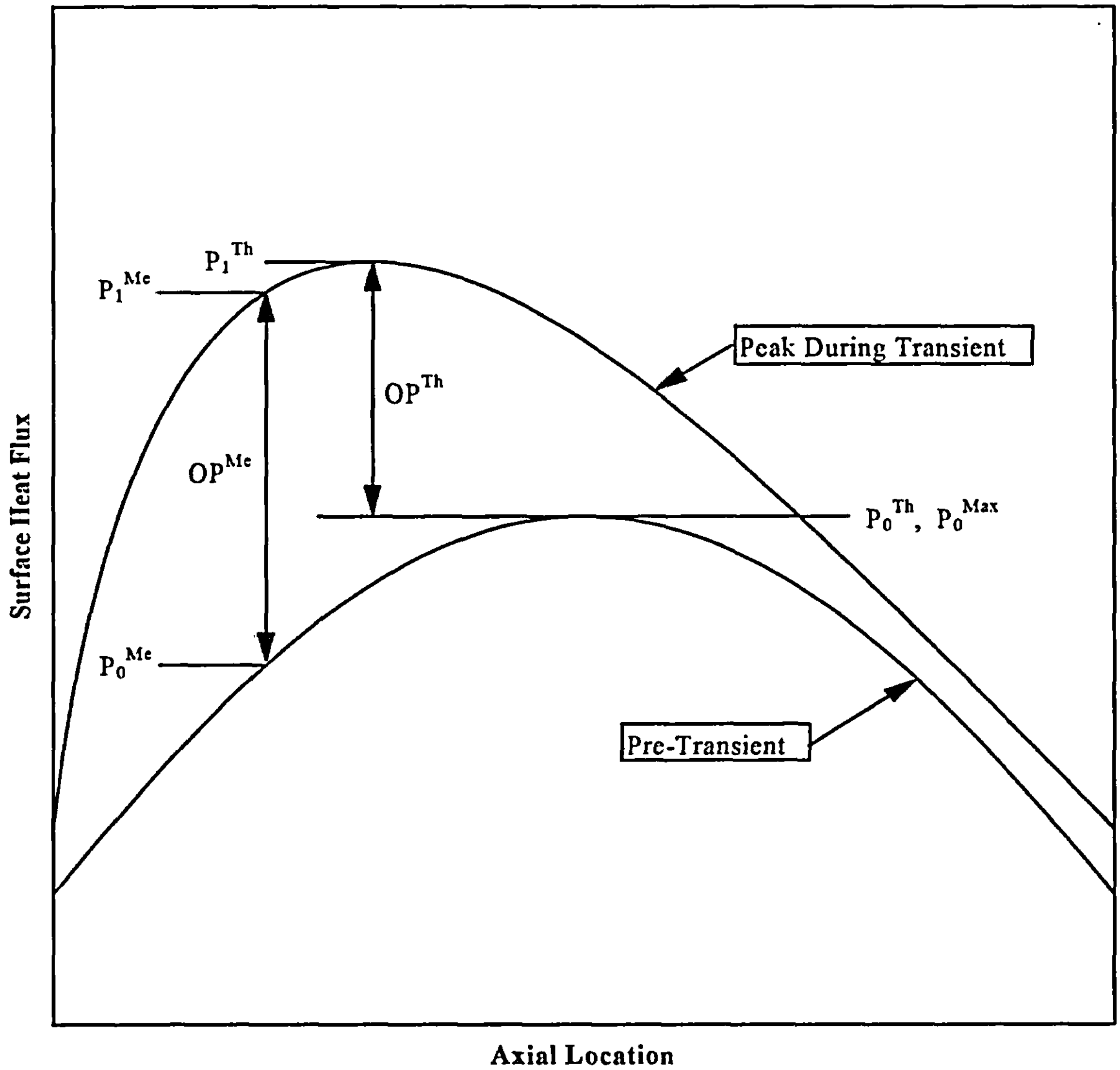

Figure 4.1 - Graph of Thermal and Mechanical Overpowers

For use with the 3–D model, the thermal overpower is defined as:

$$OP^{Th} = \left[\frac{MFLPD_{1}^{Th} - MFLPD_{0}^{Th}}{MFLPD_{0}^{Th}}\right] \times 100 \tag{4.2}$$

where:

OP^{Th} = The thermal overpower for a particular fuel design during an AOO, %. A fuel design is the quantity of fuel loaded in the core which has the same fuel rod thermal-mechanical limits for both steady-state operation and AOOs and the OP^{Th} is the maximum value for the event considering all fuel bundles of that design present in the core.

$MFLPD_{0}^{Th}$ = The maximum fraction of linear power density (MFLPD), relative to the steady-state thermal-mechanical limit prior to the event for any fuel bundle in the core which is located no more than two (2) positions away from the fuel bundle for which the OP^{Th} is being calculated.

$MFLPD_{1}^{Th}$ = The maximum fraction of linear power density relative to the steady-state thermal-mechanical limit during the event for any fuel bundle in the core.

Alternately, for use with the 3-D model, the thermal overpower can also be defined as:

$$OP^{Th} = \left[\frac{MAPRAT_{1}^{Th} - MAPRAT_{0}^{Th}}{MAPRAT_{0}^{Th}}\right] \times 100 \tag{4.3}$$

where:

OP^{Th} = The thermal overpower for a particular fuel design during an AOO, %. A fuel design is the quantity of fuel loaded in the core which has the same fuel rod thermal-mechanical limits for both steady-state operation and AOOs and the OP^{Th} is the maximum value for the event considering all fuel bundles of that design present in the core.

$MAPRAT_{0}^{Th}$ = The maximum ratio of the average planar linear heat generation rate (APLHGR) relative to the APLHGR limit (MAPLHGR) prior to the event for any fuel bundle in the core which is located no more than two (2) positions away from the fuel bundle for which the OP^{Th} is being calculated.

$MAPRAT_{1}^{Th}$ = The maximum ratio of the APLHGR relative to the APLHGR limit (MAPLHGR) during the event for any fuel bundle in the core.

Equations (4.2) and (4.3) differ in that equation (4.2) will include any differences and changes in the local power and exposure peaking in the nodes being evaluated as compared with that used for establishing the MAPLHGR.

4.2.2.2 Mechanical Overpower

The mechanical overpower is used to evaluate the potential for overstraining of the cladding. The incremental cladding strain during an AOO is proportional to the change in fuel volume average temperature, which is proportional to the change in either the fuel rod linear power or the fuel rod surface heat flux at a particular axial location or cross-section of the fuel rod. This overpower is therefore evaluated based on the change in heat flux at a specific fuel rod axial location. As with the thermal overpower, the fuel volume average temperature change is evaluated differently depending on the nuclear methods used to evaluate the transient.

For use with the point model or the 1–D model, the mechanical overpower is therefore defined as:

$$OP^{Me} = \left[\frac{P_1^{Me} - P_0^{Me}}{P_0^{Max}}\right] \times 100 \qquad (4.4)$$

where:

OP^{Me} = The mechanical overpower for a particular fuel design during an AOO, %. A fuel design is the quantity of fuel loaded in the core, which has the same fuel rod thermal-mechanical limits for both steady-state operation and AOOs .

P_0^{Me} = The steady-state heat flux prior to the event in the fuel rod of a particular fuel design for the axial location that experiences the largest heat flux increase during the event. A fuel design is the quantity of fuel loaded in the core, which has the same fuel rod thermal-mechanical limits for both steady-state operation and AOOs . The largest surface heat flux increase at a particular node in a fuel rod is measured as the absolute value for the magnitude of the surface heat flux change at that node and not as a percentage value.

P_1^{Me} = The maximum heat flux reached during the event in the same fuel rod at the same axial location.

P_0^{Max} = The maximum steady-state heat flux in the same fuel rod prior to the event. This may occur at a different axial node than P_0^{Me} and P_1^{Me} when evaluated based on the 1–D model results.

A graphical illustration of the mechanical overpower is shown in Figure 4.1.

For use with the 3–D model, the mechanical overpower is defined as:

$$OP^{Me} = \left[\frac{FLPD_1^{Me} - FLPD_0^{Me}}{MFLPD_{Max}^{Me}}\right] \times 100 \qquad (4.5)$$

where:

OP^{Me} = The mechanical overpower for a particular fuel design during an AOO, %. A fuel design is the quantity of fuel loaded in the core which has the same fuel rod thermal-mechanical limits for both steady-state operation and AOOs and the OP^{Me} is the maximum value for the event considering all fuel bundles of that design present in the core. Evaluation of the peak power rod in a node can be assumed to bound all rods in that node if the controlled state of the node has not changed during the event.

$FLPD_0^{Me}$ = The fraction of linear power density (FLPD), relative to the steady-state thermal-mechanical limit prior to the event for any fuel bundle and rod at the axial location which experiences the largest increase in fuel rod power during the AOO. The largest power increase at a particular node in a fuel rod is measured as the absolute value for the magnitude of the power change at that node and not as a percentage value.

$FLPD_1^{Me}$ = The fraction of linear power density relative to the steady-state thermal-mechanical limit during the event for any fuel bundle and rod at the axial location which experiences the largest increase in fuel rod power during the AOO for a particular fuel design. This will therefore be for the same fuel bundle and rod and at the same axial node as $FLPD_0^{Me}$ when evaluated based on the 3–D model results.

$MFLPD_{Max}^{Me}$ = The maximum fraction of linear power density (MFLPD), relative to the steady-state thermal-mechanical limit prior to the event for any fuel bundle in the core which is located no more than two (2) positions away from the fuel bundle for which the OP^{Me} is being calculated.

Alternately, for use with the 3–D model, the mechanical overpower can also be defined as:

$$OP^{Me} = \left[\frac{RAPLHGR_1^{Me}\text{-}RAPLHGR_0^{Me}}{MAPRAT_{Max}^{Me}}\right] \times 100 \qquad (4.6)$$

where:

OP^{ME} = The mechanical overpower for a particular fuel design during an AOO, %. A fuel design is the quantity of fuel loaded in the core which has the same fuel rod thermal-mechanical limits for both steady-state operation and AOOs and the OP^{ME} is the maximum value for the event considering all fuel bundles of that design present in the core.

$RAPLHGR_0^{Me}$ = The ratio of the average planar linear heat generation rate (APLHGR) relative to the APLHGR limit (MAPLHGR limit) prior to the event for any fuel bundle at the axial node which experiences the largest increase in nodal power during the AOO. The largest power increase at a particular node is measured as the absolute value for the magnitude of the power change at that node and not as a percentage value.

$RAPLHGR_1^{Me}$ = The ratio of the APLHGR relative to the APLHGR limit (MAPLHGR limit) during the event for the same fuel bundle and at the same axial node as $RAPLHGR_0^{Me}$.

$MAPRAT_{Max}^{Me}$ = The maximum ratio of the APLHGR relative to the APLHGR limit (MAPLHGR limit) at the axial node with the largest value for RAPLHGR prior to the event for any fuel bundle in the core which is located no more than two (2) positions away from the fuel bundle for which the OP^{Me} is being calculated.

Equations (4.5) and (4.6) differ in that equation (4.5) will include any differences and changes in the local power and exposure peaking for the rod being evaluated as compared with that used for establishing the MAPLHGR.

4.2.3 Limiting Thermal and Mechanical Overpowers for AOOs at Rated Power and Flow

4.2.3.1 Rod Withdrawal Error (RWE)

The UO_2 and $UO_2 - Gd_2O_3$ RWE mechanical overpower (MOP, % above the steady-state envelope) is 50% above the steady-state envelope defined in Table 4.1 for UO_2 Rods and 13% above the steady-state envelope defined in Table 4.3 for Gd Rods, for any axial node of any fuel rod located in the Error Cell. The RWE mechanical overpower for any axial node of any fuel rod located outside of the Error Cell shall not exceed the value specified in Table 4.4 or Table 4.5. No thermal overpower limit is applied to the RWE.

4.2.3.2 Loss of Feedwater Heater/Inadvertent Actuation of Auxiliary Cold Water Supply Systems (HPCI, HPCS, RCIC)

These events are characteristically similar and are of sufficient duration that the fuel thermal response is steady-state. Therefore, the surface heat flux values from the steady-state or transient BWR Simulator models can be compared to the surface heat flux values determined acceptable by the steady-state fuel rod thermal-mechanical analysis methods. Table 4.4 and 4.5 show the fuel rod thermal and mechanical overpowers corresponding to design and licensing limits.

4.2.3.3 Short Duration Pressurization Transients

The remaining AOOs (e.g., Load Rejection with Bypass Failure, Feedwater Controller Failure) occur quite rapidly relative to the fuel thermal time constant such that the calculated surface heat flux is not a valid indicator of the thermal and mechanical consequences of these events. The limits for these short duration events are therefore expressed in terms which can be related to the transient analysis method used for the evaluations of the events.

4.2.3.3.1 Short Duration Pressurization Transients with GE Methods

The limits for these short duration events are expressed as an allowable thermal and mechanical overpower based on the surface heat flux values from the BWR transient model. These overpowers are calculated by the transient model based on the definitions for thermal and mechanical overpower presented in Section 4.2.2 and are compared with the limits for these overpowers presented in Tables 4.6 and 4.7.

The short duration pressurization transients are subcategorized according to the nature of the event and the specific analyses performed to evaluate those event types.

4.2.3.3.1.1 Generator Load Rejection with Bypass Failure (LRNBP) Type

This category of pressurization transient events is characterized by a rapid increase in neutron flux followed by a prompt reactor scram resulting in a total event duration of <3 seconds. Included in this category are the following events:

- Generator Load Rejection with Bypass Failure
- Turbine Trip with Bypass Failure
- Generator Load Rejection
- Turbine Trip
- Loss of Normal Condenser Vacuum
- MSIV Closure-Position Scram
- Inadvertent Closure One MSIV

The limits for thermal and mechanical overpower for this type of event are presented in Tables 4.6 and 4.7.

4.2.3.3.1.2 Feedwater Controller Failure (FWCF) Type

This category of pressurization transient events is characterized by a slow (approximately 13-30 seconds) increase in power followed by a rapid (<1.5 seconds) increase in neutron flux and prompt reactor scram. The only event in this category is the feedwater controller failure.

The limits for thermal and mechanical overpower for this type of event are presented in Tables 4.6 and 4.7.

Table 4.1 - UO_2 Rod BWREDB_FUEL Limits

[[

{3}]]

Table 4.2 - UO_2 and $(U,Gd)O_2$ Fuel Rod Maximum Power, kW/ft

[[

[3]]]

Table 4.3 - UO_2 and (U, Gd)O_2 Rod/Section BWREDB_FUEL Limits

[[

{3}]]

To convert linear power (P, kW/ft) to heat flux at the cladding outer surface (Q/A, Btu/hr-ft^2):

$$\left[\frac{Q}{A}\right]\left[\frac{\text{Btu}}{\text{hr-ft}^2}\right]=P\left[\frac{\text{kW}}{\text{ft}}\right]\left[\frac{3412.14\times12}{\pi\times0.3787}\right]\left[\frac{\text{Btu}}{\text{hr-kW}}\right]\left[\frac{\text{in}}{\text{in-ft}}\right]=34416.2\times P \quad (4.7)$$

Table 4.4 - LFWH, Inadvertent HPCS, HPCI, RCIC Injection, RWE-Outside Error Cell Overpower Limits for UO_2 Rods

Maximum Allowable Surface Heat Flux Increase, %	
Thermal	Mechanical
[[{3}]]	[[{3}]]

For a definition of Thermal and Mechanical Overpowers, please see Sections 4.2.2.1 and 4.2.2.2.

Table 4.5 - LFWH, Inadvertent HPCS, HPCI, RCIC Injection, RWE-Outside Error Cell Overpower Limits for Gd Rods

[[

{3}]]

Table 4.6 - Overpower Transient Magnitude Guideline Limits for Short Duration Pressurization Transients using Gemini Method for UO_2 Rods

[[

{3}]]

Table 4.7 - Overpower Transient Magnitude Guideline Limits for Short Duration Pressurization Transients using Gemini Method for Gd Rods

[[

{3}]]

5.0 GE14 / SVEA 96+ Demonstration Cycle Analysis Description – Cycle 13

This section of the MCAR provides the results of the Reference Loading Pattern (RLP) core operation simulation of the first reload of GE14 into the Hope Creek Generating Station. The RLP is developed to meet all design bases set for the upcoming cycle (Cycle 13) and is used as the basis for deriving the actual loading pattern. The RLP is the basis for the licensing calculations that are documented in the Supplemental Reload Licensing Report (SRLR) that is reported in Section 7.0 of this report.

5.1 Reload Bundle Design Description

The reload bundle nuclear design process is closely coupled with the core nuclear design process in demonstrating compliance with safety and performance criteria. An iterative process was used between bundle design and core design to obtain an optimal balance among performance objectives while satisfying all safety criteria.

This process resulted in a two-stream GE14 reload design strategy using GE14 bundles with axial and radial isotopic configurations shown in Figures 5.1 and 5.2. The average content and specific distributions of gadolinium and enriched uranium used for the GE14 bundle designs were selected to accomplish the following goals:

1. Meet PSEG specified cycle energy and operating strategy for an 18-month operating cycle. The average enrichment of the fuel bundles was 4.02 wt% U235. The gadolinium loading of 4.0 and 6.0 wt% Gd_2O_3 was chosen to compensate for the natural decrease in hot excess reactivity of the legacy fuel resulting in a relatively flat overall core hot excess reactivity throughout the majority of the operating cycle and to control radial and axial power shapes without leaving significant amounts of undepleted gadolinium at the end of the cycle.
2. Maintain adequate thermal margins. Lattice enrichment and gadolinium distributions were optimized to obtain desired relative rod-to-rod thermal performance. This included analysis of the local power peaking factors used to calculate linear heat generation rates and the bundle R-factors used to calculate critical power ratios. These parameters were minimized, consistent with other goals, throughout the bundle exposure range associated with expected high power operation for these GE14 designs. Relative powers for gadolinia rods were suppressed to provide adequate margin to meet thermal-mechanical design requirements.
3. Maintain adequate reactivity margins. To demonstrate one stuck rod sub-criticality, design margin to criticality is calculated with the 3D simulator (PANACEA) in conjunction with critical eigenvalue determinations at the reactor during plant startup. Reactivity control of the fresh fuel is accomplished through the choice of gadolinia design. Cold shutdown margin at beginning of cycle is influenced primarily by the number of gadolinia rods used, while cold shutdown margin later in the cycle is influenced primarily by the concentration of gadolinia used.

4. Minimize the number and complexity of unique pellet and rod types. The number of pellet and rod types are determined primarily to optimize relative rod-to-rod thermal performance. There are 51 unique (non-symmetric) lattice locations for fueled rods in the GE14 bundle configuration. The two GE14 reload bundles both utilize 11 unique pellet types in a total of 15 unique rod types (including two types of tie rods).

5.2 Cycle 13 Core Design Description

5.2.1 Core Configuration Description

Changing the design of the fuel utilized in a nuclear power reactor requires a wide range of analyses to support acceptance relative to operational and safety requirements. The purpose of the core design analysis is to demonstrate feasibility of operation, assure compliance with safety limits and provide operating state points for further safety analyses.

Hot operating analyses with projected control rod patterns were performed at different burn-up points through Cycle 13 to demonstrate that the specified operating strategies can be supported and that all operating limits can be satisfied. These analysis conditions also provide the beginning state points for other safety analyses. Cold shutdown calculations have been performed throughout the cycle to demonstrate compliance with the stuck control rod criteria.

5.2.2 Design Limits and Targets

The target core flow range is 98.0 – 103.0% rated flow. The critical k_{eff} design target for hot, rated operation is shown in Figure 3.1. The distributed critical k_{eff} design target for cold shutdown evaluations is shown in Figure 3.2. Core design limits are provided in Table 5.1 and parameters for tracking the core design limits are provided in Table 5.2.

The cold critical k_{eff} values are based on the local, cold, critical k_{eff} predicted for Cycle 13 operation. The local cold critical k_{eff} = (distributed cold critical k_{eff}) - 0.003, where the distributed cold, critical k_{eff} are based on observed plant data from in-sequence cold critical cases.

MCPR margin is tracked via the parameter MFLCPR; MLHGR (pellet power margin) is tracked via the parameter MFLPD; and, nodal power margin is tracked via the parameter MAPRAT, where:

$$\text{MFLCPR} = \frac{\text{MCPR Operating Limit}}{\text{MCPR}} \tag{5.1}$$

$$\text{MFLPD} = \frac{\text{Peak LHGR}}{\text{LHGR Operating Limit}} \tag{5.2}$$

$$\text{MAPRAT} = \frac{\text{Maximum Average Planar LHGR}}{\text{MAPLHGR Operating Limit}} \tag{5.3}$$

5.3 Cycle 13 Performance Summary

The resultant Cycle 13 RLP for the upper left quarter core loading configuration is provided in Figure 5.3.[a] The table below Figure 5.3 lists all fuel types and how many of each type are included in the Cycle 13 core configuration.

Table 5.3 compares the calculated thermal limit core performance parameters to the Table 5.2 thermal limit design margin targets. Table 5.4 provides hot excess reactivity vs. cycle exposure. Tables 5.5 and 5.6 compare cold shutdown and standby liquid control system (SLCS) reactivity performance parameters, respectively, to the Table 5.2 reactivity limit design margin targets.

Figure 5.4 provides the Cycle 13 core control blade configuration for the upper left quadrant[b], calculated thermal margins[c] and k_{eff} eigenvalue as a function of cycle exposure. Figure 5.5 plots the thermal limit parameters vs. cycle exposure. Figure 5.6 plots core hot excess reactivity vs. cycle exposure. Figures 5.7 and 5.8 plot cold shutdown and SLCS reactivity margins, respectively, versus cycle exposure.

As is seen in the above referenced tables and figures, all core operating and design margins are met by the Cycle 13 RLP, except for MFLPD at the beginning of cycle (BOC). The MFLPD exception at BOC has been dispositioned to be acceptable based on the MFLPD comparisons at BOC shown in Section 3.1.

---

[a] The RLP was evaluated on a full-core basis.
[b] All control blade patterns are quarter-core mirror symmetric.
[c] Minimum margin in full-core reported.

Table 5.1 - Core Design Limits

Minimum Critical Power Ratio (MCPR) - Design operating limit for RLP core design (Actual operating limits as determined by reload analyses are presented in Section 7.0)	GE14 [[{3}]] BOC to 8022 MWd/ST [[{3}]] after 8022 MWd/ST
	SVEA 96+ [[{3}]] BOC to 8022 MWd/ST [[{3}]] after 8022 MWd/ST
Maximum Linear Heat Generation Rate (MLHGR) Cold Shutdown Margin - One Stuck Control Rod Boron Injection Shutdown Margin Peak Pellet Exposure	Fuel Dependent Limit in kW/ft [[{3}]] kW/ft (GE14) [[{3}]] kW/ft (SVEA 96+) 1.0% Δk 1.0% Δk [[{3}]] GWd/MTU (GE14) [[{3}]] GWd/MTU (SVEA 96+)

Table 5.2 - Core Design Margin Targets

MFLCPR	0.93
MFLPD	0.85
MAPRAT	0.89
Cold Shutdown Margin - One Stuck Control Rod	1.3% Δk
Boron Injection Shutdown Margin	1.0% Δk
Peak Pellet Exposure	[[{3}]] GWd/MTU (GE14) [[{3}]] GWd/MTU (SVEA 96+)

Table 5.3 - Cycle 13 RLP Summary of Rod Pattern Results

[[

{3}]]

Table 5.4 - Cycle 13 RLP Hot Excess Reactivity

[[

{3}]]

Table 5.5 - Cycle 13 RLP Cold Shutdown Reactivity Margin

*** CARI AND SDM RESULTS ***

CASE CONVERGENCE: PASSED
DESIGN CRITERIA: MET

[[

{3}]]

Table 5.6 - Cycle 13 RLP Standby Liquid Control Shutdown Margin

SLCS ANALYSIS - PANACEA SLCS RESULTS

PLANT NAME : HOPE CREEK 1
EIS CODE : KT1
CYCLE NUMBER : 13

PANACEA VERSION: PANAC11V
NITER: 15
ANALYSIS TEMP: 160. C
ANALYSIS BORON: 726. PPM

SLCS SDM REQUIREMENT DETERMINATION:

IAT NO.	NO. BUNDLES IN THE CORE	PRODUCT LINE	SDM REQ
1	89	SVEA 96+	0.010
2	38	SVEA 96+	0.010
3	166	SVEA 96+	0.010
4	69	SVEA 96+	0.010
5	164	SVEA 96+	0.010
6	62	SVEA 96+	0.010
7	56	GE14C	0.010
8	108	GE14C	0.010
9	2	SVEA 96+	0.010
10	2	SVEA 96+	0.010
11	2	SVEA 96+	0.010
12	4	SVEA 96+	0.010
13	2	SVEA 96+	0.010

SDM REQUIREMENT (MOST RESTRICTIVE VALUE): 0.010

[[

{3}]]

[[

{3}]]

Figure 5.1 - Fresh GE14 Reload Bundle 2757 Configuration

[[

[3]]]

Figure 5.2 - Fresh GE14 Reload Bundle 2758 Configuration

[[

[3]]]

Figure 5.3 - Cycle 13 (Quarter Core)

Figure 5.4 - Cycle 13 Reference Loading Pattern Control Rod Operating Sequence

[[

{3}]]

Figure 5.4 - Cycle 13 Reference Loading Pattern Control Rod Operating Sequence

[[

{3}]]

Figure 5.4 - Cycle 13 Reference Loading Pattern Control Rod Operating Sequence

[[

{3}]]

Figure 5.4 - Cycle 13 Reference Loading Pattern Control Rod Operating Sequence

[[

{3}]]

Figure 5.4 - Cycle 13 Reference Loading Pattern Control Rod Operating Sequence

[[

{3}]]

Figure 5.4 - Cycle 13 Reference Loading Pattern Control Rod Operating Sequence

[[

{3}]]

Figure 5.4 - Cycle 13 Reference Loading Pattern Control Rod Operating Sequence

[[

[3]]]

Figure 5.4 - Cycle 13 Reference Loading Pattern Control Rod Operating Sequence

[[

{3}]]

[[

{3}]]

Figure 5.5 - Cycle 13 RLP Rod Pattern Thermal Design Ratio Results

[[

{3}]]

Figure 5.6 - Cycle 13 RLP Hot Excess Reactivity

[[

{3}]]

Figure 5.7 - Cycle 13 RLP Cold Shutdown Margin

[[

{3}]]

Figure 5.8 - Cycle 13 RLP Standby Liquid Control System Shutdown Margin

6.0 Safety Limit Minimum Critical Power Ratio (SLMCPR)

This section of the MCAR provides the results of the SLMCPR evaluation of the Reference Loading Pattern containing legacy SVEA 96+ and the first reload of GE14 in the Hope Creek Generating Station, as reported in Section 5.0 of this report. SLMCPR information developed with GNF NRC approved methodologies and uncertainties[1] is also included to allow for a comparison to the cycle previous to the introduction of GE14 (Cycle 12). The purpose of the evaluation is to determine the minimum allowable MCPR during the most limiting full core transients under which at least 99.9% of the rods in the core would be expected to avoid boiling transition. The minimum allowable MCPR established in this way is defined as the safety limit minimum critical power ratio (SLMCPR).

6.1 Discussion

The Safety Limit Minimum Critical Power Ratio (SLMCPR) evaluations for Hope Creek Cycle 13 were performed using NRC approved methodology and uncertainties. Table 6.1 summarizes the relevant input parameters and results for Cycle 13. Additional information is provided in response to NRC questions related to similar submittals regarding changes in Technical Specification values of SLMCPR. NRC questions pertaining to how GE14 applications satisfy the conditions of the NRC SER[1] have been addressed in Reference 2. Other generically applicable questions related to application of the GEXL14 correlation, and to the applicable range for the R-factor methodology, are addressed in Reference 3. Items that require a plant/cycle specific response are presented below.

Previously, the SLMCPR was calculated on the upper boundary of the power/flow operating map only at 100% flow / 100% power (rated flow/rated power) with limiting control blade patterns developed at the rated flow/rated power point. This approach had been shown in NEDC-32601P-A to result in conservative SLMCPR evaluation values. As reported in Reference 4, recent SLMCPR evaluations performed by GNF have shown that limiting control blade patterns developed for less than rated flow at the rated power condition sometimes yield more limiting bundle-by-bundle MCPR distributions and/or more limiting bundle axial power shapes than the limiting control blade patterns developed at the rated flow/rated power evaluation point. Consequently, in addition to the rated flow/rated power evaluation point, an SLMCPR calculation has been performed for Hope Creek at a lower flow/rated power evaluation point. The current Hope Creek licensing basis minimum allowable core flow at rated power is 87% rated flow. However, to account for future operation at lower flow/rated power conditions, SLMCPR evaluations were performed at a reduced core flow rate of 76.6% rated flow at the rated power condition for the same exposure points that were previously calculated for the rated flow/rated power evaluations. The SLMCPR results for Hope Creek Cycle 13 at the 76.6% rated flow condition are equivalent to or bound the SLMCPR results calculated at the rated flow condition and the 87% flow condition.

The core loading information for Hope Creek Cycle 13 is provided in Figure 6.2.

In general, the calculated safety limit is dominated by two key parameters: (1) flatness of the core bundle-by-bundle MCPR distributions, and (2) flatness of the bundle pin-by-pin power/ R-factor distributions. Greater flatness in either parameter yields more rods susceptible to boiling transition and thus a higher calculated SLMCPR. The value of these parameters for Hope Creek Cycle 13 is summarized in Table 6.1 as the MIP (MCPR Importance Parameter) and the RIP (R-factor Importance Parameter), respectively.

The impact of the fuel loading pattern differences on the calculated SLMCPR is correlated to the values of MIP and RIP. The calculated MIP value for the Hope Creek Cycle 13 core at EOR using a limiting rod pattern is [[{3}]]

Pin-by-pin power distributions are characterized in terms of R-factors using the NRC approved methodology.[5] For the Hope Creek Cycle 13 limiting case analyzed at EOR, the weighted RIP value, considering the participation of the contributing bundles, was calculated to be [[{3}]]

The revised power distribution methodology was used for the Hope Creek Cycle 13 analysis. This methodology has been justified, reviewed and approved by the NRC (reference NEDC-32601P-A). When applying the revised model to calculate a lower SLMCPR, the conservatism that remains was reviewed, approved and documented by the USNRC. It was noted on page A-24 of NEDC-32601P-A [[{3}]]

The SLMCPR was calculated for Hope Creek Cycle 13 using the reduced power distribution uncertainties described in Reference 1.

Table 6.1 summarizes the relevant input parameters and results of Cycle 13 evaluated at the condition of 76.6% rated flow/rated power. The SLMCPR values were calculated for Hope Creek using uncertainties that have been previously reviewed and approved by the NRC as listed in Table 6.2 and described in Reference 1 and, where warranted, higher plant-cycle-specific uncertainties as listed in Table 6.3. A [[{3}]] consistent with current GNF fuel operation. For the Hope Creek Cycle 13 lower flow evaluations, the Core Flow Rate and Random effective TIP reading uncertainties were [[{3}]]

These calculations use the GEXL14 correlation for GE14 fuel and GEXL80 correlation for SVEA 96+ fuel (Reference 6). [[{3}]]

The Two Loop and SLO SLMCPR values calculated for Hope Creek Cycle 13 are shown in Table 6.1.[a]

6.2 Summary

The calculated 1.06 SLMCPR and 1.07 SLO SLMCPR for Hope Creek Cycle 13 are consistent with expectations given the ratios for MIP and RIP that have been calculated and the use of the reduced uncertainties described in Reference 1. Correlations of MIP and RIP directly to the calculated SLMCPR have been performed for this plant/cycle which show that these values are appropriate when the approved methodology and the reduced uncertainties given in NEDC-32601P-A and NEDC-32694P-A are used.

Based on all of the information and discussion presented above, it is concluded that a 1.06 SLMCPR and 1.08 SLO SLMCPR for the Hope Creek Cycle 13 core are appropriate.

6.3 References

1. Letter, Frank Akstulewicz (NRC) to Glen A. Watford (GE), "Acceptance for Referencing of Licensing Topical Reports NEDC-32601P, *Methodology and Uncertainties for Safety Limit MCPR Evaluations*; NEDC-32694P, *Power Distribution Uncertainties for Safety Limit MCPR Evaluation*; and Amendment 25 to NEDE-24011-P-A on Cycle Specific Safety Limit MCPR," (TAC Nos. M97490, M99069 and M97491), March 11, 1999.
2. Letter, Glen A. Watford (GNF-A) to U. S. Nuclear Regulatory Commission Document Control Desk with attention to R. Pulsifer (NRC), "Confirmation of 10x10 Fuel Design Applicability to Improved SLMCPR, Power Distribution and R-Factor Methodologies", FLN-2001-016, September 24, 2001.
3. Letter, Glen A. Watford (GNF-A) to U. S. Nuclear Regulatory Commission Document Control Desk with attention to J. Donoghue (NRC), "Confirmation of the Applicability of the GEXL14 Correlation and Associated R-Factor Methodology for Calculating SLMCPR Values in Cores Containing GE14 Fuel", FLN-2001-017, October 1, 2001.
4. Letter, Jason S. Post (GE Energy) to U.S. Nuclear Regulatory Commission Document Control Desk, "Part 21 Reportable Condition and 60-Day Interim Report Notification: Non-conservative SLMCPR", MFN-04-081, August 24, 2004.

[a] The calculated SLO SLMCPR is 1.07, however, the Hope Creek Cycle 13 NRC approved SLO value is 1.08. Hope Creek requested a SLO SLMCPR of 1.08 in Hope Creek's initial license change request for the Cycle 13 SLMCPR. Due to an earlier than planned shutdown at the end of Cycle 12 and the removal of two fuel defects found during core offload, the Cycle 13 core was redesigned after the initial Cycle 13 SLMCPR license change request. SLMCPR information based on the redesigned core was provided to the NRC as a supplement to the initial license change request. In the supplement, Hope Creek chose to keep the SLO SLMCPR value of 1.08 that was initially calculated since the value is bounding for the redesigned core. The SLO SLMCPR value of 1.07 is presented in this report to provide an exact numerical base for comparison with Hope Creek constant pressure power uprate SLMCPR results.

5. Letter, Thomas H. Essig (NRC) to Glen A. Watford (GE), "Acceptance for Referencing of Licensing Topical Report NEDC-32505P, Revision 1, *R-Factor Calculation Method for GE11, GE12 and GE13 Fuel*," (TAC Nos. M99070 and M95081), January 11, 1999.
6. *GEXL80 Correlation for SVEA 96+ Fuel*, NEDC-33107P, Revision 0, Class III, September 2003.
7. Letter, Glen A. Watford (GNF-A) to U. S. Nuclear Regulatory Commission Document Control Desk with attention to J. Donoghue (NRC), "Final Presentation Material for GEXL Presentation – February 11, 2002", FLN-2002-004, February 12, 2002.

Table 6.1 - Comparison of the Hope Creek Generating Station Cycle 13 and Cycle 12 SLMCPR

DESCRIPTION	Hope Creek Cycle 12	Hope Creek Cycle 13	Hope Creek Cycle 13
Number of Bundles in Core	764	764	764
Limiting Cycle Exposure Point[a]	EOR	EOR	EOR
Cycle Exposure at Limiting Point (MWd/MTU)	12020 (EOR – 1102)	10472 (EOR – 1467)	10472 (EOR – 1467)
Core Flow, % Rated	100.0	100.0	76.6
Reload Fuel Type	SVEA 96+	GE14	GE14
Latest Reload Batch Fraction, %	31.4	21.5	21.5
Latest Reload Average Batch Weight % Enrichment	3.61	4.02	4.02
Core Fuel Fraction for GE14 (%)	0.0	21.5	21.5
Core Fuel Fraction for GE9B (%)	6.9	0.0	0.0
Core Fuel Fraction for SVEA 96+ (%)	93.1	78.5	78.5
Core Average Weight % Enrichment	3.44	3.63	3.63
Core MCPR (for limiting rod pattern)	1.38	1.42	1.38
[[			{3}]]
[[			{3}]]
[[			{3}]]
Power distribution methodology	Revised NEDC-32601P-A	Revised NEDC-32601P-A	Revised NEDC-32601P-A
Power distribution uncertainty	Reduced NEDC-32694P-A	Reduced NEDC-32694P-A	Reduced NEDC-32694P-A
Non-power distribution uncertainty	Revised NEDC-32601P-A	Revised NEDC-32601P-A	Revised NEDC-32601P-A
Calculated Safety Limit MCPR (Two Loop)	1.09	1.05	1.06
Calculated Safety Limit MCPR (SLO)	1.10	1.06	1.07

[a] End of Rated (EOR) is defined as end-of-cycle all rods out, 100% power / 100% flow and normal feedwater temperature. The actual analysis is performed prior to EOR in order to have sufficient control rod density to force some bundles near to the OLMCPR.

Table 6.2 - Standard Uncertainties

DESCRIPTION	Hope Creek Cycle 12 100% Flow	Hope Creek Cycle 13 100% Flow	Hope Creek Cycle 13 76.6% Flow
Non-power Distribution Uncertainties	**Revised NEDC-32601P-A**	**Revised NEDC-32601P-A**	**Revised NEDC-32601P-A**
Core flow rate (derived from pressure drop)	2.5 Two Loop 6.0 SLO	2.5 Two Loop 6.0 SLO	2.5 Two Loop 6.0 SLO
Individual channel flow area	[[{3}]]	[[{3}]]	[[{3}]]
Individual channel friction factor	5.0	5.0	5.0
Friction factor multiplier	[[{3}]]	[[{3}]]	[[{3}]]
Reactor pressure	[[{3}]]	[[{3}]]	[[{3}]]
Core inlet temperature	0.2	0.2	0.2
Feedwater temperature	[[{3}]]	[[{3}]]	[[{3}]]
Feedwater flow rate	[[{3}]]	[[{3}]]	[[{3}]]
Power Distribution Uncertainties	Reduced NEDC-32694P-A	Reduced NEDC-32694P-A	Reduced NEDC-32694P-A
GEXL R-factor	[[{3}]]	[[{3}]]	[[{3}]]
Random effective TIP reading	1.2 Two Loop 2.85 SLO	1.2 Two Loop 2.85 SLO	1.2 Two Loop 2.85 SLO
Systematic effective TIP reading	[[{3}]]	[[{3}]]	[[{3}]]
Integrated effective TIP reading	[[{3}]]	[[{3}]]	[[{3}]]
Bundle power	[[{3}]]	[[{3}]]	[[{3}]]
Effective total bundle power uncertainty	[[{3}]]	[[{3}]]	[[{3}]]

Table 6.3 - Exceptions to the Standard Uncertainties Used in Hope Creek Cycle 13 and Cycle 12

Reactor pressure	2.04	2.04	2.04
Core Flow Rate	--	--	[[{3}]]
Random Effective TIP Reading	--	--	[[{3}]]
GEXL R-factor	[[{3}]]	[[{3}]]	[[{3}]]

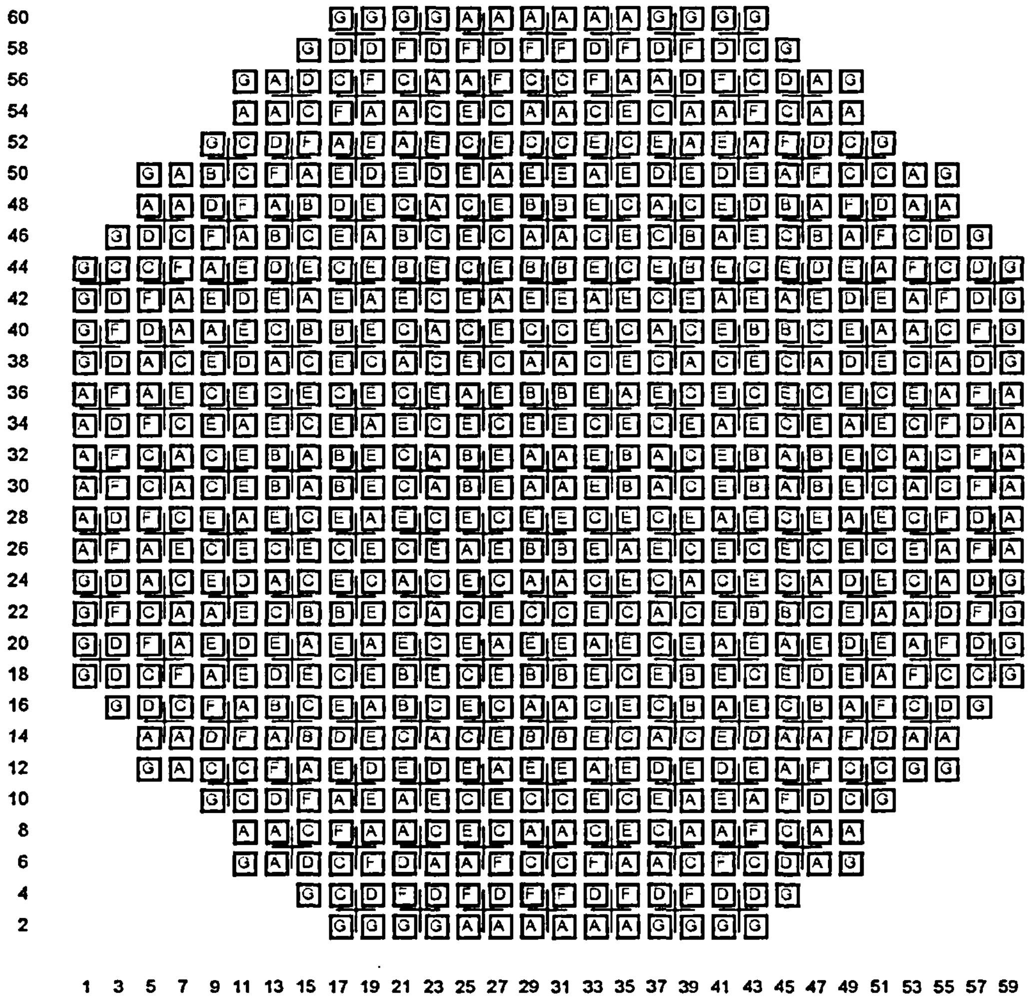

Code	Bundle Name	Number Loaded	Cycle Loaded
A	SVEA96-P10CASB326-11GZ-568U-4WR-150-T6-2654	184	10
B	SVEA96-P10CASB326-11G4.5-568U-4WR-150-T6-2655	48	10
C	SVEA96-P10CASB360-12GZ-568U-4WR-150-T6-2656	167	11
D	SVEA96-P10CASB360-12G5.0-568U-4WR-150-T6-2657	72	11
E	SVEA96-P10CASB361-14GZ-568U-4WR-150-T6-2658	176	12
F	SVEA96-P10CASB360-12G5.5/2G2.5-568U-4WR-150-T6-2659	64	12
G	GE9B-P8CWB280-8G4.0-80U-150-T6	53	9

Figure 6.1 - Reference Core Loading Pattern – Cycle 12

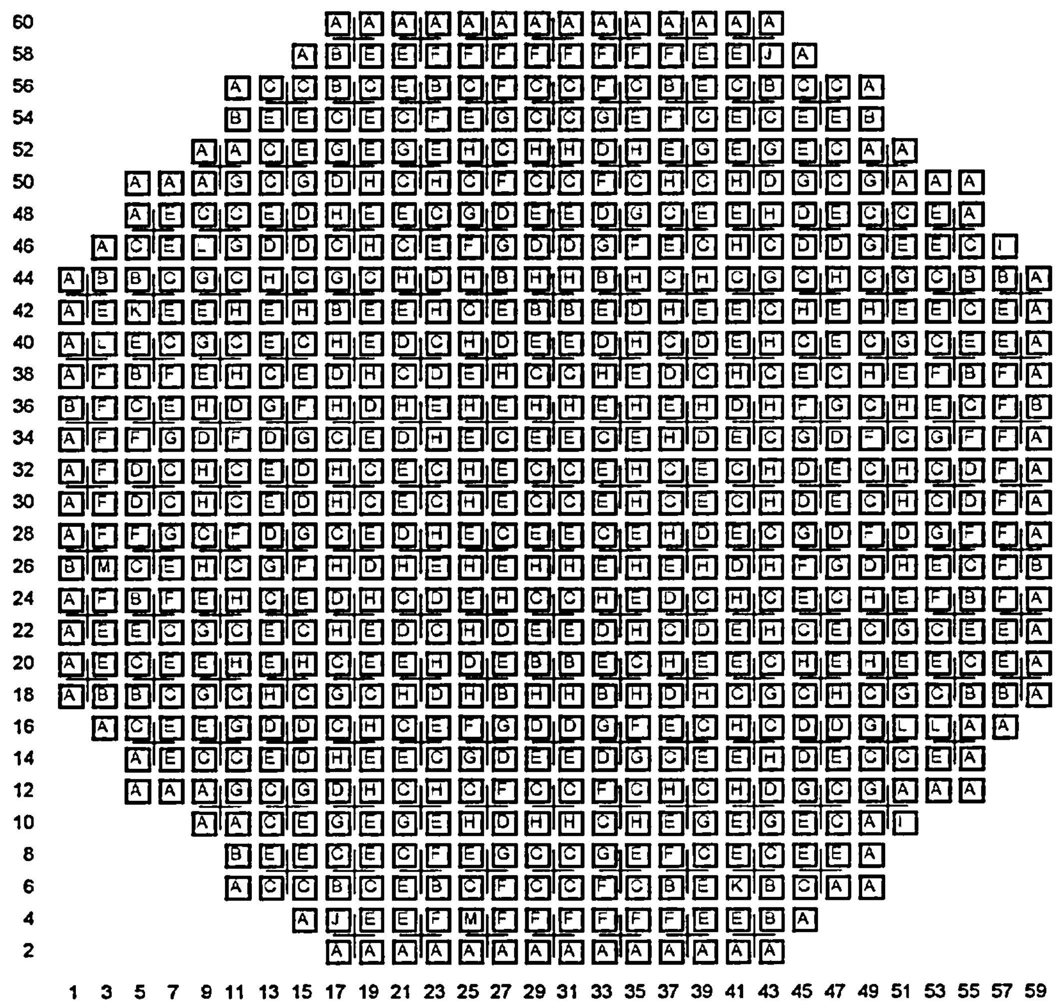

Code	Bundle Name	Number Loaded	Cycle Loaded
A	SVEA96-P10CASB326-11GZ-568U-4WR-150-T6-2654	89	10
B	SVEA96-P10CASB326-11G4.5-568U-4WR-150-T6-2655	38	10
C	SVEA96-P10CASB360-12GZ-568U-4WR-150-T6-2656	166	11
D	SVEA96-P10CASB360-12G5.0-568U-4WR-150-T6-2657	69	11
E	SVEA96-P10CASB361-14GZ-568U-4WR-150-T6-2658	164	12
F	SVEA96-P10CASB360-12G5.5/2G2.5-568U-4WR-150-T6-2659	62	12
G	GE14-P10CNAB402-4G6.0/16G4.0-100T-150-T6-2757	56	13
H	GE14-P10CNAB402-5G6.0/14G4.0-100T-150-T6-2758	108	13
I	SVEA96-P10CASB326-11GZ-568U-4WR-150-T6-2654	2	10
J	SVEA96-P10CASB326-11G4.5-568U-4WR-150-T6-2655	2	10
K	SVEA96-P10CASB360-12G5.0-568U-4WR-150-T6-2657	2	11
L	SVEA96-P10CASB361-14GZ-568U-4WR-150-T6-2658	4	12
M	SVEA96-P10CASB360-12G5.5/2G2.5-568U-4WR-150-T6-2659	2	12

Figure 6.2 - Reference Core Loading Pattern – Cycle 13

7.0 Cycle 13 Supplemental Reload Licensing Report (SRLR)

A copy of the Cycle 13 SRLR follows this analysis. The SRLR sections, tables, figures, appendices and page numbering are self contained as in the original report and therefore have not been modified to be consistent with Sections 1.0 – 6.0 of the MCAR. Accordingly, individual SRLR sections, tables and figures are not contained in the MCAR Table of Contents, List of Tables or List of Figures.

Global Nuclear Fuel
A Joint Venture of GE, Toshiba, & Hitachi

0000-0031-0596-SRLR
Revision 1
Class I
December 2004

0000-0031-0596-SRLR, Rev. 1

Supplemental Reload Licensing Report

for

Hope Creek Unit 1

Reload 12 Cycle 13

Approved M. E. Harding
M. E. Harding, Manager
Fuel Engineering Services

Approved
R. E. Kingston
Customer Account Leader

Important Notice Regarding Contents of This Report

Please Read Carefully

This report was prepared by Global Nuclear Fuel - Americas, LLC (GNF-A) solely for PSEG Nuclear, LLC and the U.S. Nuclear Regulatory Commission (USNRC). The information contained in this report is believed by GNF-A to be an accurate and true representation of the facts known, obtained or provided to GNF-A at the time this report was prepared.

The only undertakings of GNF-A respecting information in this document are contained in the contract between PSEG Nuclear, LLC and GNF-A for nuclear fuel and related services for the nuclear system for Hope Creek Generating Station Unit 1 and nothing contained in this document shall be construed as changing said contract. The use of this information except as defined by said contract, or for any purpose other than that for which it is intended, is not authorized; and with respect to any such unauthorized use, neither GNF-A nor any of the contributors to this document makes any representation or warranty (express or implied) as to the completeness, accuracy or usefulness of privately owned rights; nor do they assume any responsibility for liability or damage of any kind which may result from such use of such information.

Acknowledgement

The engineering and reload licensing analyses, which form the technical basis of this Supplemental Reload Licensing Report, were performed by G. N. Marrotte, R. H. Szilard, S. C. Gupta, S. J. Peters, A. E. Horna and W. Wong. The Supplemental Reload Licensing Report was prepared by G. N. Marrotte. This document has been verified by R. H. Szilard.

The basis for this report is *General Electric Standard Application for Reactor Fuel*, NEDE-24011-P-A-14, June 2000; and the U.S. Supplement, NEDE-24011-P-A-14-US, June 2000.

1. Plant-unique Items

Appendix A: Analysis Conditions
Appendix B: List of Acronyms
Appendix C: Decrease In Core Coolant Temperature Events
Appendix D: Basis for K_f curve
Appendix E: Option B Licensing Basis
Appendix F: Reactor Recirculation Pump Seizure Event

2. Reload Fuel Bundles

Fuel Type	Cycle Loaded	Number
Irradiated:		
SVEA96-P10CASB326-11GZ-568U-4WR-150-T6-2654 (SVEA-96+)	10	91
SVEA96-P10CASB326-11G4.5-568U-4WR-150-T6-2655 (SVEA-96+)	10	40
SVEA96-P10CASB360-12GZ-568U-4WR-150-T6-2656 (SVEA-96+)	11	166
SVEA96-P10CASB360-12G5.0-568U-4WR-150-T6-2657 (SVEA-96+)	11	71
SVEA96-P10CASB361-14GZ-568U-4WR-150-T6-2658 (SVEA-96+)	12	168
SVEA96-P10CASB360-12G5.5/2G2.5-568U-4WR-150-T6-2659 (SVEA-96+)	12	64
New:		
GE14-P10CNAB402-5G6.0/14G4.0-100T-150-T6-2758 (GE14C)	13	108
GE14-P10CNAB402-4G6.0/16G4.0-100T-150-T6-2757 (GE14C)	13	56
Total		764

3. Reference Core Loading Pattern

Nominal previous cycle core average exposure at end of cycle:	25828 MWd/MT (23430 MWd/ST)
Minimum previous cycle core average exposure at end of cycle from cold shutdown considerations[1]:	25828 MWd/MT (23430 MWd/ST)
Assumed reload cycle core average exposure at beginning of cycle:	17839 MWd/MT (16183 MWd/ST)
Assumed reload cycle core average exposure at end of cycle (rated conditions):	29777 MWd/MT (27013 MWd/ST)
Reference core loading pattern:	Figure 1

4. Calculated Core Effective Multiplication and Control System Worth - No Voids, 20°C

Beginning of Cycle, $k_{effective}$	
Uncontrolled	1.103
Fully controlled	0.947
Strongest control rod out	0.983
R, Maximum increase in cold core reactivity with exposure into cycle, Δk	0.001

5. Standby Liquid Control System Shutdown Capability

Boron (ppm) (at 20°C)	Shutdown Margin (Δk) (at 160°C, Xenon Free)
660	0.035

[1] The licensing analyses are based on the actual shutdown exposure for the previous cycle.

6. Reload Unique GETAB Anticipated Operational Occurrences (AOO) Analysis Initial Condition Parameters[2]

Operating domain: ICF (HBB)
Exposure range : BOC13 to EOR13-3245 MWd/MT (2944 MWd/ST)

	Peaking Factors						
Fuel Design	Local	Radial	Axial	R-Factor	Bundle Power (MWt)	Bundle Flow (1000 lb/hr)	Initial MCPR
GE14C	1.45	1.57	1.40	1.040	6.688	105.5	1.32
SVEA-96+	1.45	1.62	1.40	1.040	6.922	101.4	1.33

Operating domain: ICF (HBB)
Exposure range : EOR13-3245 MWd/MT (2944 MWd/ST) to EOC13

	Peaking Factors						
Fuel Design	Local	Radial	Axial	R-Factor	Bundle Power (MWt)	Bundle Flow (1000 lb/hr)	Initial MCPR
GE14C	1.45	1.51	1.54	1.040	6.453	109.3	1.30
SVEA-96+	1.45	1.56	1.54	0.990	6.661	104.8	1.33

Operating domain: MELLLA (HBB)
Exposure range : BOC13 to EOR13-3245 MWd/MT (2944 MWd/ST)

	Peaking Factors						
Fuel Design	Local	Radial	Axial	R-Factor	Bundle Power (MWt)	Bundle Flow (1000 lb/hr)	Initial MCPR
GE14C	1.45	1.43	1.34	1.040	6.109	78.7	1.32
SVEA-96+	1.45	1.46	1.34	0.990	6.208	74.9	1.35

[2] End of Rated (EOR) is defined as end-of-cycle all rods out, 100% power/100% flow, and normal feedwater temperature.

Operating domain: MELLLA (HBB) Exposure range : EOR13-3245 MWd/MT (2944 MWd/ST) to EOC13							
	Peaking Factors						
Fuel Design	Local	Radial	Axial	R-Factor	Bundle Power (MWt)	Bundle Flow (1000 lb/hr)	Initial MCPR
GE14C	1.45	1.39	1.44	1.040	5.922	80.9	1.33
SVEA-96+	1.45	1.41	1.44	0.990	6.020	76.6	1.36

Operating domain: ICF (UB) Exposure range : EOR13-3245 MWd/MT (2944 MWd/ST) to EOC13							
	Peaking Factors						
Fuel Design	Local	Radial	Axial	R-Factor	Bundle Power (MWt)	Bundle Flow (1000 lb/hr)	Initial MCPR
GE14C	1.45	1.58	1.29	1.040	6.760	104.4	1.33
SVEA-96+	1.45	1.64	1.29	0.990	6.977	100.7	1.34

Operating domain: MELLLA (UB) Exposure range : EOR13-3245 MWd/MT (2944 MWd/ST) to EOC13							
	Peaking Factors						
Fuel Design	Local	Radial	Axial	R-Factor	Bundle Power (MWt)	Bundle Flow (1000 lb/hr)	Initial MCPR
GE14C	1.45	1.49	1.21	1.040	6.365	76.1	1.30
SVEA-96+	1.45	1.52	1.21	0.990	6.487	72.8	1.31

Operating domain: ICF & MFWT[3] (HBB) Exposure range : BOC13 to EOR13-3245 MWd/MT (2944 MWd/ST)							
	Peaking Factors						
Fuel Design	Local	Radial	Axial	R-Factor	Bundle Power (MWt)	Bundle Flow (1000 lb/hr)	Initial MCPR
GE14C	1.45	1.61	1.40	1.040	6.883	104.1	1.29
SVEA-96+	1.45	1.66	1.40	0.990	7.060	100.1	1.31

[3] MFWT, minimum feedwater temperature, is allowed by plant Technical Specifications as low as 400 °F at rated power.

Operating domain: ICF & MFWT (HBB) Exposure range : EOR13-3245 MWd/MT (2944 MWd/ST) to EOC13							
	Peaking Factors						
Fuel Design	Local	Radial	Axial	R-Factor	Bundle Power (MWt)	Bundle Flow (1000 lb/hr)	Initial MCPR
GE14C	1.45	1.55	1.54	1.040	6.620	108.2	1.28
SVEA-96+	1.45	1.60	1.54	0.990	6.837	103.3	1.30

Operating domain: MELLLA & MFWT (HBB) Exposure range : BOC13 to EOR13-3245 MWd/MT (2944 MWd/ST)							
	Peaking Factors						
Fuel Design	Local	Radial	Axial	R-Factor	Bundle Power (MWt)	Bundle Flow (1000 lb/hr)	Initial MCPR
GE14C	1.45	1.49	1.34	1.040	6.323	77.3	1.28
SVEA-96+	1.45	1.51	1.34	0.990	6.402	73.6	1.31

Operating domain: MELLLA & MFWT (HBB) Exposure range : EOR13-3245 MWd/MT (2944 MWd/ST) to EOC13							
	Peaking Factors						
Fuel Design	Local	Radial	Axial	R-Factor	Bundle Power (MWt)	Bundle Flow (1000 lb/hr)	Initial MCPR
GE14C	1.45	1.45	1.44	1.040	6.164	79.5	1.28
SVEA-96+	1.45	1.47	1.44	0.990	6.238	75.2	1.31

Operating domain: ICF & MFWT (UB) Exposure range : EOR13-3245 MWd/MT (2944 MWd/ST) to EOC13							
	Peaking Factors						
Fuel Design	Local	Radial	Axial	R-Factor	Bundle Power (MWt)	Bundle Flow (1000 lb/hr)	Initial MCPR
GE14C	1.45	1.63	1.29	1.040	6.949	103.1	1.30
SVEA-96+	1.45	1.68	1.29	0.990	7.139	99.3	1.31

Operating domain: MELLLA & MFWT (UB) Exposure range : EOR13-3245 MWd/MT (2944 MWd/ST) to EOC13							
	Peaking Factors						
Fuel Design	Local	Radial	Axial	R-Factor	Bundle Power (MWt)	Bundle Flow (1000 lb/hr)	Initial MCPR
GE14C	1.45	1.54	1.21	1.040	6.555	75.0	1.26
SVEA-96+	1.45	1.57	1.21	0.990	6.686	71.5	1.27

Operating domain: ICF with RPTOOS (HBB) Exposure range : BOC13 to EOR13-3245 MWd/MT (2944 MWd/ST)							
	Peaking Factors						
Fuel Design	Local	Radial	Axial	R-Factor	Bundle Power (MWt)	Bundle Flow (1000 lb/hr)	Initial MCPR
GE14C	1.45	1.54	1.40	1.040	6.586	106.2	1.35
SVEA-96+	1.45	1.59	1.40	0.990	6.797	102.3	1.36

Operating domain: ICF with RPTOOS (HBB) Exposure range : EOR13-3245 MWd/MT (2944 MWd/ST) to EOC13							
	Peaking Factors						
Fuel Design	Local	Radial	Axial	R-Factor	Bundle Power (MWt)	Bundle Flow (1000 lb/hr)	Initial MCPR
GE14C	1.45	1.49	1.54	1.040	6.342	110.0	1.33
SVEA-96+	1.45	1.54	1.54	0.990	6.583	105.3	1.35

Operating domain: MELLLA with RPTOOS (HBB) Exposure range : BOC13 to EOR13-3245 MWd/MT (2944 MWd/ST)							
	Peaking Factors						
Fuel Design	Local	Radial	Axial	R-Factor	Bundle Power (MWt)	Bundle Flow (1000 lb/hr)	Initial MCPR
GE14C	1.45	1.43	1.34	1.040	6.077	78.8	1.33
SVEA-96+	1.45	1.45	1.34	0.990	6.174	75.1	1.36

Operating domain: MELLLA with RPTOOS (HBB) Exposure range : EOR13-3245 MWd/MT (2944 MWd/ST) to EOC13							
	Peaking Factors						
Fuel Design	Local	Radial	Axial	R-Factor	Bundle Power (MWt)	Bundle Flow (1000 lb/hr)	Initial MCPR
GE14C	1.45	1.39	1.44	1.040	5.906	80.9	1.34
SVEA-96+	1.45	1.41	1.44	0.990	6.009	76.7	1.37

Operating domain: ICF with RPTOOS (UB) Exposure range : EOR13-3245 MWd/MT (2944 MWd/ST) to EOC13							
	Peaking Factors						
Fuel Design	Local	Radial	Axial	R-Factor	Bundle Power (MWt)	Bundle Flow (1000 lb/hr)	Initial MCPR
GE14C	1.45	1.55	1.29	1.040	6.613	105.4	1.37
SVEA-96+	1.45	1.60	1.29	0.990	6.838	101.7	1.37

Operating domain: MELLLA with RPTOOS (UB) Exposure range : EOR13-3245 MWd/MT (2944 MWd/ST) to EOC13							
	Peaking Factors						
Fuel Design	Local	Radial	Axial	R-Factor	Bundle Power (MWt)	Bundle Flow (1000 lb/hr)	Initial MCPR
GE14C	1.45	1.48	1.21	1.040	6.301	76.4	1.31
SVEA-96+	1.45	1.51	1.21	0.990	6.428	73.1	1.33

Operating domain: ICF & MFWT with RPTOOS (HBB) Exposure range : BOC13 to EOR13-3245 MWd/MT (2944 MWd/ST)							
	Peaking Factors						
Fuel Design	Local	Radial	Axial	R-Factor	Bundle Power (MWt)	Bundle Flow (1000 lb/hr)	Initial MCPR
GE14C	1.45	1.58	1.40	1.040	6.758	104.9	1.32
SVEA-96+	1.45	1.64	1.40	0.990	6.965	100.8	1.33

Operating domain: ICF & MFWT with RPTOOS (HBB) Exposure range : EOR13-3245 MWd/MT (2944 MWd/ST) to EOC13							
	Peaking Factors						
Fuel Design	Local	Radial	Axial	R-Factor	Bundle Power (MWt)	Bundle Flow (1000 lb/hr)	Initial MCPR
GE14C	1.45	1.53	1.54	1.040	6.524	108.8	1.30
SVEA-96+	1.45	1.58	1.54	0.990	6.733	104.1	1.32

Operating domain: MELLLA & MFWT with RPTOOS (HBB) Exposure range : BOC13 to EOR13-3245 MWd/MT (2944 MWd/ST)							
	Peaking Factors						
Fuel Design	Local	Radial	Axial	R-Factor	Bundle Power (MWt)	Bundle Flow (1000 lb/hr)	Initial MCPR
GE14C	1.45	1.48	1.34	1.040	6.289	77.5	1.29
SVEA-96+	1.45	1.50	1.34	0.990	6.380	73.7	1.31

Operating domain: MELLLA & MFWT with RPTOOS (HBB) Exposure range : EOR13-3245 MWd/MT (2944 MWd/ST) to EOC13							
	Peaking Factors						
Fuel Design	Local	Radial	Axial	R-Factor	Bundle Power (MWt)	Bundle Flow (1000 lb/hr)	Initial MCPR
GE14C	1.45	1.44	1.44	1.040	6.142	79.6	1.29
SVEA-96+	1.45	1.46	1.44	0.990	6.215	75.3	1.32

Operating domain: ICF & MFWT with RPTOOS (UB) Exposure range : EOR13-3245 MWd/MT (2944 MWd/ST) to EOC13							
	Peaking Factors						
Fuel Design	Local	Radial	Axial	R-Factor	Bundle Power (MWt)	Bundle Flow (1000 lb/hr)	Initial MCPR
GE14C	1.45	1.59	1.29	1.040	6.795	104.1	1.33
SVEA-96+	1.45	1.65	1.29	0.990	7.017	100.2	1.34

Operating domain: MELLLA & MFWT with RPTOOS (UB) Exposure range : EOR13-3245 MWd/MT (2944 MWd/ST) to EOC13							
	Peaking Factors						
Fuel Design	Local	Radial	Axial	R-Factor	Bundle Power (MWt)	Bundle Flow (1000 lb/hr)	Initial MCPR
GE14C	1.45	1.53	1.21	1.040	6.497	75.3	1.27
SVEA-96+	1.45	1.55	1.21	0.990	6.599	72.0	1.29

7. Selected Margin Improvement Options [4]

Recirculation pump trip: Yes

Rod withdrawal limiter: No

Thermal power monitor: Yes

Improved scram time: Yes (ODYN Option B)

Measured scram time: No

Exposure dependent limits: Yes

Exposure points analyzed: 2

[4] Refer to GESTAR for those margin improvement options that are referenced and supported within GESTAR.

8. Operating Flexibility Options [5]

Extended Operating Domain (EOD): Yes

EOD type: Maximum Extended Load Line Limit (MELLLA) [6]

Minimum core flow at rated power: 76.6 %

Increased Core Flow: Yes

Flow point analyzed throughout cycle: 105.0 %

Feedwater Temperature Reduction: No

ARTS Program: No

Single-loop operation: Yes

Equipment Out of Service:

Safety/relief valves Out of Service: Yes
(credit taken for 13 of 14 valves)

RPTOOS Yes

9. Core-wide AOO Analysis Results

Methods used: GEMINI; GEXL-PLUS

Operating domain: ICF (HBB) **Exposure range : BOC13 to EOR13-3245 MWd/MT (2944 MWd/ST)**					
			Uncorrected ΔCPR		
Event	**Flux (%NBR)**	**Q/A (%NBR)**	**GE14C**	**SVEA-96+**	**Fig.**
FW Controller Failure	272	118	0.23	0.25	2
Turbine Trip w/o Bypass	340	117	0.26	0.27	3
Load Reject w/o Bypass	327	116	0.26	0.27	4

[5] Refer to GESTAR for those operating flexibility options that are referenced and supported within GESTAR.
[6] MELLLA is not a licensed operating domain at Hope Creek, however these analyses results bound their current licensed operating domain, ELLLA.

Operating domain: ICF (HBB) Exposure range : EOR13-3245 MWd/MT (2944 MWd/ST) to EOC13					
			Uncorrected ΔCPR		
Event	Flux (%NBR)	Q/A (%NBR)	GE14C	SVEA-96+	Fig.
FW Controller Failure	324	122	0.21	0.24	5
Turbine Trip w/o Bypass	396	121	0.24	0.26	6
Load Reject w/o Bypass	384	121	0.24	0.26	7

Operating domain: MELLLA (HBB) Exposure range : BOC13 to EOR13-3245 MWd/MT (2944 MWd/ST)					
			Uncorrected ΔCPR		
Event	Flux (%NBR)	Q/A (%NBR)	GE14C	SVEA-96+	Fig.
FW Controller Failure	191	111	0.22	0.24	8
Load Reject w/o Bypass	238	112	0.26	0.29	9
Turbine Trip w/o Bypass	242	112	0.26	0.28	10

Operating domain: MELLLA (HBB) Exposure range : EOR13-3245 MWd/MT (2944 MWd/ST) to EOC13					
			Uncorrected ΔCPR		
Event	Flux (%NBR)	Q/A (%NBR)	GE14C	SVEA-96+	Fig.
FW Controller Failure	233	115	0.22	0.25	11
Load Reject w/o Bypass	286	116	0.27	0.30	12
Turbine Trip w/o Bypass	285	116	0.27	0.30	13

Operating domain: ICF (UB) Exposure range : EOR13-3245 MWd/MT (2944 MWd/ST) to EOC13					
			Uncorrected ΔCPR		
Event	Flux (%NBR)	Q/A (%NBR)	GE14C	SVEA-96+	Fig.
FW Controller Failure	231	114	0.23	0.24	14
Turbine Trip w/o Bypass	306	115	0.27	0.28	15
Load Reject w/o Bypass	301	114	0.27	0.28	16

Operating domain: MELLLA (UB) Exposure range : EOR13-3245 MWd/MT (2944 MWd/ST) to EOC13					
			Uncorrected ΔCPR		
Event	Flux (%NBR)	Q/A (%NBR)	GE14C	SVEA-96+	Fig.
FW Controller Failure	147	106	0.18	0.19	17
Turbine Trip w/o Bypass	200	108	0.24	0.25	18
Load Reject w/o Bypass	198	107	0.23	0.25	19

Operating domain: ICF & MFWT (HBB) Exposure range : BOC13 to EOR13-3245 MWd/MT (2944 MWd/ST)					
			Uncorrected ΔCPR		
Event	Flux (%NBR)	Q/A (%NBR)	GE14C	SVEA-96+	Fig.
FW Controller Failure	283	119	0.23	0.25	20

Operating domain: ICF & MFWT (HBB) Exposure range : EOR13-3245 MWd/MT (2944 MWd/ST) to EOC13					
			Uncorrected ΔCPR		
Event	Flux (%NBR)	Q/A (%NBR)	GE14C	SVEA-96+	Fig.
FW Controller Failure	331	123	0.21	0.24	21

Operating domain: MELLLA & MFWT (HBB) Exposure range : BOC13 to EOR13-3245 MWd/MT (2944 MWd/ST)					
			Uncorrected ΔCPR		
Event	Flux (%NBR)	Q/A (%NBR)	GE14C	SVEA-96+	Fig.
FW Controller Failure	199	112	0.22	0.25	22

Operating domain: MELLLA & MFWT (HBB) Exposure range : EOR13-3245 MWd/MT (2944 MWd/ST) to EOC13					
			Uncorrected ΔCPR		
Event	Flux (%NBR)	Q/A (%NBR)	GE14C	SVEA-96+	Fig.
FW Controller Failure	243	116	0.22	0.25	23

Operating domain: ICF & MFWT (UB) Exposure range : EOR13-3245 MWd/MT (2944 MWd/ST) to EOC13					
			Uncorrected ΔCPR		
Event	**Flux (%NBR)**	**Q/A (%NBR)**	**GE14C**	**SVEA-96+**	**Fig.**
FW Controller Failure	236	116	0.24	0.25	24

Operating domain: MELLLA & MFWT (UB) Exposure range : EOR13-3245 MWd/MT (2944 MWd/ST) to EOC13					
			Uncorrected ΔCPR		
Event	**Flux (%NBR)**	**Q/A (%NBR)**	**GE14C**	**SVEA-96+**	**Fig.**
FW Controller Failure	151	107	0.19	0.21	25

Operating domain: ICF with RPTOOS (HBB) Exposure range : BOC13 to EOR13-3245 MWd/MT (2944 MWd/ST)					
			Uncorrected ΔCPR		
Event	**Flux (%NBR)**	**Q/A (%NBR)**	**GE14C**	**SVEA-96+**	**Fig.**
FW Controller Failure	301	121	0.25	0.27	26
Turbine Trip w/o Bypass	385	121	0.28	0.30	27
Load Reject w/o Bypass	378	120	0.28	0.29	28

Operating domain: ICF with RPTOOS (HBB) Exposure range : EOR13-3245 MWd/MT (2944 MWd/ST) to EOC13					
			Uncorrected ΔCPR		
Event	**Flux (%NBR)**	**Q/A (%NBR)**	**GE14C**	**SVEA-96+**	**Fig.**
FW Controller Failure	355	125	0.24	0.26	29
Turbine Trip w/o Bypass	442	125	0.27	0.29	30
Load Reject w/o Bypass	436	125	0.27	0.28	31

Operating domain: MELLLA with RPTOOS (HBB) Exposure range : BOC13 to EOR13-3245 MWd/MT (2944 MWd/ST)					
			Uncorrected ΔCPR		
Event	Flux (%NBR)	Q/A (%NBR)	GE14C	SVEA-96+	Fig.
FW Controller Failure	200	113	0.23	0.25	32
Load Reject w/o Bypass	254	114	0.27	0.29	33
Turbine Trip w/o Bypass	256	114	0.27	0.29	34

Operating domain: MELLLA with RPTOOS (HBB) Exposure range : EOR13-3245 MWd/MT (2944 MWd/ST) to EOC13					
			Uncorrected ΔCPR		
Event	Flux (%NBR)	Q/A (%NBR)	GE14C	SVEA-96+	Fig.
FW Controller Failure	240	117	0.23	0.26	35
Load Reject w/o Bypass	305	118	0.27	0.30	36
Turbine Trip w/o Bypass	293	118	0.27	0.30	37

Operating domain: ICF with RPTOOS (UB) Exposure range : EOR13-3245 MWd/MT (2944 MWd/ST) to EOC13					
			Uncorrected ΔCPR		
Event	Flux (%NBR)	Q/A (%NBR)	GE14C	SVEA-96+	Fig.
FW Controller Failure	257	118	0.27	0.27	38
Load Reject w/o Bypass	355	118	0.31	0.31	39
Turbine Trip w/o Bypass	342	118	0.30	0.31	40

Operating domain: MELLLA with RPTOOS (UB) Exposure range : EOR13-3245 MWd/MT (2944 MWd/ST) to EOC13					
			Uncorrected ΔCPR		
Event	Flux (%NBR)	Q/A (%NBR)	GE14C	SVEA-96+	Fig.
FW Controller Failure	167	108	0.20	0.21	41
Load Reject w/o Bypass	223	110	0.25	0.27	42
Turbine Trip w/o Bypass	221	111	0.25	0.26	43

Operating domain: ICF & MFWT with RPTOOS (HBB) **Exposure range : BOC13 to EOR13-3245 MWd/MT (2944 MWd/ST)**					
			Uncorrected ΔCPR		
Event	**Flux (%NBR)**	**Q/A (%NBR)**	**GE14C**	**SVEA-96+**	**Fig.**
FW Controller Failure	313	122	0.26	0.27	44

Operating domain: ICF & MFWT with RPTOOS (HBB) **Exposure range : EOR13-3245 MWd/MT (2944 MWd/ST) to EOC13**					
			Uncorrected ΔCPR		
Event	**Flux (%NBR)**	**Q/A (%NBR)**	**GE14C**	**SVEA-96+**	**Fig.**
FW Controller Failure	364	126	0.24	0.26	45

Operating domain: MELLLA & MFWT with RPTOOS (HBB) **Exposure range : BOC13 to EOR13-3245 MWd/MT (2944 MWd/ST)**					
			Uncorrected ΔCPR		
Event	**Flux (%NBR)**	**Q/A (%NBR)**	**GE14C**	**SVEA-96+**	**Fig.**
FW Controller Failure	205	114	0.23	0.25	46

Operating domain: MELLLA & MFWT with RPTOOS (HBB) **Exposure range : EOR13-3245 MWd/MT (2944 MWd/ST) to EOC13**					
			Uncorrected ΔCPR		
Event	**Flux (%NBR)**	**Q/A (%NBR)**	**GE14C**	**SVEA-96+**	**Fig.**
FW Controller Failure	253	118	0.23	0.26	47

Operating domain: ICF & MFWT with RPTOOS (UB) **Exposure range : EOR13-3245 MWd/MT (2944 MWd/ST) to EOC13**					
			Uncorrected ΔCPR		
Event	**Flux (%NBR)**	**Q/A (%NBR)**	**GE14C**	**SVEA-96+**	**Fig.**
FW Controller Failure	263	119	0.27	0.28	48

Operating domain: MELLLA & MFWT with RPTOOS (UB) Exposure range : EOR13-3245 MWd/MT (2944 MWd/ST) to EOC13					
			Uncorrected ΔCPR		
Event	Flux (%NBR)	Q/A (%NBR)	GE14C	SVEA-96+	Fig.
FW Controller Failure	169	110	0.21	0.23	49

10. Local Rod Withdrawal Error (With Limiting Instrument Failure) AOO Summary

Assuming the worst channel response and 50% availability of the LPRM's yields a ΔCPR of 0.21 for all RBM setpoints including the unblocked response.

11. Cycle MCPR Values [7]

Two loop operation safety limit: 1.06

Single loop operation safety limit: 1.08

ECCS OLMCPR Design Basis: See Section 16 (Initial MCPR)

Non-pressurization events:

Exposure range: BOC13 to EOC13		
	GE14C	SVEA-96+
Loss of Feedwater Heating (110°F)	1.20	1.20
Control Rod Withdrawal Error (unblocked)	1.27	1.27
Fuel Loading Error (mislocated)	1.21	1.21
Fuel Loading Error (misoriented)	1.18	1.28

[7] For single-loop operation, the MCPR operating limit is 0.02 greater than the two-loop value.

Limiting Pressurization Events OLMCPR Summary Table: [8]

Appl. Cond.[9]	Exposure Range	Option A		Option B	
		GE14C	SVEA-96+	GE14C	SVEA-96+
1	**EQUIPMENT IN SERVICE**				
	BOC13 to EOR13-3245 MWd/MT (2944 MWd/ST)	1.45	1.47	1.34	1.36
	EOR13-3245 MWd/MT (2944 MWd/ST) to EOC13	1.56	1.60	1.39	1.43
2	**RPTOOS**				
	BOC13 to EOR13-3245 MWd/MT (2944 MWd/ST)	1.47	1.48	1.36	1.37
	EOR13-3245 MWd/MT (2944 MWd/ST) to EOC13	1.59	1.60	1.42	1.43

Pressurization events: [10]

Operating domain: ICF (HBB)
Exposure range : BOC13 to EOR13-3245 MWd/MT (2944 MWd/ST)
Application condition: 1, 2

	Option A		Option B	
	GE14C	SVEA-96+	GE14C	SVEA-96+
FW Controller Failure	1.42	1.43	1.31	1.32
Turbine Trip w/o Bypass	1.44	1.46	1.33	1.35
Load Reject w/o Bypass	1.44	1.46	1.33	1.35

[8] Each application condition (Appl. Cond.) covers the entire range of licensed flow and feedwater temperature unless specified otherwise. The OLMCPR values presented apply to rated power operation.
[9] One SRV out-of-service allowed.
[10] The application condition number(s) shown for each of the following pressurization events represents the application condition(s) for which this event contributed in the determination of the limiting OLMCPR value.

Operating domain: ICF (HBB) Exposure range : EOR13-3245 MWd/MT (2944 MWd/ST) to EOC13 Application condition: 1, 2				
	Option A		Option B	
	GE14C	SVEA-96+	GE14C	SVEA-96+
FW Controller Failure	1.49	1.53	1.32	1.36
Turbine Trip w/o Bypass	1.52	1.55	1.35	1.38
Load Reject w/o Bypass	1.52	1.55	1.35	1.38

Operating domain: MELLLA (HBB) Exposure range : BOC13 to EOR13-3245 MWd/MT (2944 MWd/ST) Application condition: 1, 2				
	Option A		Option B	
	GE14C	SVEA-96+	GE14C	SVEA-96+
FW Controller Failure	1.40	1.42	1.29	1.31
Load Reject w/o Bypass	1.45	1.47	1.34	1.36
Turbine Trip w/o Bypass	1.45	1.47	1.34	1.36

Operating domain: MELLLA (HBB) Exposure range : EOR13-3245 MWd/MT (2944 MWd/ST) to EOC13 Application condition: 1, 2				
	Option A		Option B	
	GE14C	SVEA-96+	GE14C	SVEA-96+
FW Controller Failure	1.50	1.54	1.33	1.37
Load Reject w/o Bypass	1.55	1.60	1.38	1.43
Turbine Trip w/o Bypass	1.55	1.59	1.38	1.42

Operating domain: ICF (UB) Exposure range : EOR13-3245 MWd/MT (2944 MWd/ST) to EOC13 Application condition: 1, 2				
	Option A		Option B	
	GE14C	SVEA-96+	GE14C	SVEA-96+
FW Controller Failure	1.51	1.53	1.34	1.36
Turbine Trip w/o Bypass	1.56	1.57	1.39	1.40
Load Reject w/o Bypass	1.56	1.57	1.39	1.40

Operating domain: MELLLA (UB) **Exposure range : EOR13-3245 MWd/MT (2944 MWd/ST) to EOC13** **Application condition: 1, 2**				
	Option A		**Option B**	
	GE14C	**SVEA-96+**	**GE14C**	**SVEA-96+**
FW Controller Failure	1.46	1.48	1.29	1.31
Turbine Trip w/o Bypass	1.52	1.54	1.35	1.37
Load Reject w/o Bypass	1.51	1.54	1.34	1.37

Operating domain: ICF & MFWT (HBB) **Exposure range : BOC13 to EOR13-3245 MWd/MT (2944 MWd/ST)** **Application condition: 1, 2**				
	Option A		**Option B**	
	GE14C	**SVEA-96+**	**GE14C**	**SVEA-96+**
FW Controller Failure	1.42	1.44	1.31	1.33

Operating domain: ICF & MFWT (HBB) **Exposure range : EOR13-3245 MWd/MT (2944 MWd/ST) to EOC13** **Application condition: 1, 2**				
	Option A		**Option B**	
	GE14C	**SVEA-96+**	**GE14C**	**SVEA-96+**
FW Controller Failure	1.49	1.53	1.32	1.36

Operating domain: MELLLA & MFWT (HBB) **Exposure range : BOC13 to EOR13-3245 MWd/MT (2944 MWd/ST)** **Application condition: 1, 2**				
	Option A		**Option B**	
	GE14C	**SVEA-96+**	**GE14C**	**SVEA-96+**
FW Controller Failure	1.41	1.43	1.30	1.32

Operating domain: MELLLA & MFWT (HBB) **Exposure range : EOR13-3245 MWd/MT (2944 MWd/ST) to EOC13** **Application condition: 1, 2**				
	Option A		**Option B**	
	GE14C	**SVEA-96+**	**GE14C**	**SVEA-96+**
FW Controller Failure	1.51	1.54	1.34	1.37

Operating domain: ICF & MFWT (UB)
Exposure range : EOR13-3245 MWd/MT (2944 MWd/ST) to EOC13
Application condition: 1, 2

	Option A		Option B	
	GE14C	SVEA-96+	GE14C	SVEA-96+
FW Controller Failure	1.52	1.54	1.35	1.37

Operating domain: MELLLA & MFWT (UB)
Exposure range : EOR13-3245 MWd/MT (2944 MWd/ST) to EOC13
Application condition: 1, 2

	Option A		Option B	
	GE14C	SVEA-96+	GE14C	SVEA-96+
FW Controller Failure	1.47	1.50	1.30	1.33

Operating domain: ICF with RPTOOS (HBB)
Exposure range : BOC13 to EOR13-3245 MWd/MT (2944 MWd/ST)
Application condition: 2

	Option A		Option B	
	GE14C	SVEA-96+	GE14C	SVEA-96+
FW Controller Failure	1.44	1.45	1.33	1.34
Turbine Trip w/o Bypass	1.47	1.48	1.36	1.37
Load Reject w/o Bypass	1.47	1.48	1.36	1.37

Operating domain: ICF with RPTOOS (HBB)
Exposure range : EOR13-3245 MWd/MT (2944 MWd/ST) to EOC13
Application condition: 2

	Option A		Option B	
	GE14C	SVEA-96+	GE14C	SVEA-96+
FW Controller Failure	1.52	1.55	1.35	1.38
Turbine Trip w/o Bypass	1.55	1.58	1.38	1.41
Load Reject w/o Bypass	1.55	1.57	1.38	1.40

Operating domain: MELLLA with RPTOOS (HBB) Exposure range : BOC13 to EOR13-3245 MWd/MT (2944 MWd/ST) Application condition: 2				
	Option A		Option B	
	GE14C	SVEA-96+	GE14C	SVEA-96+
FW Controller Failure	1.41	1.43	1.30	1.32
Load Reject w/o Bypass	1.46	1.48	1.35	1.37
Turbine Trip w/o Bypass	1.46	1.48	1.35	1.37

Operating domain: MELLLA with RPTOOS (HBB) Exposure range : EOR13-3245 MWd/MT (2944 MWd/ST) to EOC13 Application condition: 2				
	Option A		Option B	
	GE14C	SVEA-96+	GE14C	SVEA-96+
FW Controller Failure	1.51	1.55	1.34	1.38
Load Reject w/o Bypass	1.56	1.60	1.39	1.43
Turbine Trip w/o Bypass	1.55	1.59	1.38	1.42

Operating domain: ICF with RPTOOS (UB) Exposure range : EOR13-3245 MWd/MT (2944 MWd/ST) to EOC13 Application condition: 2				
	Option A		Option B	
	GE14C	SVEA-96+	GE14C	SVEA-96+
FW Controller Failure	1.55	1.56	1.38	1.39
Load Reject w/o Bypass	1.59	1.60	1.42	1.43
Turbine Trip w/o Bypass	1.59	1.60	1.42	1.43

Operating domain: MELLLA with RPTOOS (UB) Exposure range : EOR13-3245 MWd/MT (2944 MWd/ST) to EOC13 Application condition: 2				
	Option A		Option B	
	GE14C	SVEA-96+	GE14C	SVEA-96+
FW Controller Failure	1.48	1.49	1.31	1.32
Load Reject w/o Bypass	1.54	1.56	1.37	1.39
Turbine Trip w/o Bypass	1.54	1.55	1.37	1.38

Operating domain: ICF & MFWT with RPTOOS (HBB) Exposure range : BOC13 to EOR13-3245 MWd/MT (2944 MWd/ST) Application condition: 2				
	Option A		Option B	
	GE14C	SVEA-96+	GE14C	SVEA-96+
FW Controller Failure	1.44	1.46	1.33	1.35

Operating domain: ICF & MFWT with RPTOOS (HBB) Exposure range : EOR13-3245 MWd/MT (2944 MWd/ST) to EOC13 Application condition: 2				
	Option A		Option B	
	GE14C	SVEA-96+	GE14C	SVEA-96+
FW Controller Failure	1.52	1.55	1.35	1.38

Operating domain: MELLLA & MFWT with RPTOOS (HBB) Exposure range : BOC13 to EOR13-3245 MWd/MT (2944 MWd/ST) Application condition: 2				
	Option A		Option B	
	GE14C	SVEA-96+	GE14C	SVEA-96+
FW Controller Failure	1.41	1.44	1.30	1.33

Operating domain: MELLLA & MFWT with RPTOOS (HBB) Exposure range : EOR13-3245 MWd/MT (2944 MWd/ST) to EOC13 Application condition: 2				
	Option A		Option B	
	GE14C	SVEA-96+	GE14C	SVEA-96+
FW Controller Failure	1.51	1.55	1.34	1.38

Operating domain: ICF & MFWT with RPTOOS (UB) Exposure range : EOR13-3245 MWd/MT (2944 MWd/ST) to EOC13 Application condition: 2				
	Option A		Option B	
	GE14C	SVEA-96+	GE14C	SVEA-96+
FW Controller Failure	1.55	1.57	1.38	1.40

Operating domain: MELLLA & MFWT with RPTOOS (UB) **Exposure range : EOR13-3245 MWd/MT (2944 MWd/ST) to EOC13** **Application condition: 2**				
	Option A		**Option B**	
	GE14C	**SVEA-96+**	**GE14C**	**SVEA-96+**
FW Controller Failure	1.49	1.51	1.32	1.34

12. Overpressurization Analysis Summary

Event	**Psl (psig)**	**Pdome (psig)**	**Pv (psig)**	**Plant Response**
MSIV Closure (Flux Scram)	1244	1246	1265	Figure 50

13. Loading Error Results

Variable water gap misoriented bundle analysis: Yes [11]

Misoriented Fuel Bundle	**ΔCPR**
GE14-P10CNAB402-4G6.0/16G4.0-100T-150-T6-2757 (GE14C)	0.08
GE14-P10CNAB402-5G6.0/14G4.0-100T-150-T6-2758 (GE14C)	0.12
SVEA96-P10CASB326-11GZ-568U-4WR-150-T6-2654	0.17
SVEA96-P10CASB326-11G4.5-568U-4WR-150-T6-2655	0.17
SVEA96-P10CASB360-12GZ-568U-4WR-150-T6-2656	0.20
SVEA96-P10CASB360-12G5.0-568U-4WR-150-T6-2657	0.20
SVEA96-P10CASB361-14GZ-568U-4WR-150-T6-2658	0.22
SVEA96-P10CASB360-12G5.5/2G2.5-568U-4WR-150-T6-2659	0.21

14. Control Rod Drop Analysis Results

Banked Position Withdrawal Sequence is utilized at Hope Creek Generating Station Unit 1; therefore, the control rod drop accident analysis is not required. NRC approval is documented in NEDE-24011-P-A-US.

[11] Includes a 0.02 penalty due to variable water gap R-factor uncertainty.

15. Stability Analysis Results

GE SIL-380 recommendations, BWROG Interim Corrective Actions (Reference 15.1) and Backup Stability Protection for Inoperable Option III Solution (Reference 15.2) have been included in the Hope Creek Cycle 13 operating procedures. Regions of restricted operation defined in Attachment 1 to NRC Bulletin No 88-07, Supplement 1, *Power Oscillations in Boiling Water Reactors (BWRs)* and expanded in BWROG-94079 (Reference 15.1) and Backup Stability Protection for Inoperable Option III Solution (Reference 15.2) are used for Hope Creek Cycle 13 backup stability protection evaluation (Reference 15.3). The standard ICA stability regions are expanded as appropriate to offer stability protection per BWROG-02072 (Reference 15.4) and OG 02-0119-260 (Reference 15.2) for Hope Creek Cycle 13 ELLLA operation.

The Hope Creek Cycle 13 stability analyses discussed above are applicable to the ELLLA operation domain as specified in Reference 15.3 Additional analysis would be required to support operation in the expanded MELLLA operating domain.

References:

15.1. BWROG-94079, *BWR Owner's Group Guidelines for Stability Interim Corrective Action*, June 1994.

15.2. OG 02-0119-260, GE to BWR Owners' Group Detect and Suppress II Committee, *Backup Stability Protection (BSP) for Inoperable Option III Solution*, July 17, 2002.

15.3. GENE-0000-0029-6193-01-R1, *Backup Stability Protection Evaluation for Hope Creek Cycle 13*, November 2004.

15.4. BWROG-02072, *Review of BWR Owners' Group Guidelines for Stability Interim Corrective Action*, November 20, 2002.

16. Loss-of-Coolant Accident Results

16.1 10CFR50.46 Licensing Results

The ECCS-LOCA analysis is based on the SAFER/GESTR-LOCA methodology. The licensing results applicable to each fuel type in the new cycle are summarized in the following table:

Table 16.1-1 Licensing Results

Fuel Type	Licensing Basis PCT (°F)	Local Oxidation (%)	Core-Wide Metal-Water Reaction (%)
SVEA-96+	1540	< 1.00	< 0.10
GE14C	1370	< 1.00	< 0.10

The SAFER/GESTR-LOCA analysis results for GE14C fuel and SVEA-96+ fuel are documented in Section 5 of Reference 16.4.1.

16.2 10CFR50.46 Error Evaluation

The 10CFR50.46 errors applicable to the Licensing Basis PCT are shown in the table below.

Table 16.2 Impact on Licensing Basis Peak Cladding Temperature for GE14C and SVEA-96+

10CFR50.46 Error Notifications		
Number	**Subject**	**PCT Impact (°F)**
2003-05	Impact of Postulated Hydrogen-Oxygen Recombination on PCT	0
	Total PCT Adder (°F)	0

The GE14C and SVEA-96+ Licensing Basis PCT remain below the 10CFR50.46 limit of 2200°F.

16.3 ECCS-LOCA Operating Limits

The ECCS MAPLHGR operating limits for all fuel bundles in this cycle are shown in the tables below.

Table 16.3-1 MAPLHGR Limits for GE14C

Bundle Types: GE14-P10CNAB402-4G6.0/16G4.0-100T-150-T6-2757 (GE14C)
GE14-P10CNAB402-5G6.0/14G4.0-100T-150-T6-2758 (GE14C)

Average Planar Exposure		MAPLHGR Limit
GWd/MT	GWd/ST	kW/ft
0.00	0.00	12.82
21.09	19.13	12.82
63.50	57.61	8.00
70.00	63.50	5.00

Table 16.3-2 MAPLHGR Limits for SVEA-96+

Bundle Types: SVEA96-P10CASB326-11GZ-568U-4WR-150-T6-2654 (SVEA-96+)
SVEA96-P10CASB326-11G4.5-568U-4WR-150-T6-2655 (SVEA-96+)
SVEA96-P10CASB360-12GZ-568U-4WR-150-T6-2656 (SVEA-96+)
SVEA96-P10CASB360-12G5.0-568U-4WR-150-T6-2657 (SVEA-96+)
SVEA96-P10CASB361-14GZ-568U-4WR-150-T6-2658 (SVEA-96+)
SVEA96-P10CASB360-12G5.5/2G2.5-568U-4WR-150-T6-2659 (SVEA-96+)

Average Planar Exposure		MAPLHGR Limit
GWd/MT	GWd/ST	kW/ft
0.00	0.00	12.85
3.68	3.34	12.85
16.00	14.51	10.97
65.00	58.97	7.24

The single loop operation multiplier on LHGR and MAPLHGR, and the ECCS Initial MCPR values applicable to each fuel type in the new cycle core are shown in the table below.

Table 16.3-3 Initial MCPR and Single Loop Operation PLHGR and MAPLHGR Multiplier

Fuel Type	Initial MCPR	Single Loop Operation PLHGR and MAPLHGR Multiplier
SVEA-96+	1.250	0.80
GE14C	1.250	0.80

16.4 References

The SAFER/GESTR-LOCA analysis base report applicable to the new cycle core is listed below.

16.4.1. NEDC-33153P, *SAFER/GESTR-LOCA ECCS-LOCA Loss of Coolant Accident Analysis for Hope Creek Generation Station*, Revision 1, September 2004.

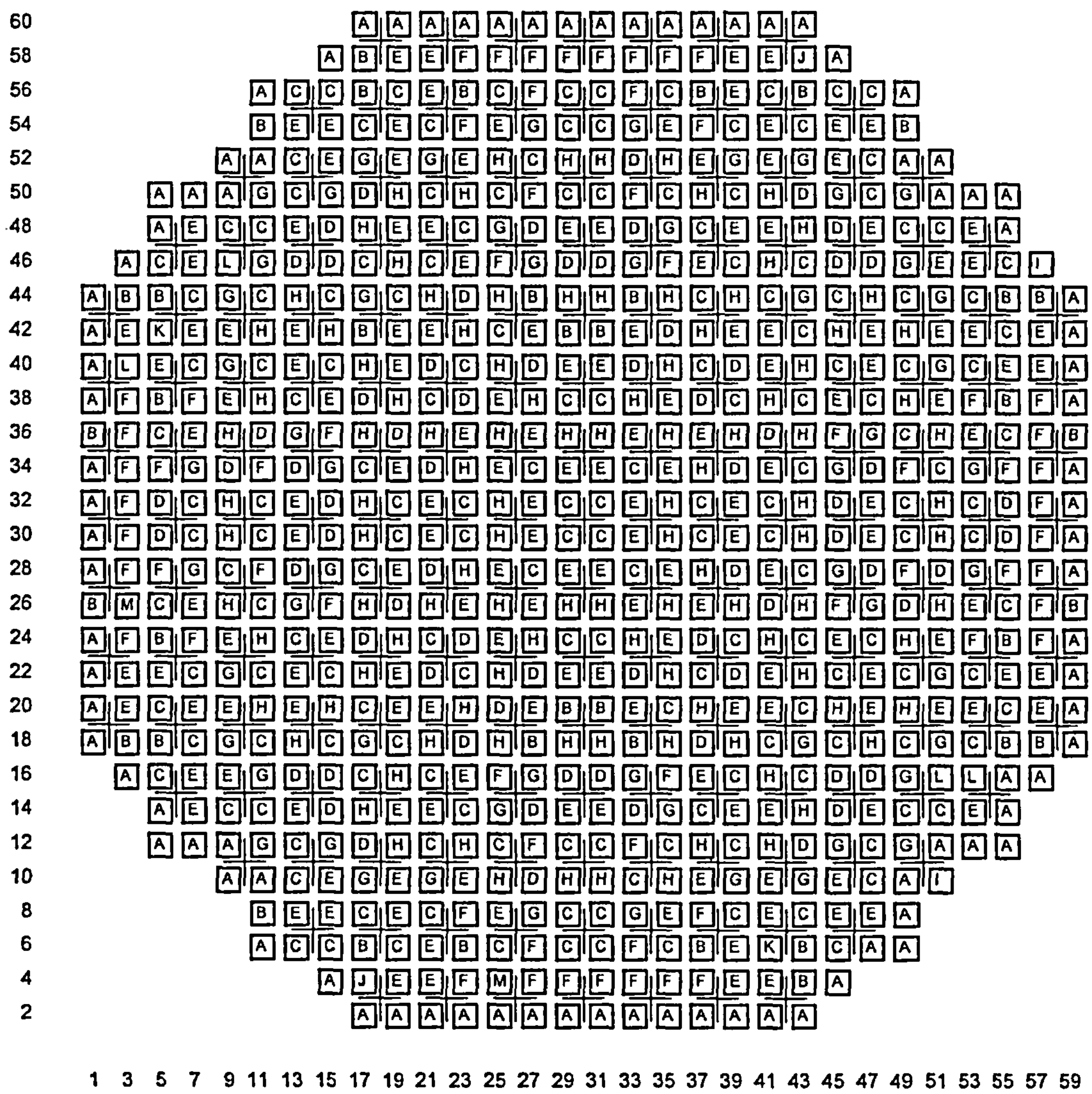

Fuel Type	
A=SVEA96-P10CASB326-11GZ-568U-4WR-150-T6-2654 (C10)	H=GE14-P10CNAB402-5G6.0/14G4.0-100T-150-T6-2758 (C13)
B=SVEA96-P10CASB326-11G4.5-568U-4WR-150-T6-2655 (C10)	I=SVEA96-P10CASB326-11GZ-568U-4WR-150-T6-2654 (C10)
C=SVEA96-P10CASB360-12GZ-568U-4WR-150-T6-2656 (C11)	J=SVEA96-P10CASB326-11G4.5-568U-4WR-150-T6-2655 (C10)
D=SVEA96-P10CASB360-12G5.0-568U-4WR-150-T6-2657 (C11)	K=SVEA96-P10CASB360-12G5.0-568U-4WR-150-T6-2657 (C11)
E=SVEA96-P10CASB361-14GZ-568U-4WR-150-T6-2658 (C12)	L=SVEA96-P10CASB361-14GZ-568U-4WR-150-T6-2658 (C12)
F=SVEA96-P10CASB360-12G5.5/2G2.5-568U-4WR-150-T6-2659 (C12)	M=SVEA96-P10CASB360-12G5.5/2G2.5-568U-4WR-150-T6-2659 (C12)
G=GE14-P10CNAB402-4G6.0/16G4.0-100T-150-T6-2757 (C13)	

Figure 1 Reference Core Loading Pattern

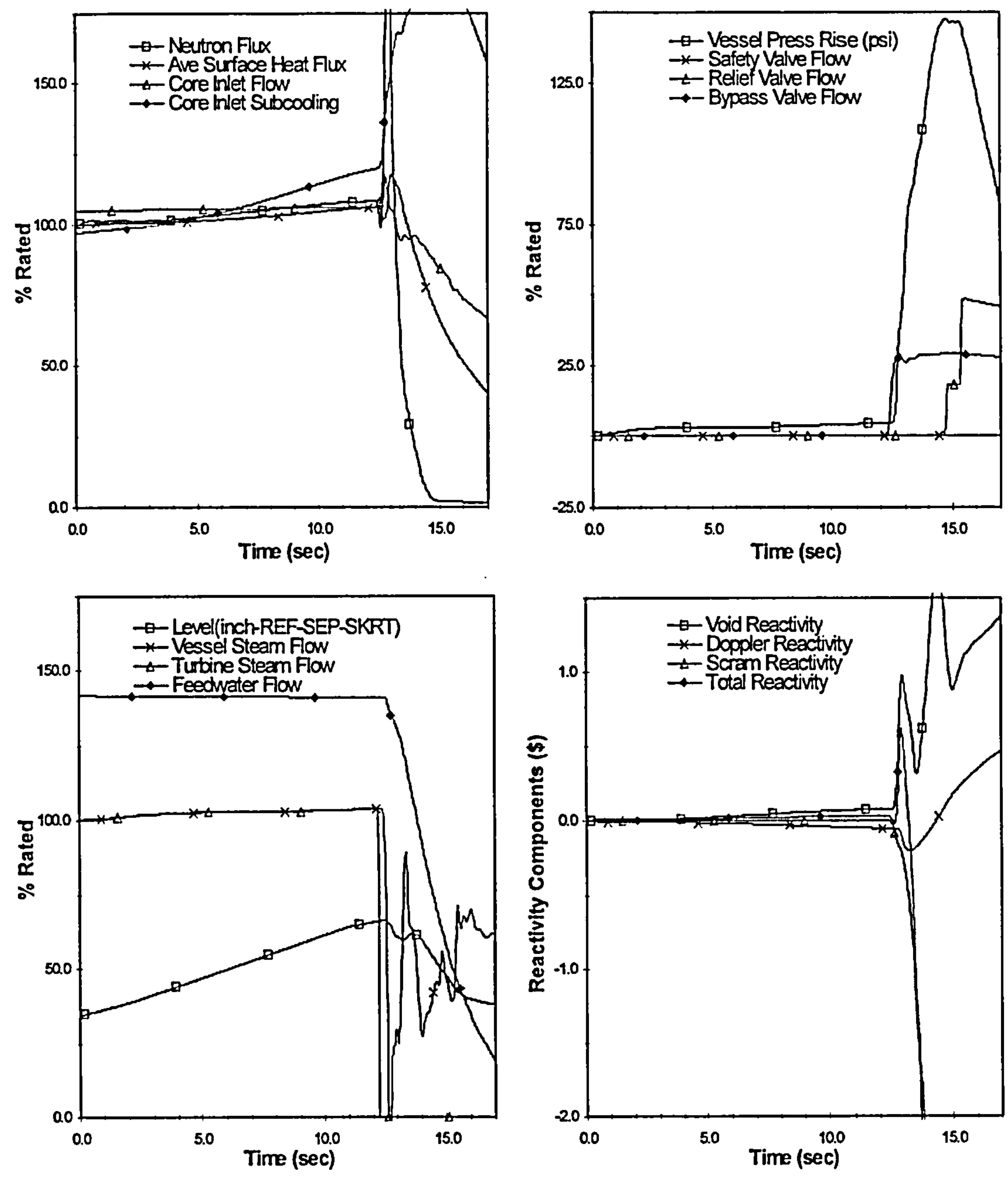

Figure 2 Plant Response to FW Controller Failure
(BOC13 to EOR13-3245 MWd/MT (2944 MWd/ST) ICF (HBB))

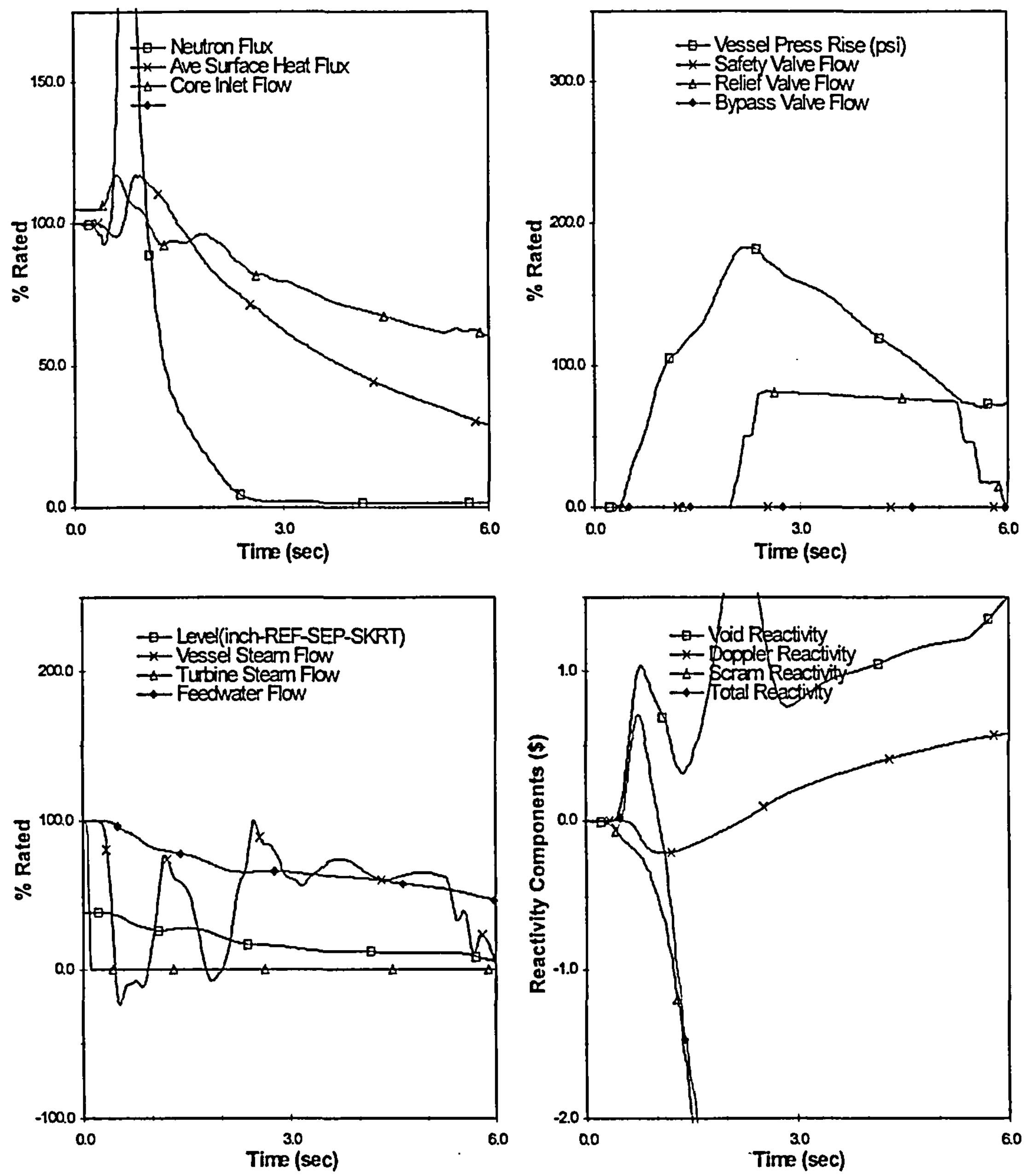

Figure 3 Plant Response to Turbine Trip w/o Bypass (BOC13 to EOR13-3245 MWd/MT (2944 MWd/ST) ICF (HBB))

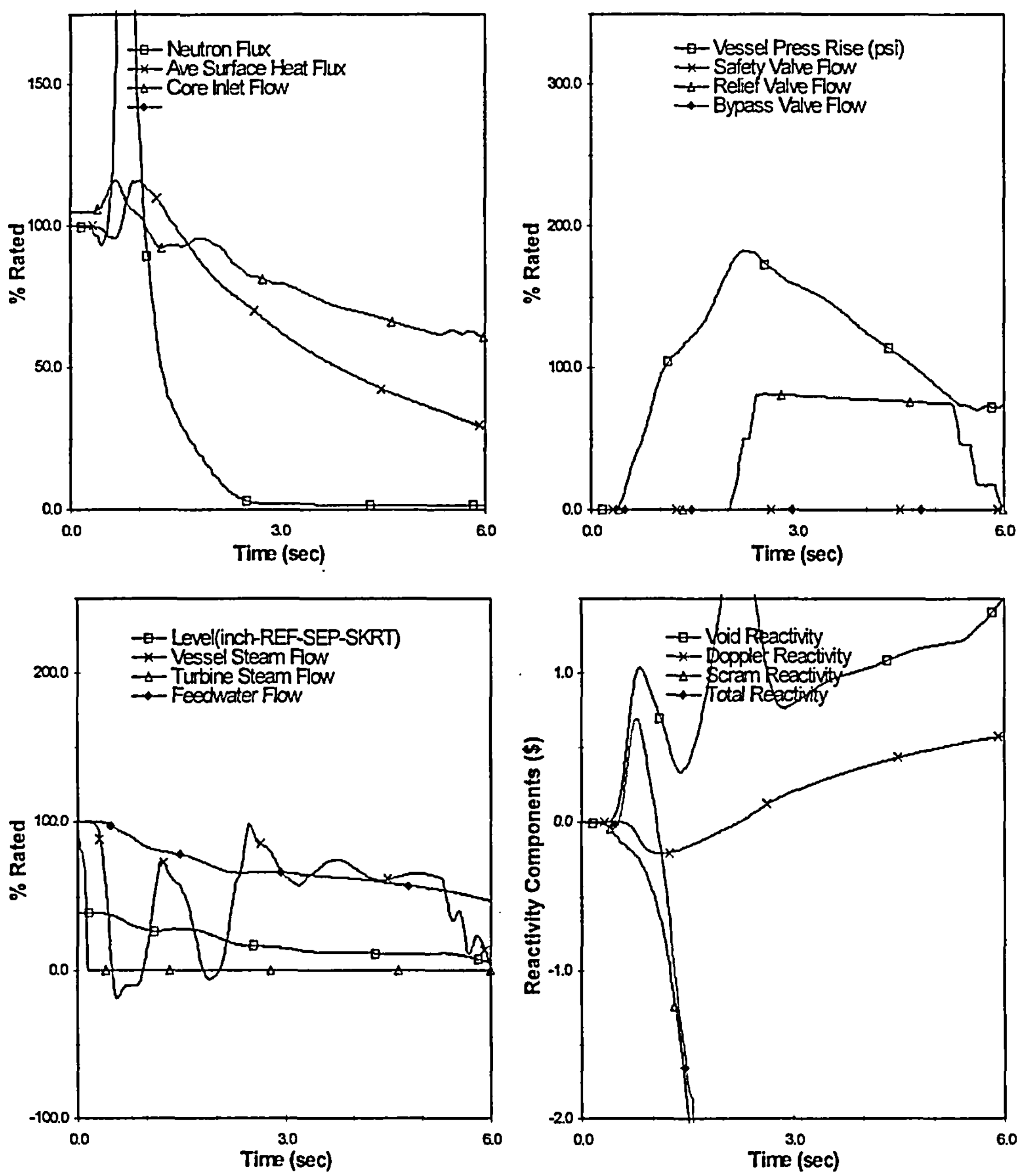

Figure 4 Plant Response to Load Reject w/o Bypass (BOC13 to EOR13-3245 MWd/MT (2944 MWd/ST) ICF (HBB))

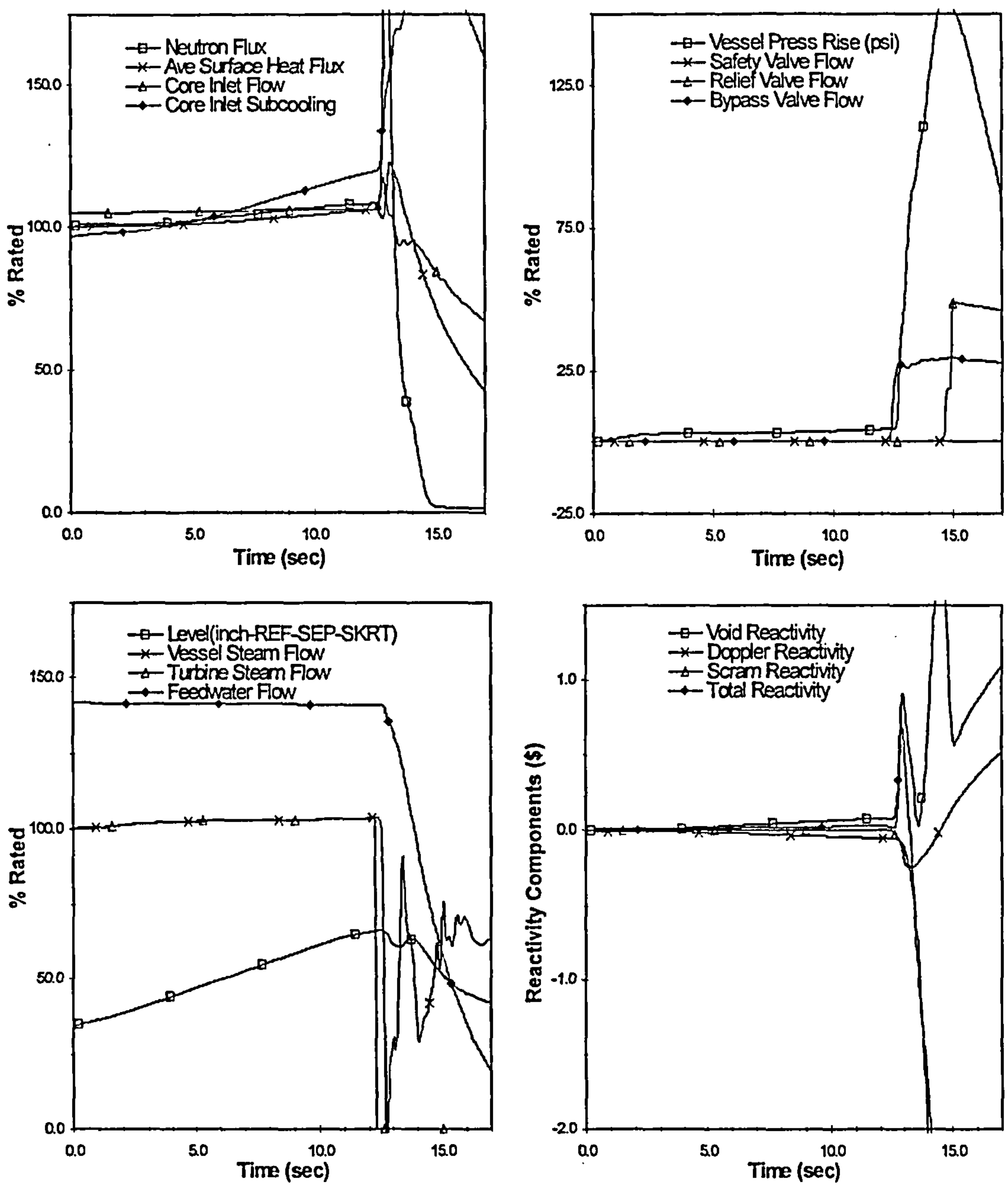

Figure 5 Plant Response to FW Controller Failure
(EOR13-3245 MWd/MT (2944 MWd/ST) to EOC13 ICF (HBB))

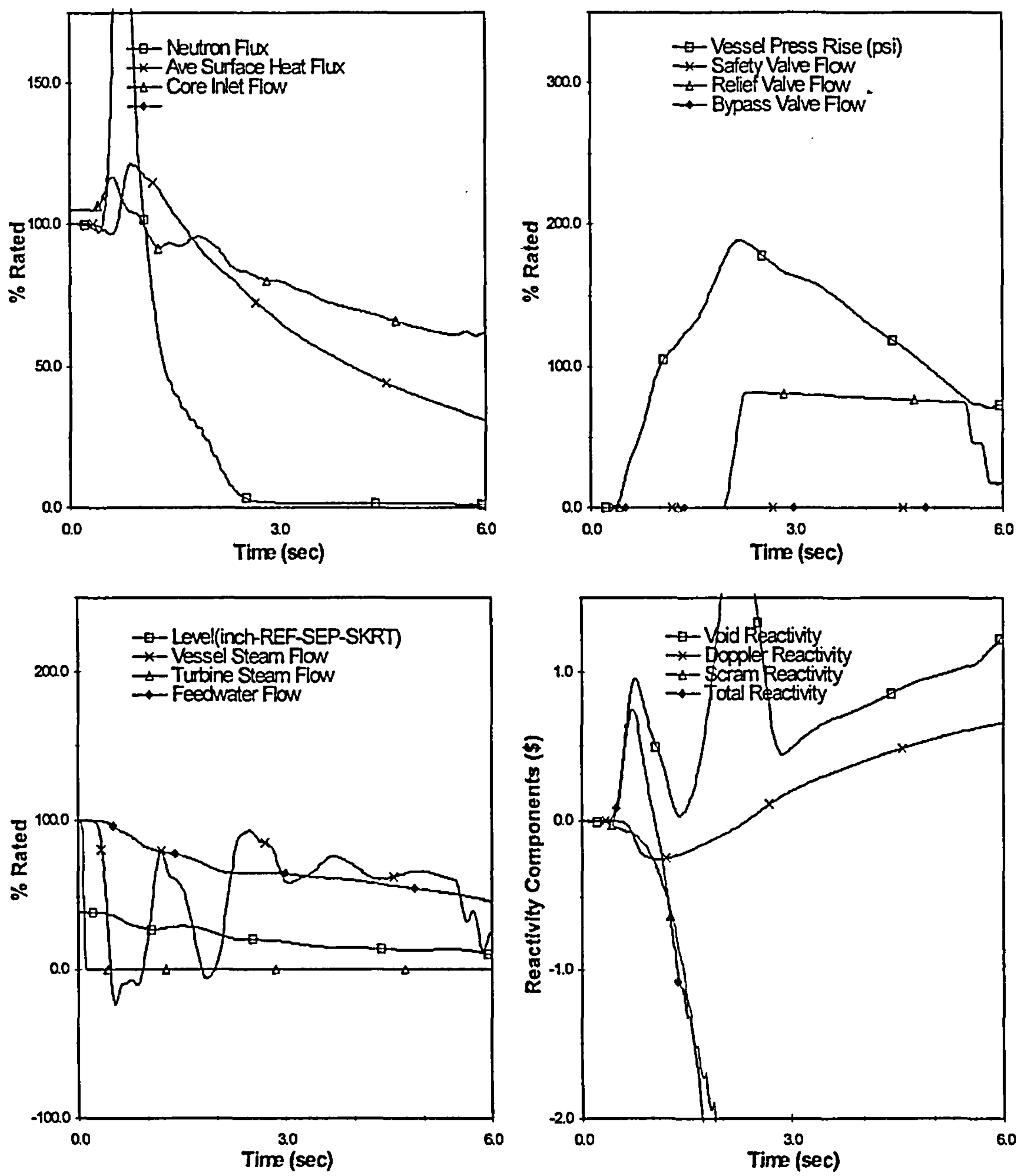

Figure 6 Plant Response to Turbine Trip w/o Bypass (EOR13-3245 MWd/MT (2944 MWd/ST) to EOC13 ICF (HBB))

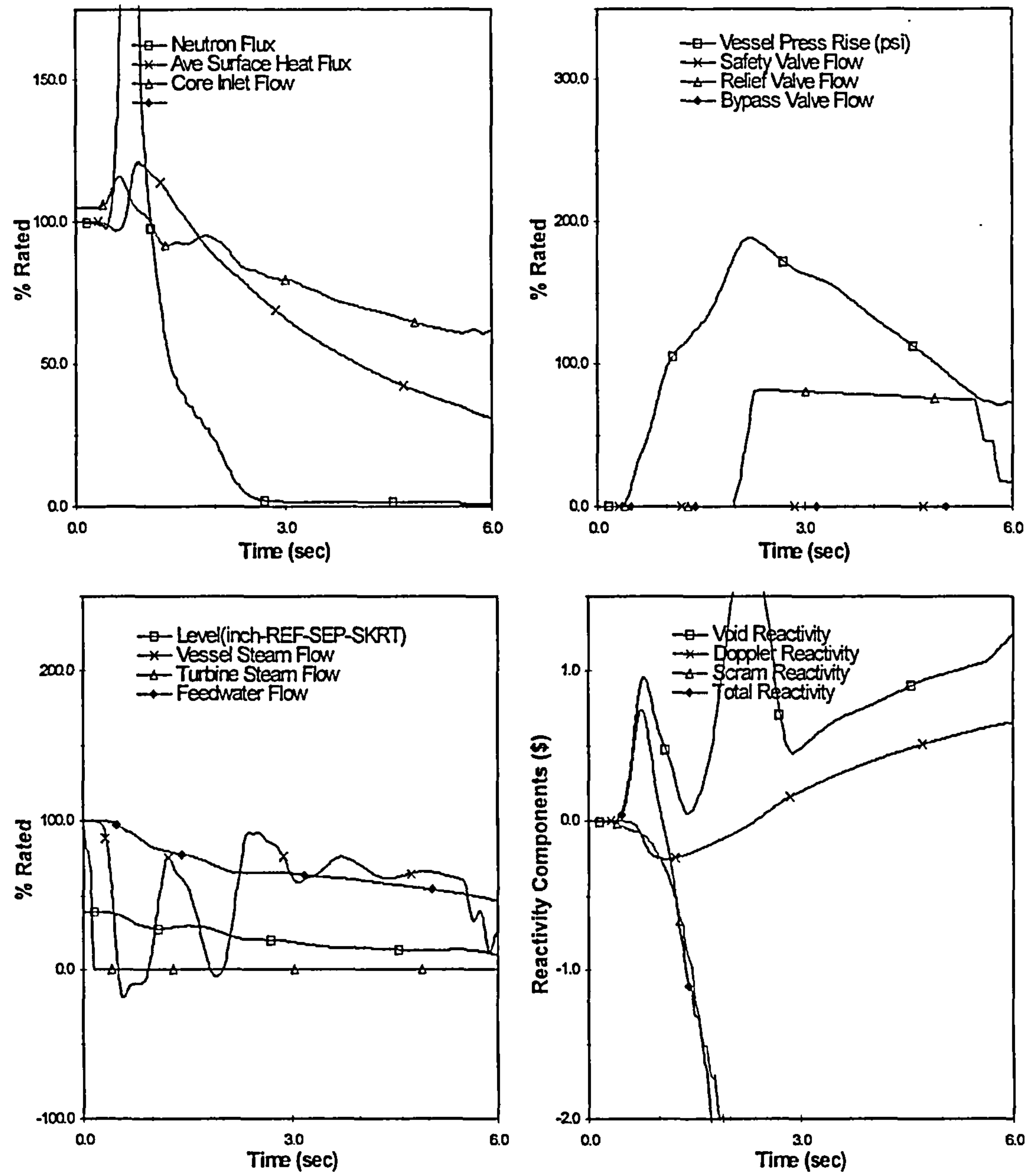

Figure 7 Plant Response to Load Reject w/o Bypass (EOR13-3245 MWd/MT (2944 MWd/ST) to EOC13 ICF (HBB))

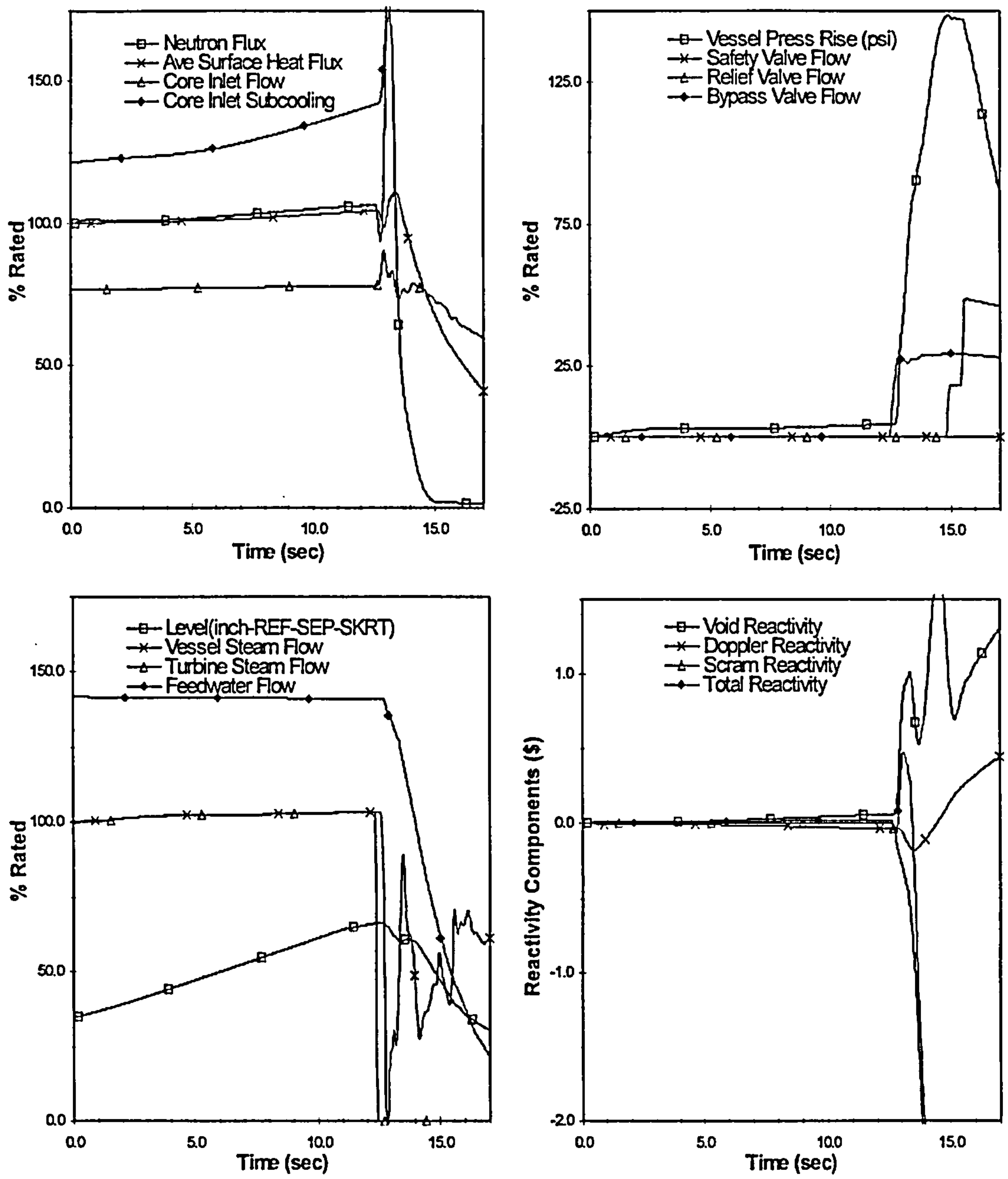

Figure 8 Plant Response to FW Controller Failure (BOC13 to EOR13-3245 MWd/MT (2944 MWd/ST) MELLLA (HBB))

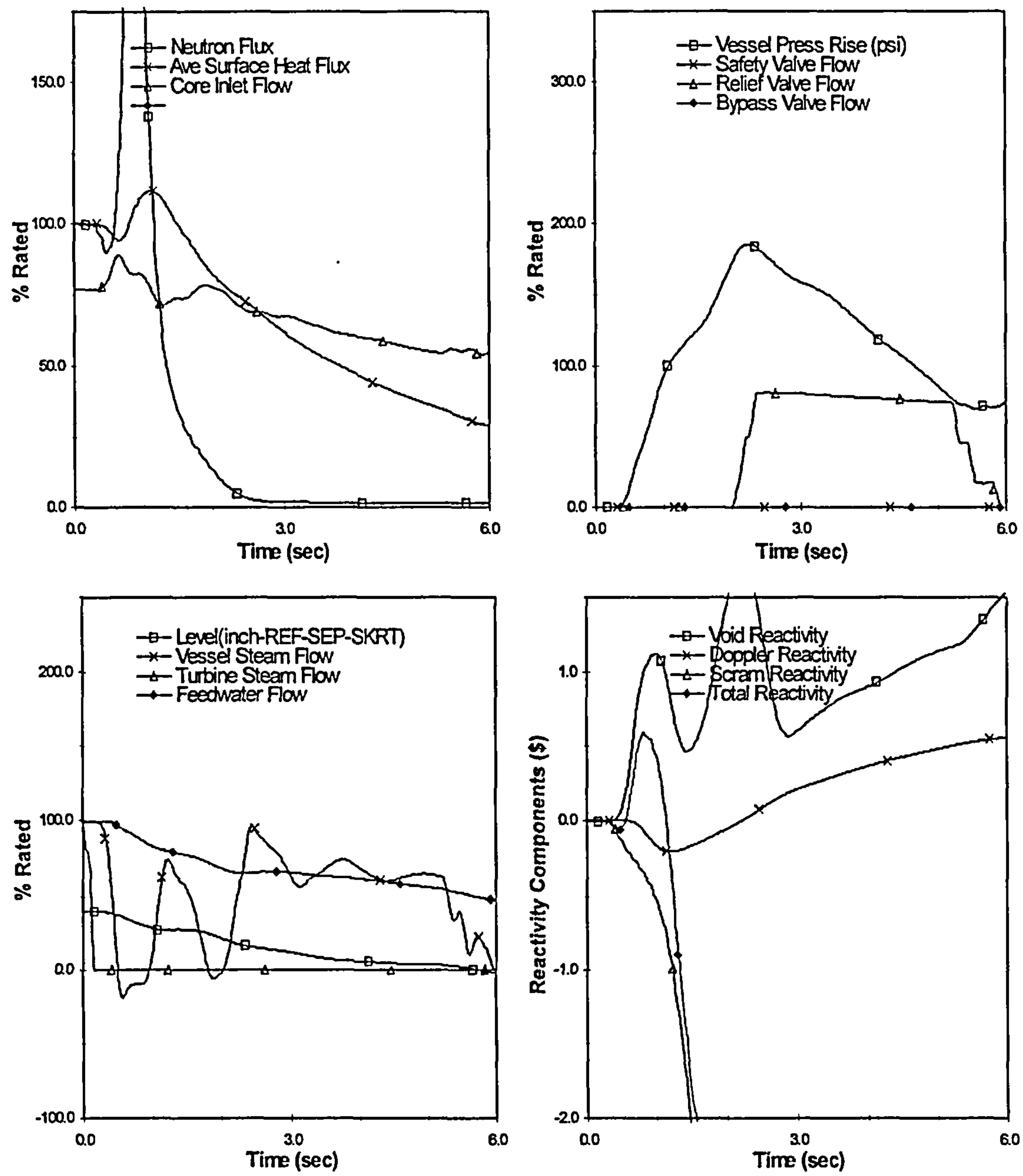

Figure 9 Plant Response to Load Reject w/o Bypass (BOC13 to EOR13-3245 MWd/MT (2944 MWd/ST) MELLLA (HBB))

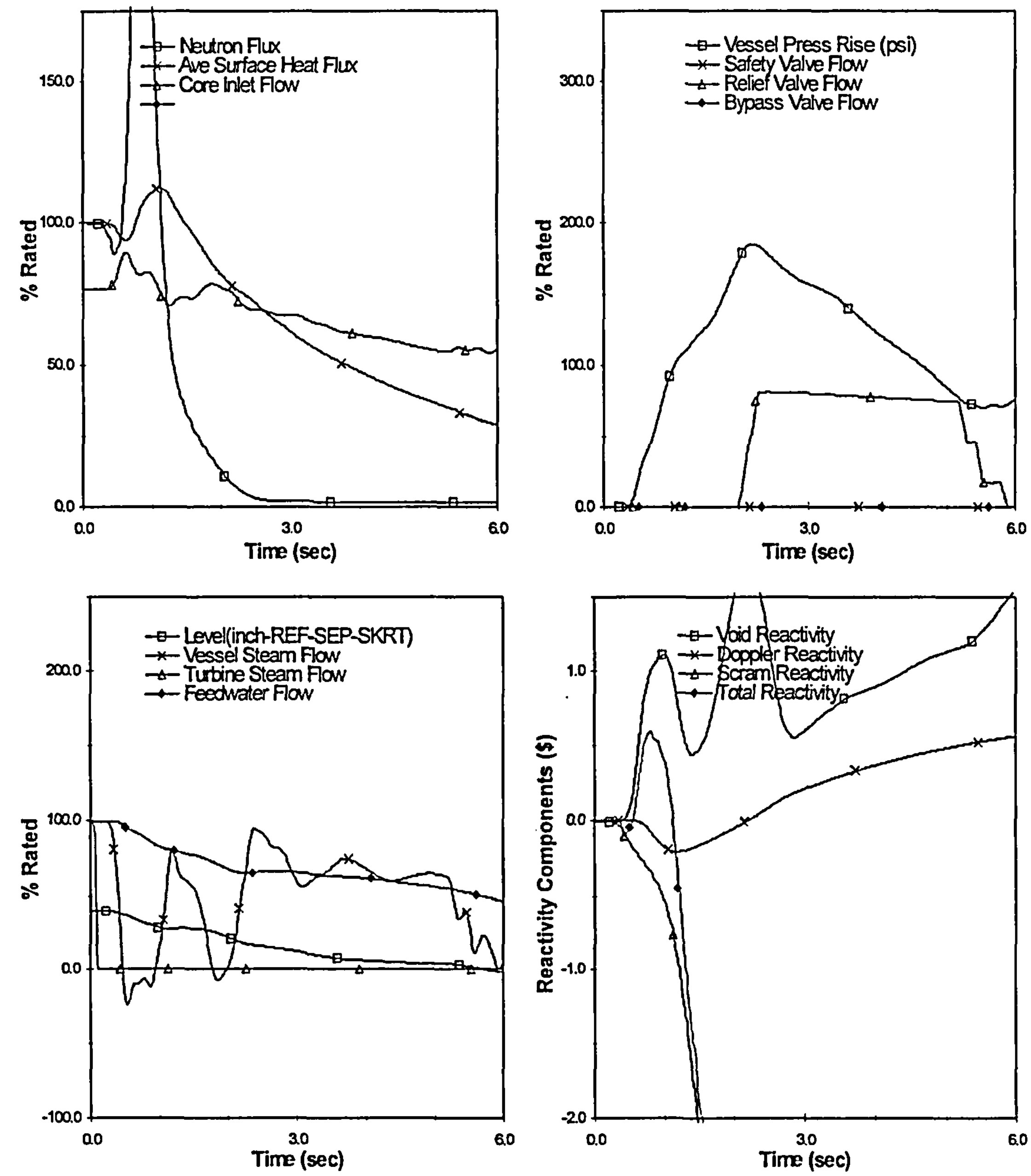

Figure 10 Plant Response to Turbine Trip w/o Bypass (BOC13 to EOR13-3245 MWd/MT (2944 MWd/ST) MELLLA (HBB))

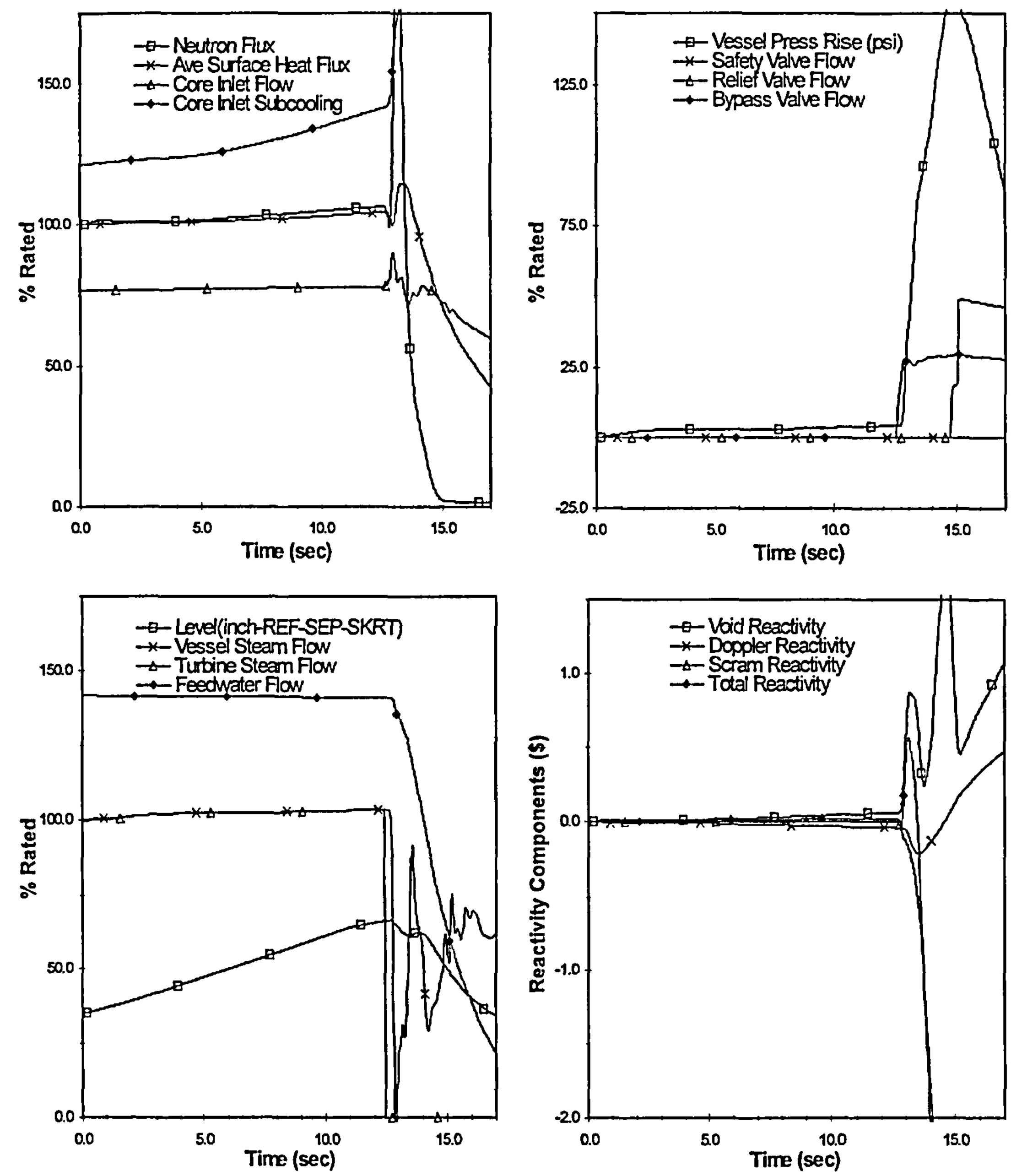

Figure 11 Plant Response to FW Controller Failure (EOR13-3245 MWd/MT (2944 MWd/ST) to EOC13 MELLLA (HBB))

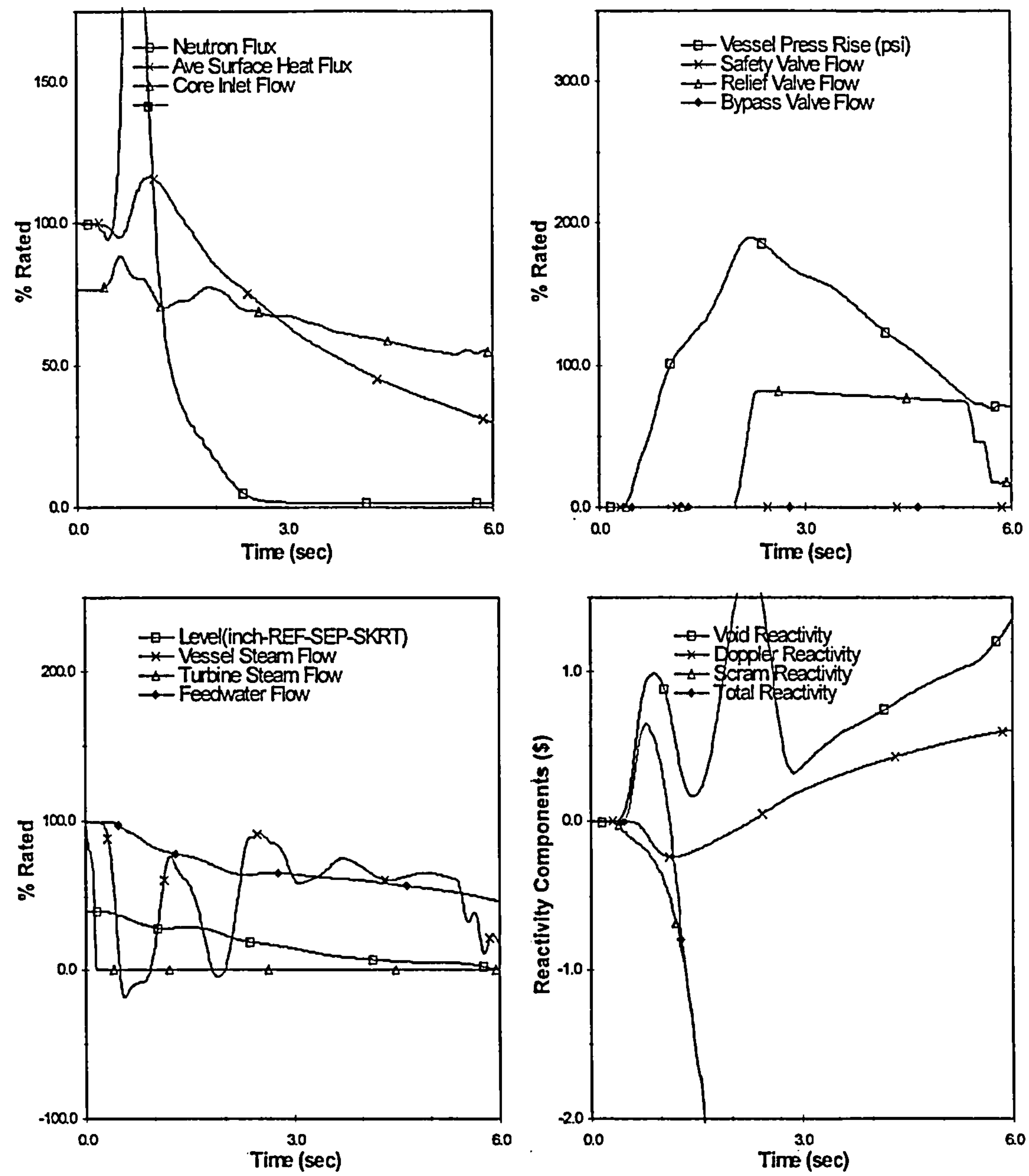

Figure 12 Plant Response to Load Reject w/o Bypass (EOR13-3245 MWd/MT (2944 MWd/ST) to EOC13 MELLLA (HBB))

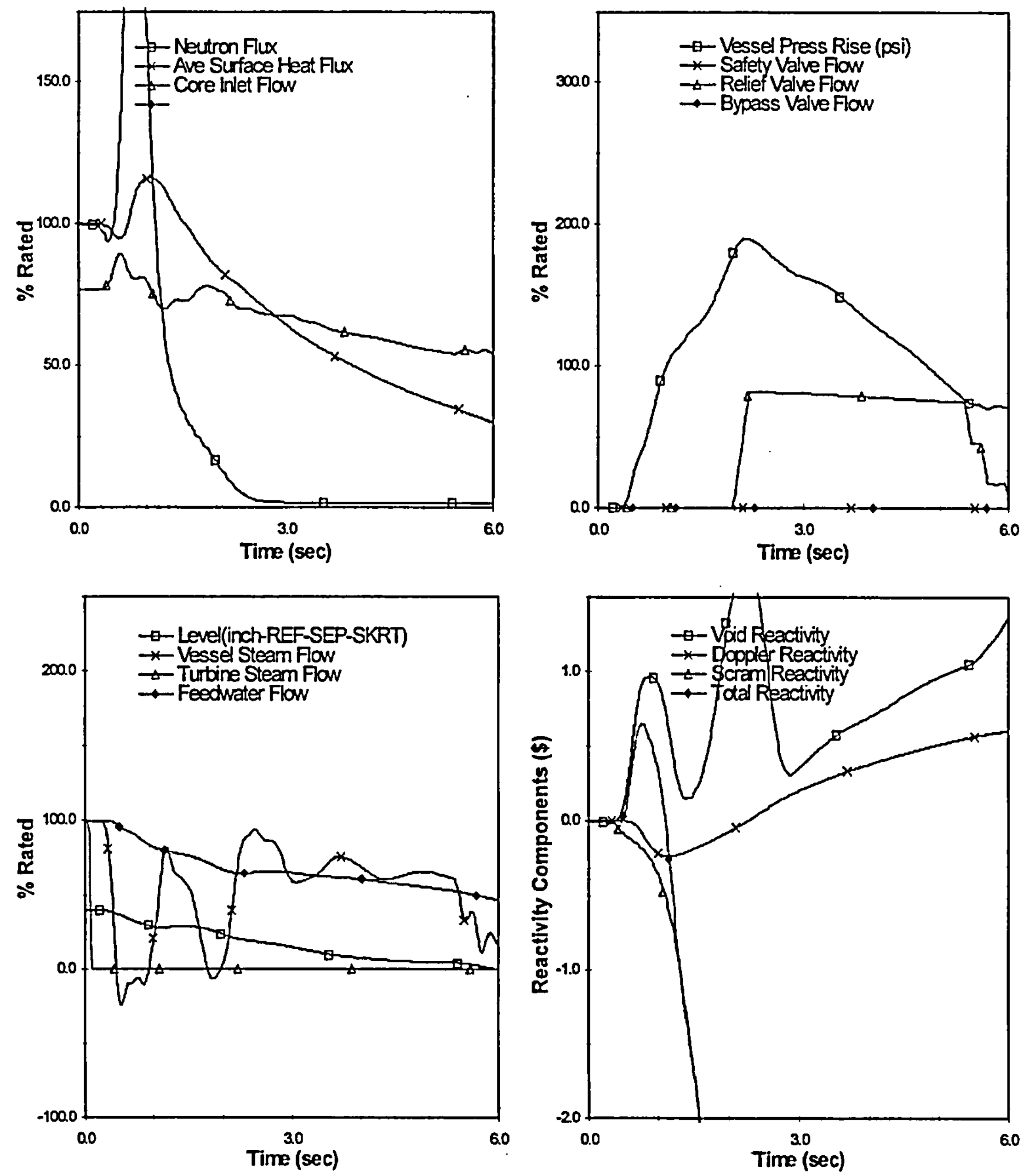

Figure 13 Plant Response to Turbine Trip w/o Bypass (EOR13-3245 MWd/MT (2944 MWd/ST) to EOC13 MELLLA (HBB))

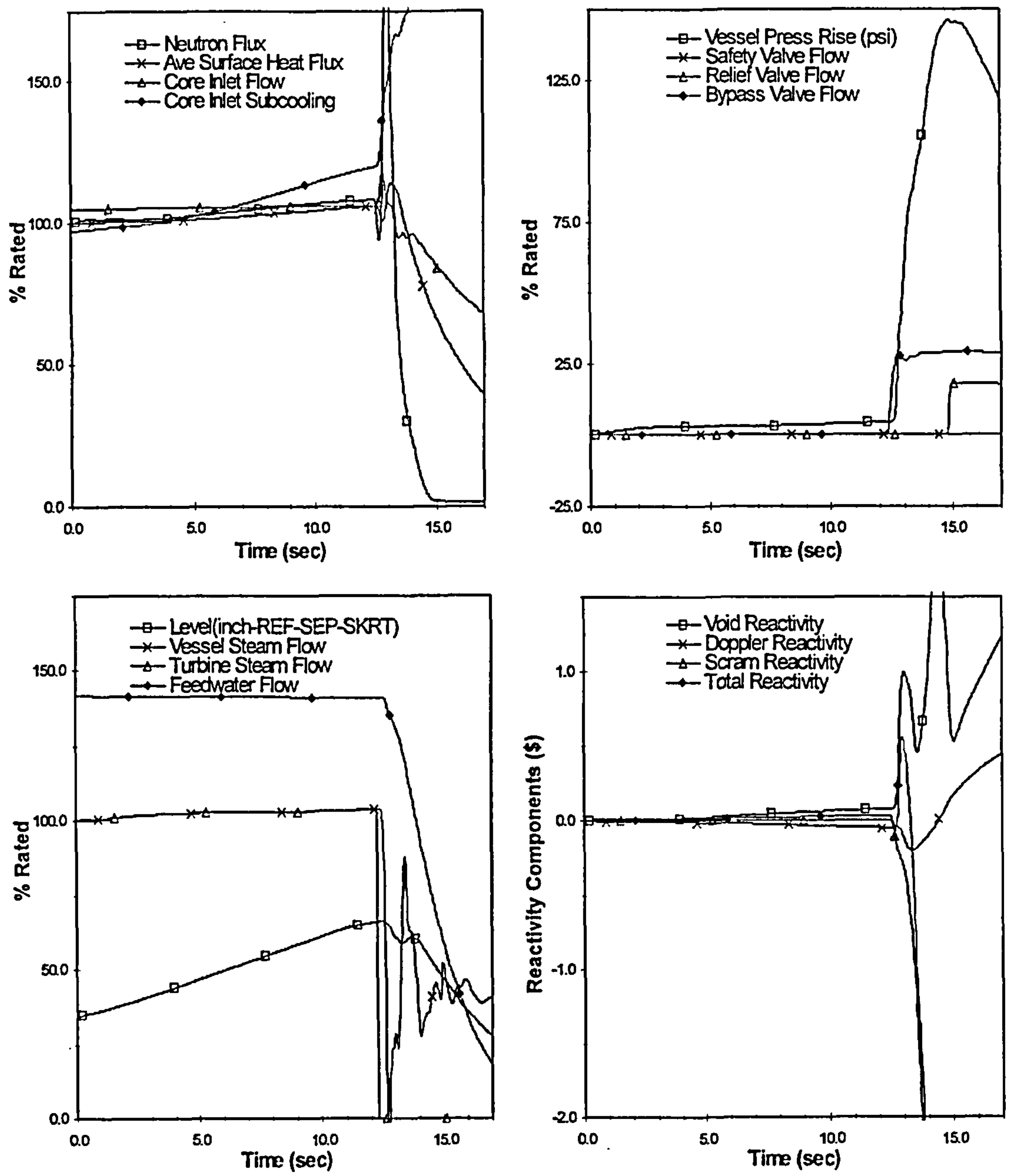

Figure 14 Plant Response to FW Controller Failure (EOR13-3245 MWd/MT (2944 MWd/ST) to EOC13 ICF (UB))

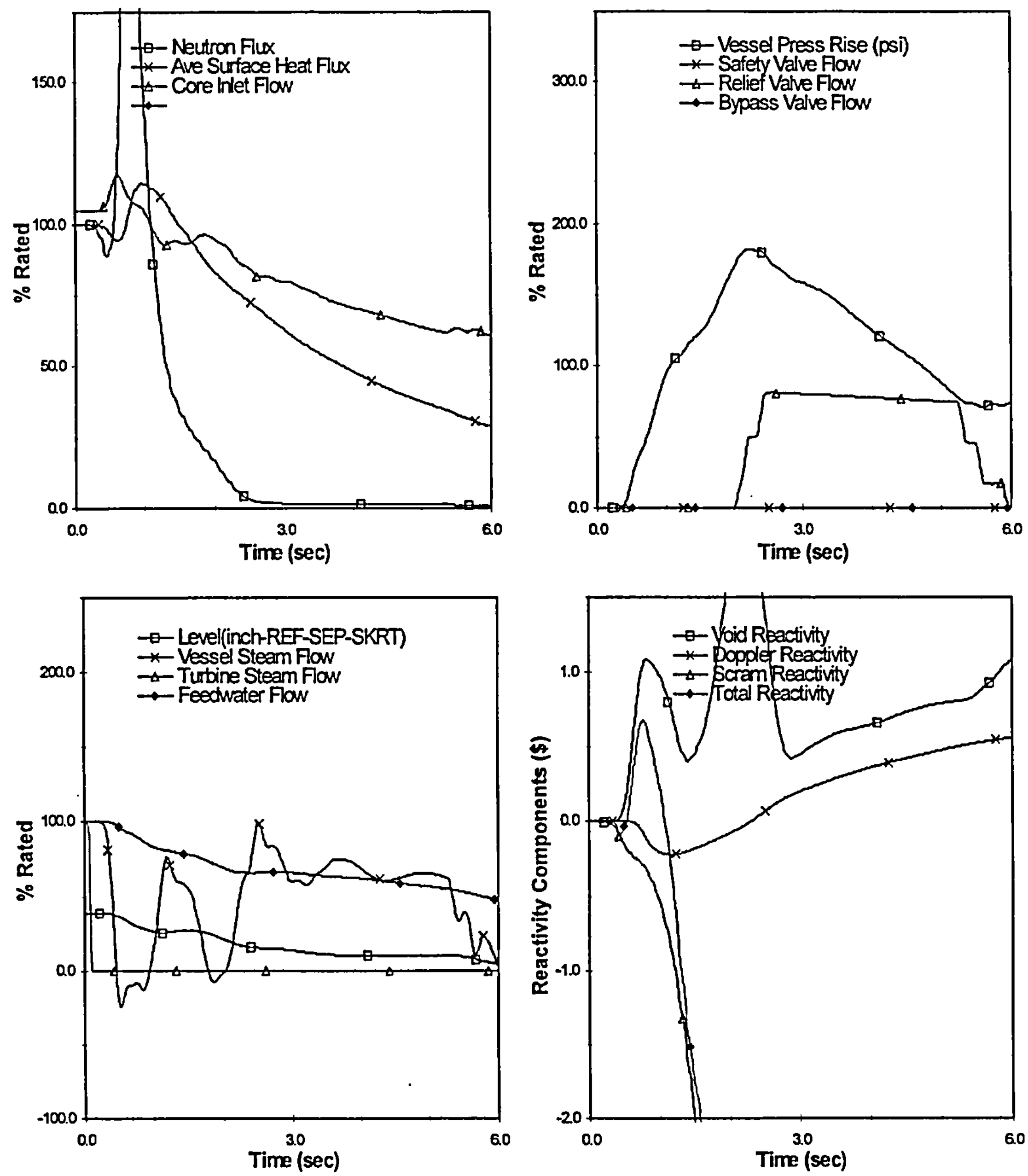

Figure 15 Plant Response to Turbine Trip w/o Bypass (EOR13-3245 MWd/MT (2944 MWd/ST) to EOC13 ICF (UB))

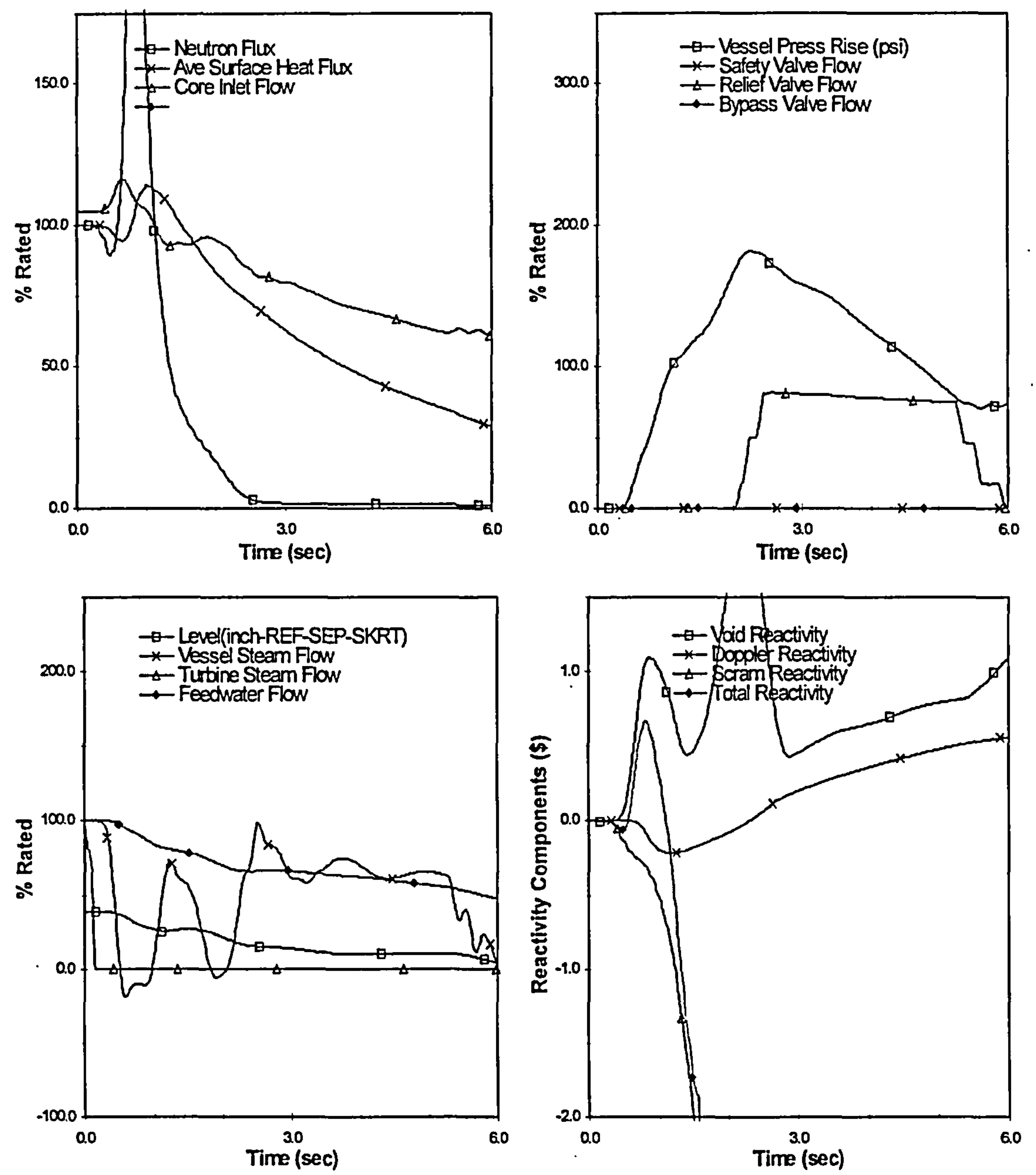

Figure 16 Plant Response to Load Reject w/o Bypass (EOR13-3245 MWd/MT (2944 MWd/ST) to EOC13 ICF (UB))

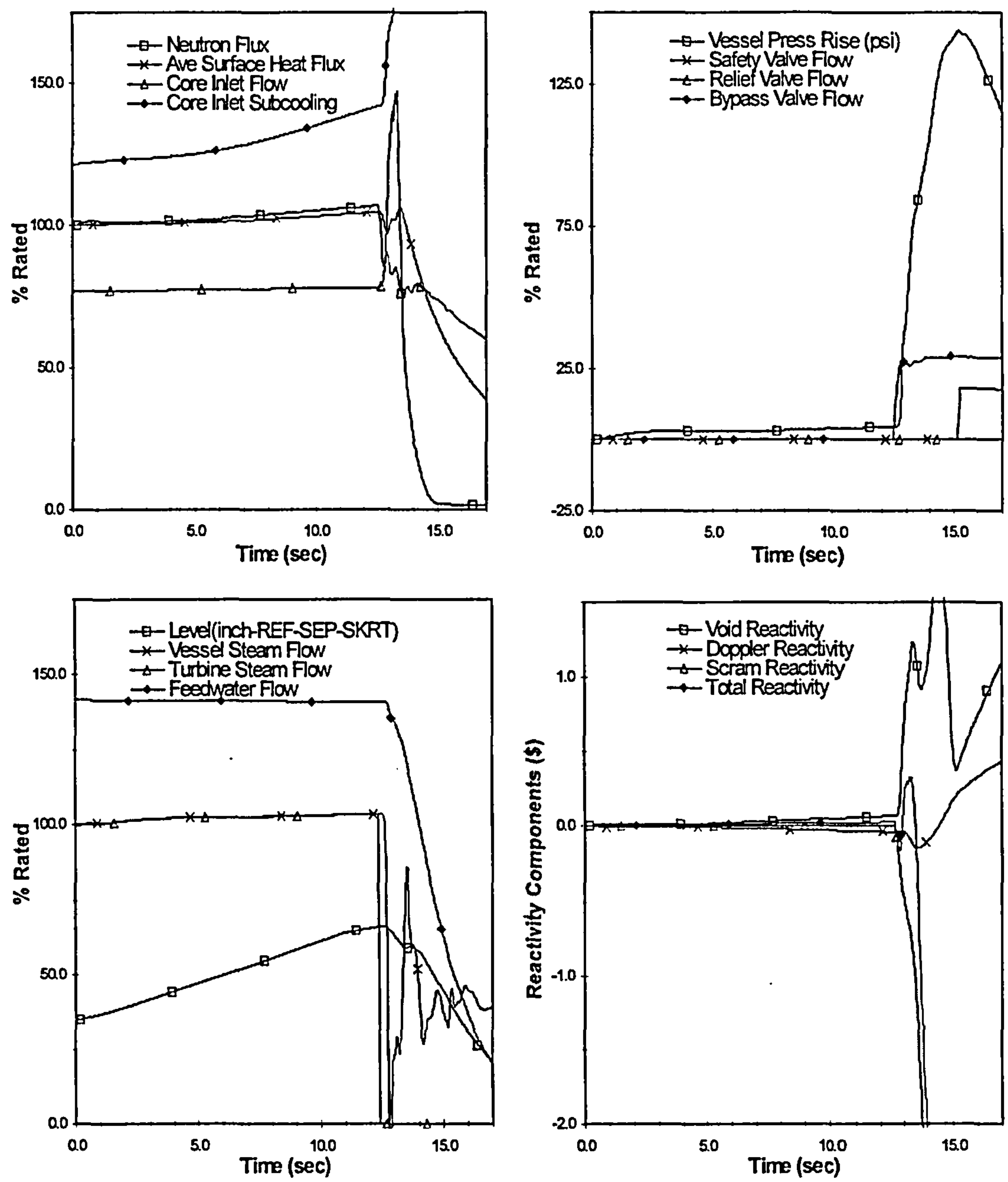

Figure 17 Plant Response to FW Controller Failure
(EOR13-3245 MWd/MT (2944 MWd/ST) to EOC13 MELLLA (UB))

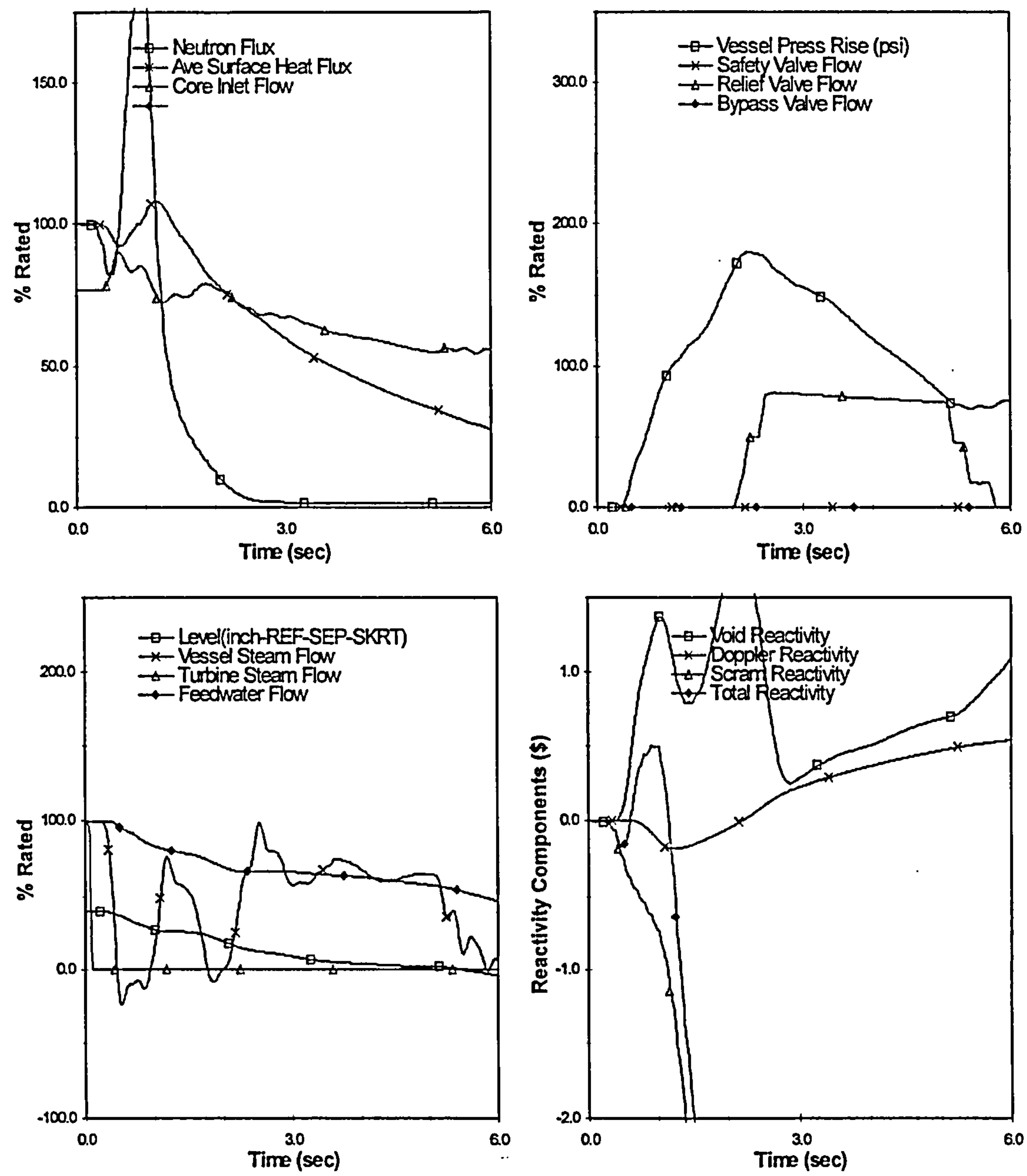

Figure 18 Plant Response to Turbine Trip w/o Bypass (EOR13-3245 MWd/MT (2944 MWd/ST) to EOC13 MELLLA (UB))

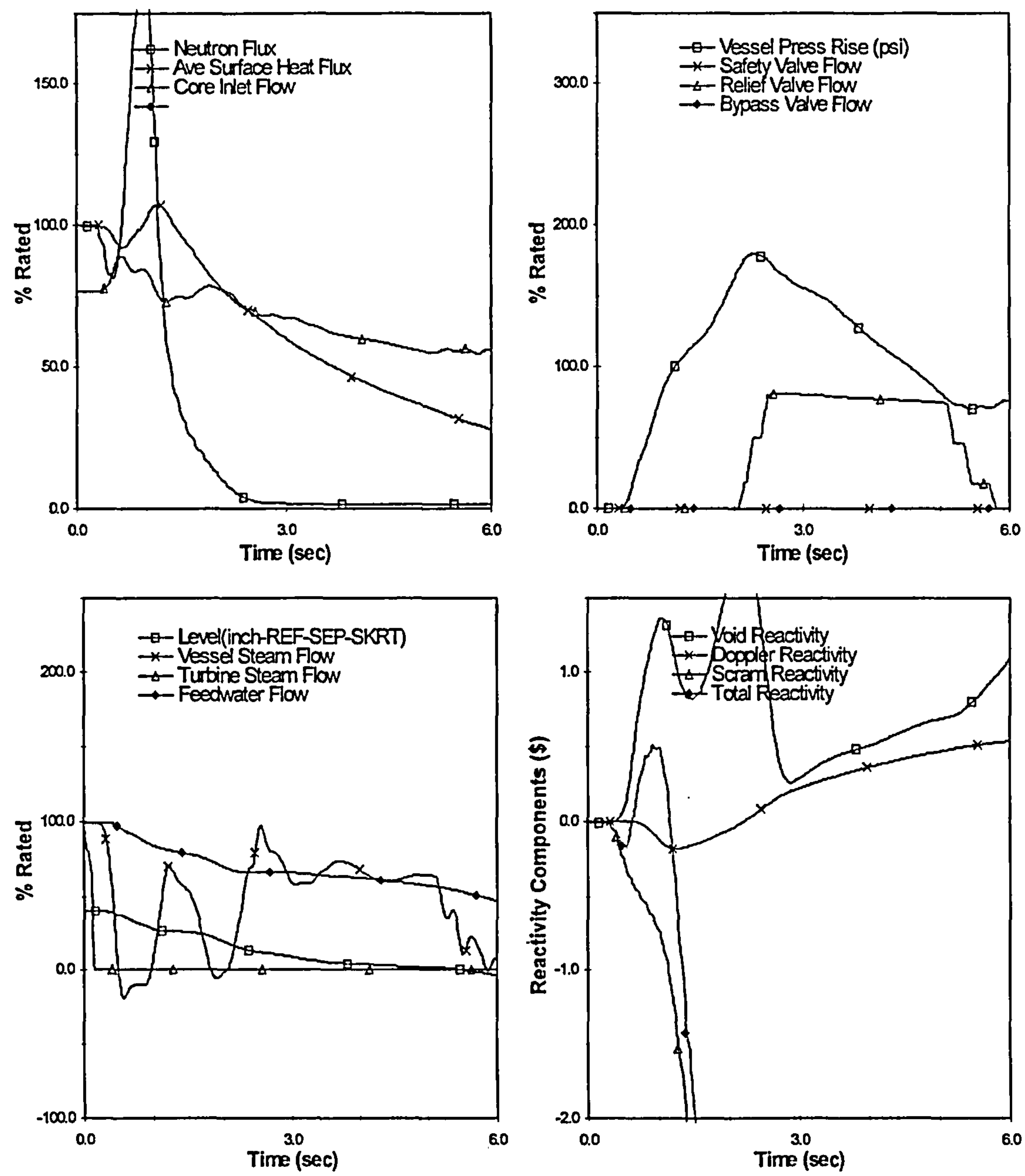

Figure 19 Plant Response to Load Reject w/o Bypass (EOR13-3245 MWd/MT (2944 MWd/ST) to EOC13 MELLLA (UB))

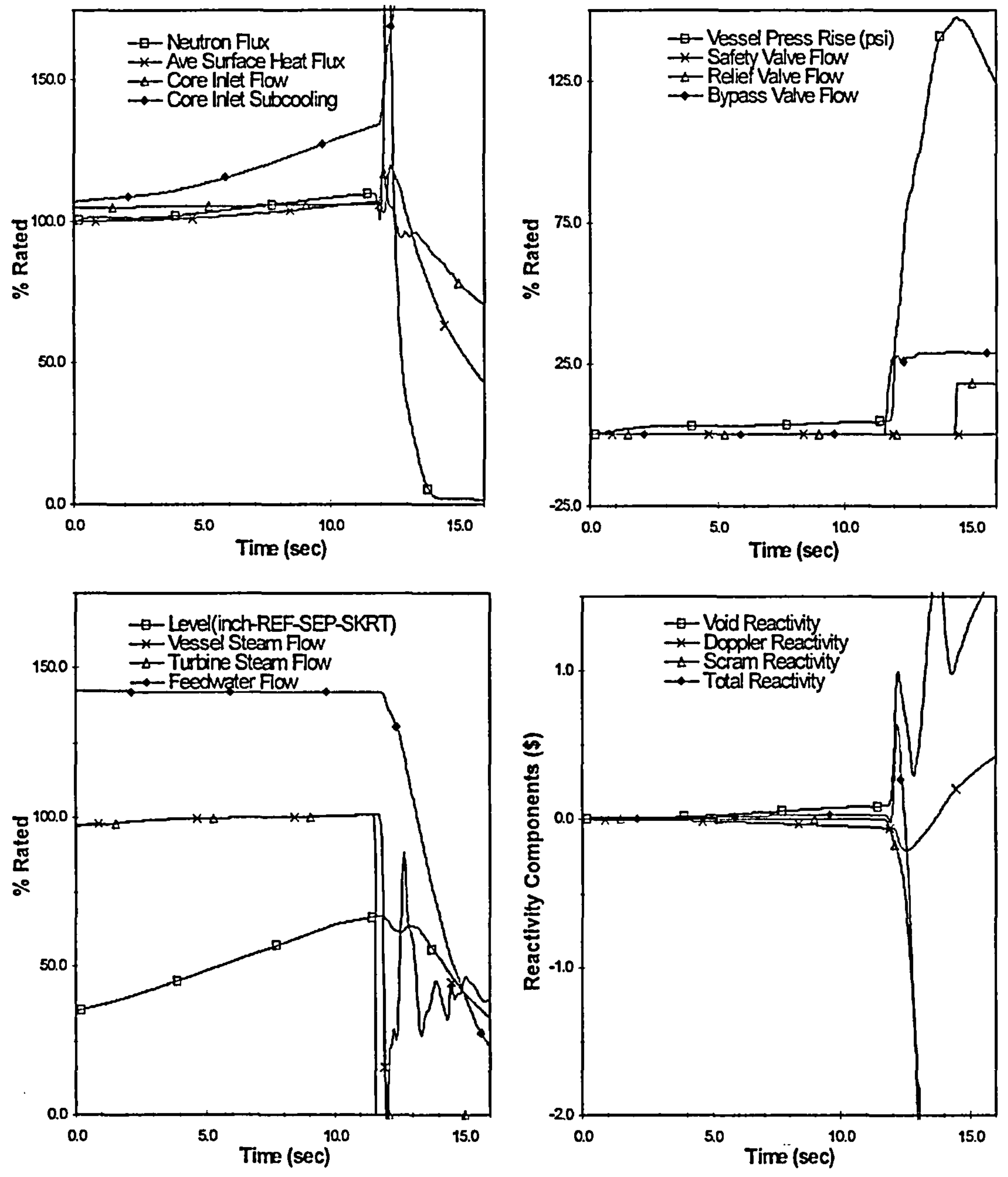

Figure 20 Plant Response to FW Controller Failure
(BOC13 to EOR13-3245 MWd/MT (2944 MWd/ST) ICF & MFWT (HBB))

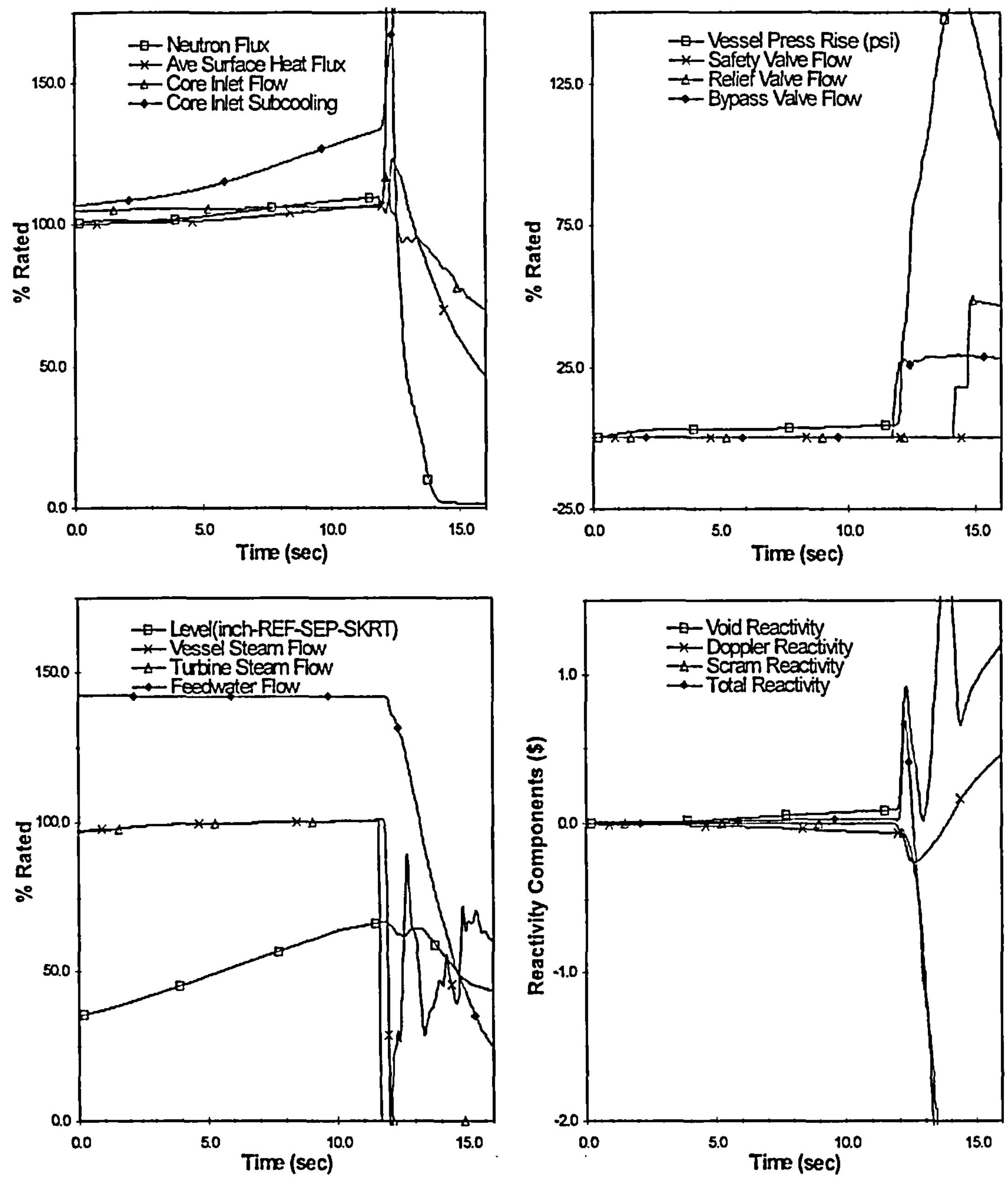

Figure 21 Plant Response to FW Controller Failure (EOR13-3245 MWd/MT (2944 MWd/ST) to EOC13 ICF & MFWT (HBB))

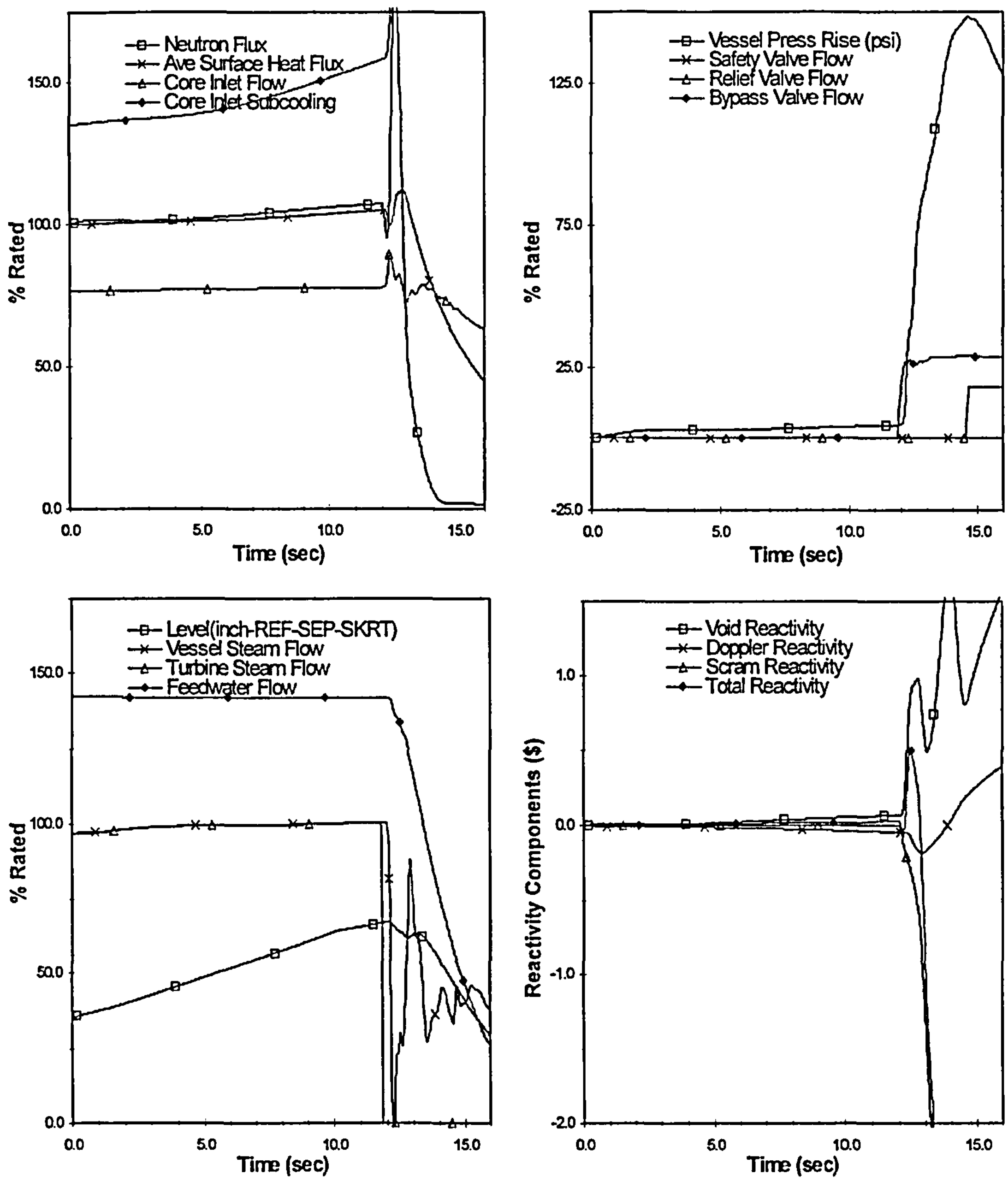

Figure 22 Plant Response to FW Controller Failure
(BOC13 to EOR13-3245 MWd/MT (2944 MWd/ST) MELLLA & MFWT (HBB))

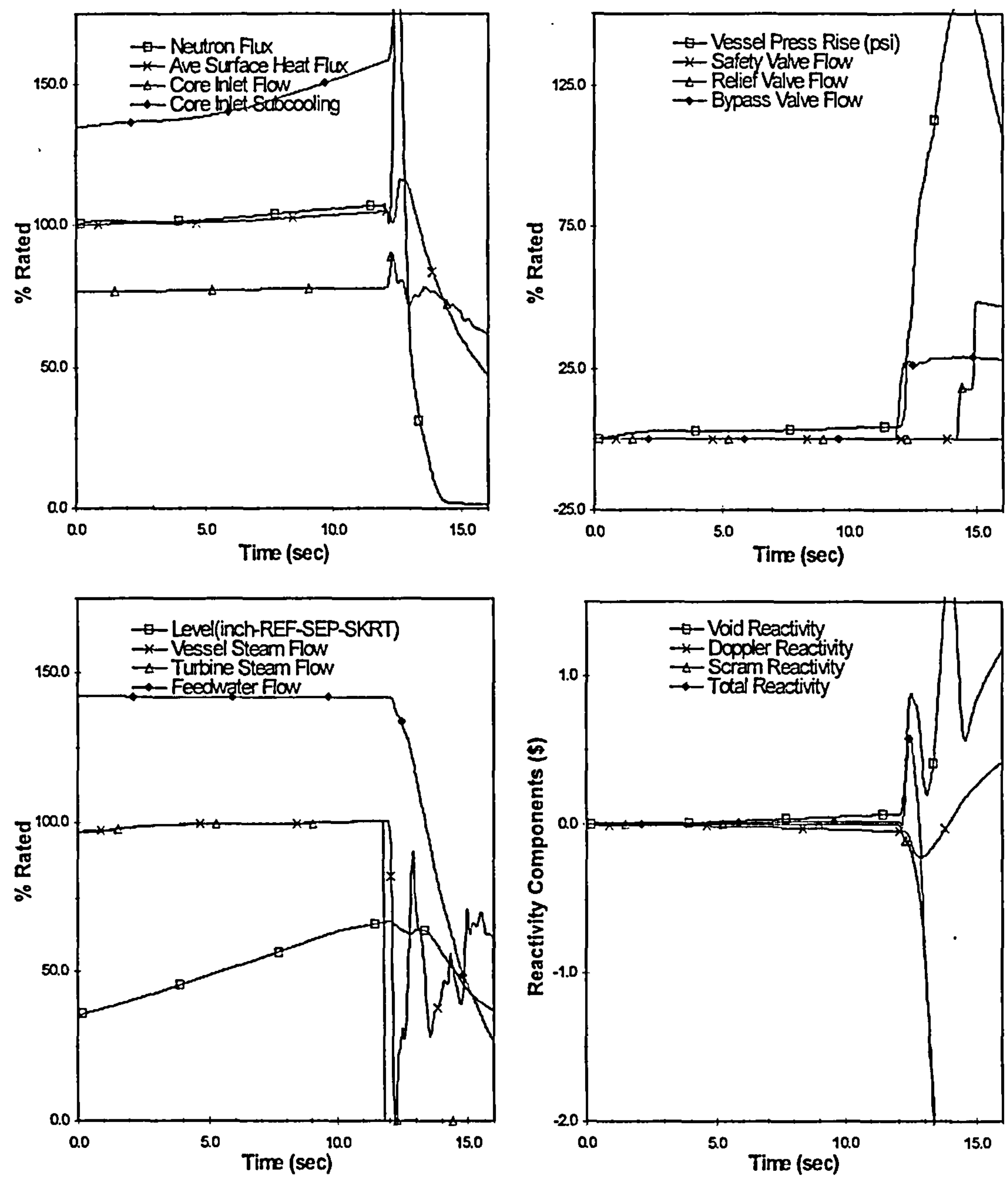

Figure 23 Plant Response to FW Controller Failure
(EOR13-3245 MWd/MT (2944 MWd/ST) to EOC13 MELLLA & MFWT (HBB))

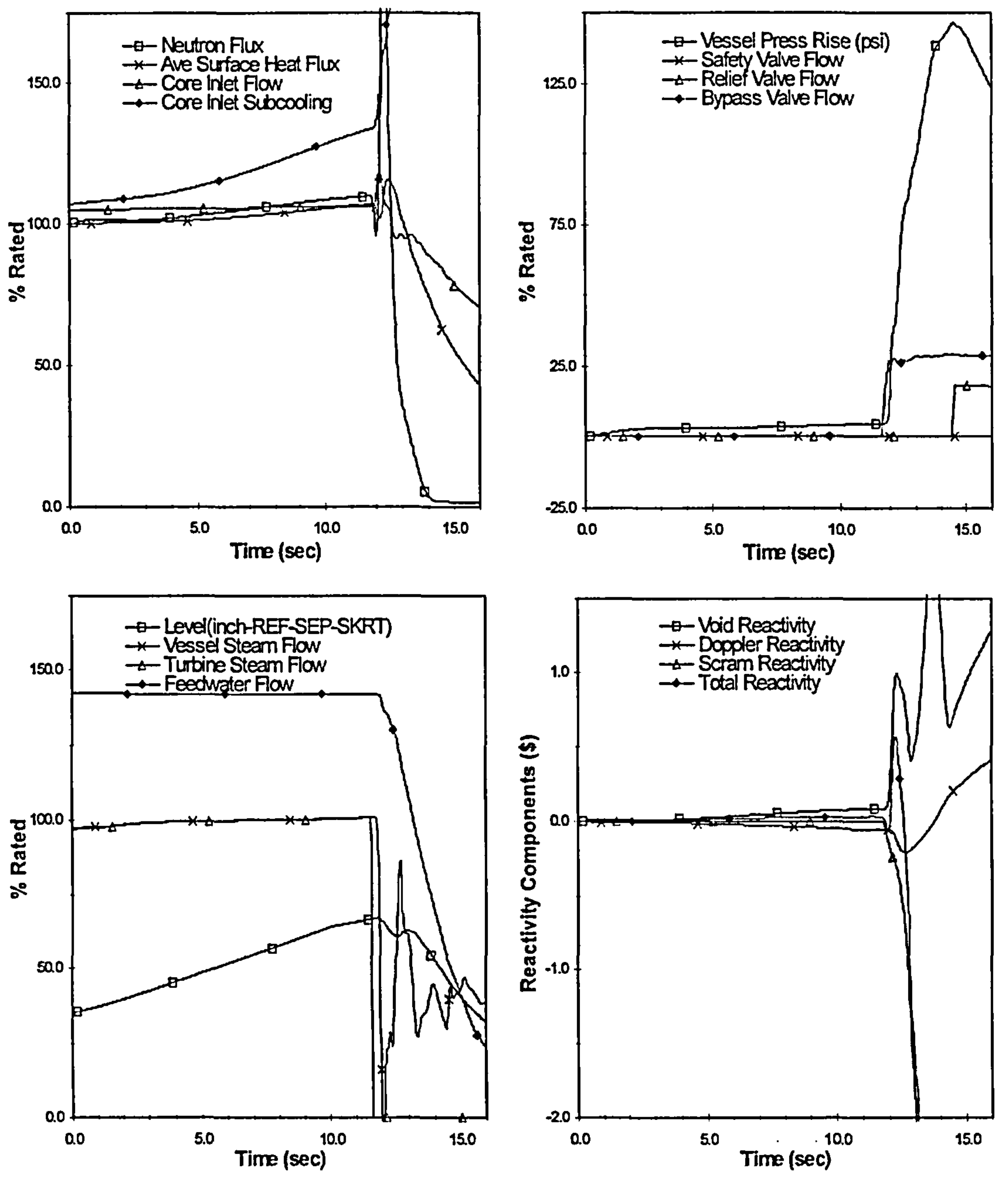

Figure 24 Plant Response to FW Controller Failure
(EOR13-3245 MWd/MT (2944 MWd/ST) to EOC13 ICF & MFWT (UB))

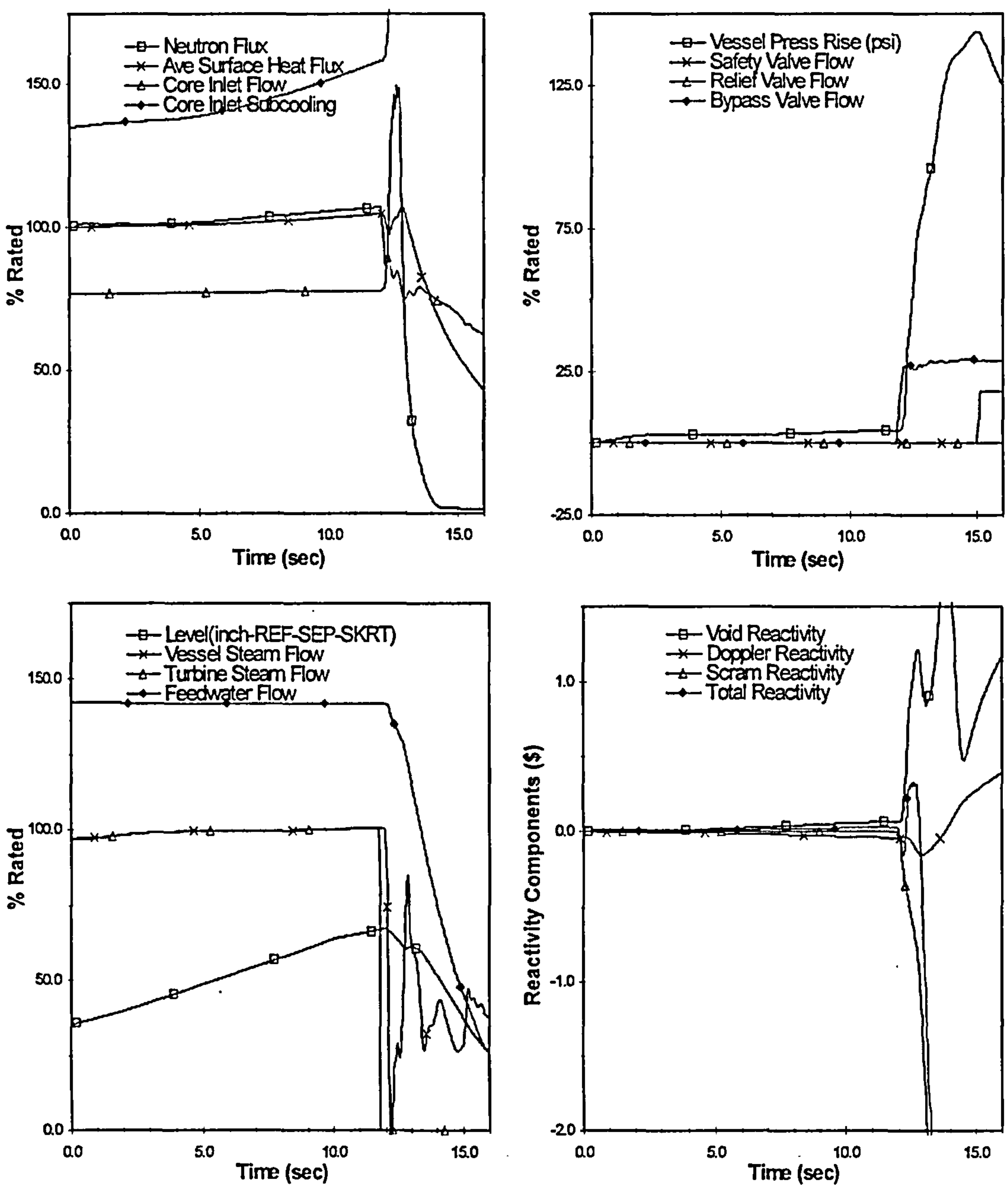

Figure 25 Plant Response to FW Controller Failure (EOR13-3245 MWd/MT (2944 MWd/ST) to EOC13 MELLLA & MFWT (UB))

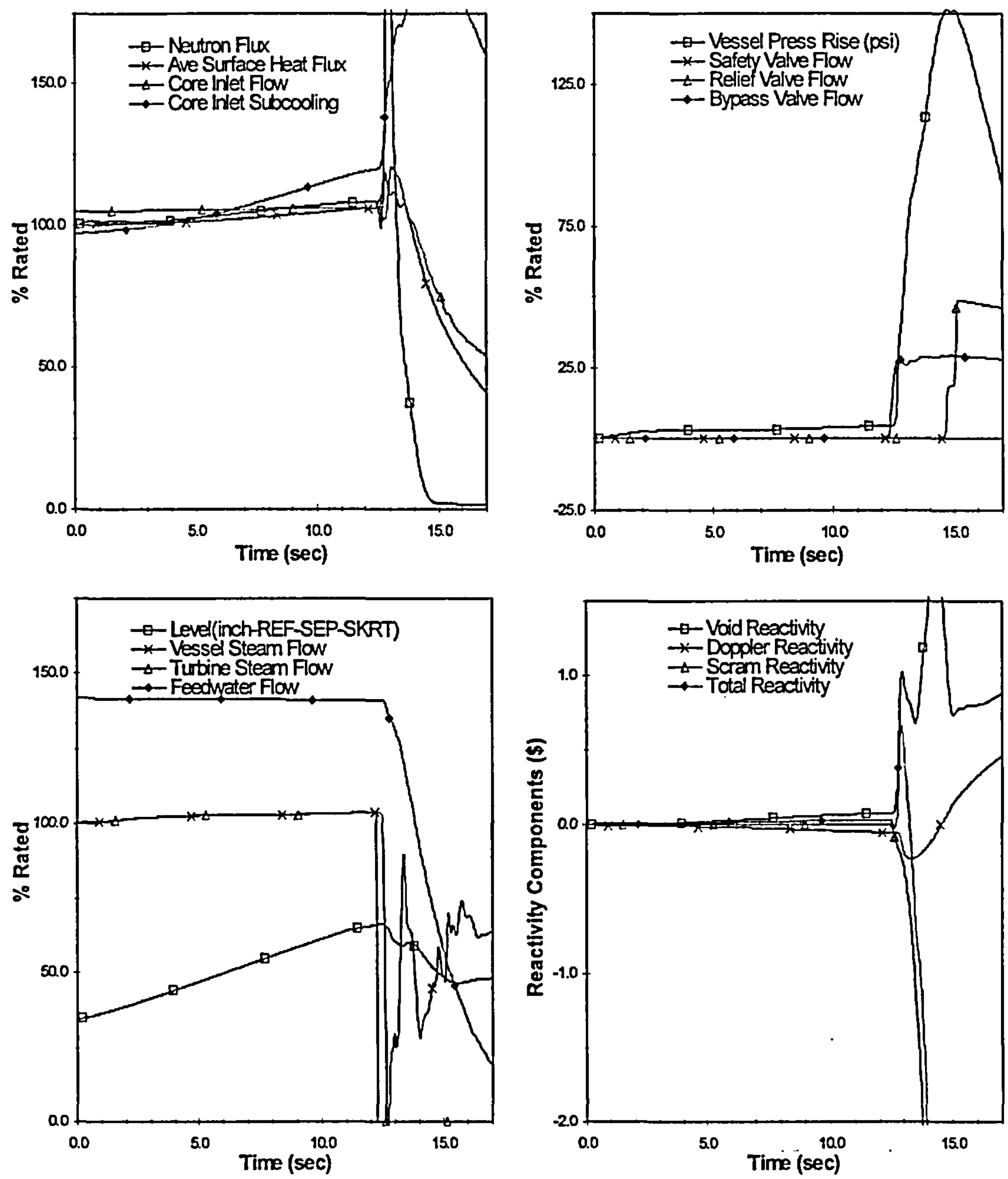

Figure 26 Plant Response to FW Controller Failure
(BOC13 to EOR13-3245 MWd/MT (2944 MWd/ST) ICF with RPTOOS (HBB))

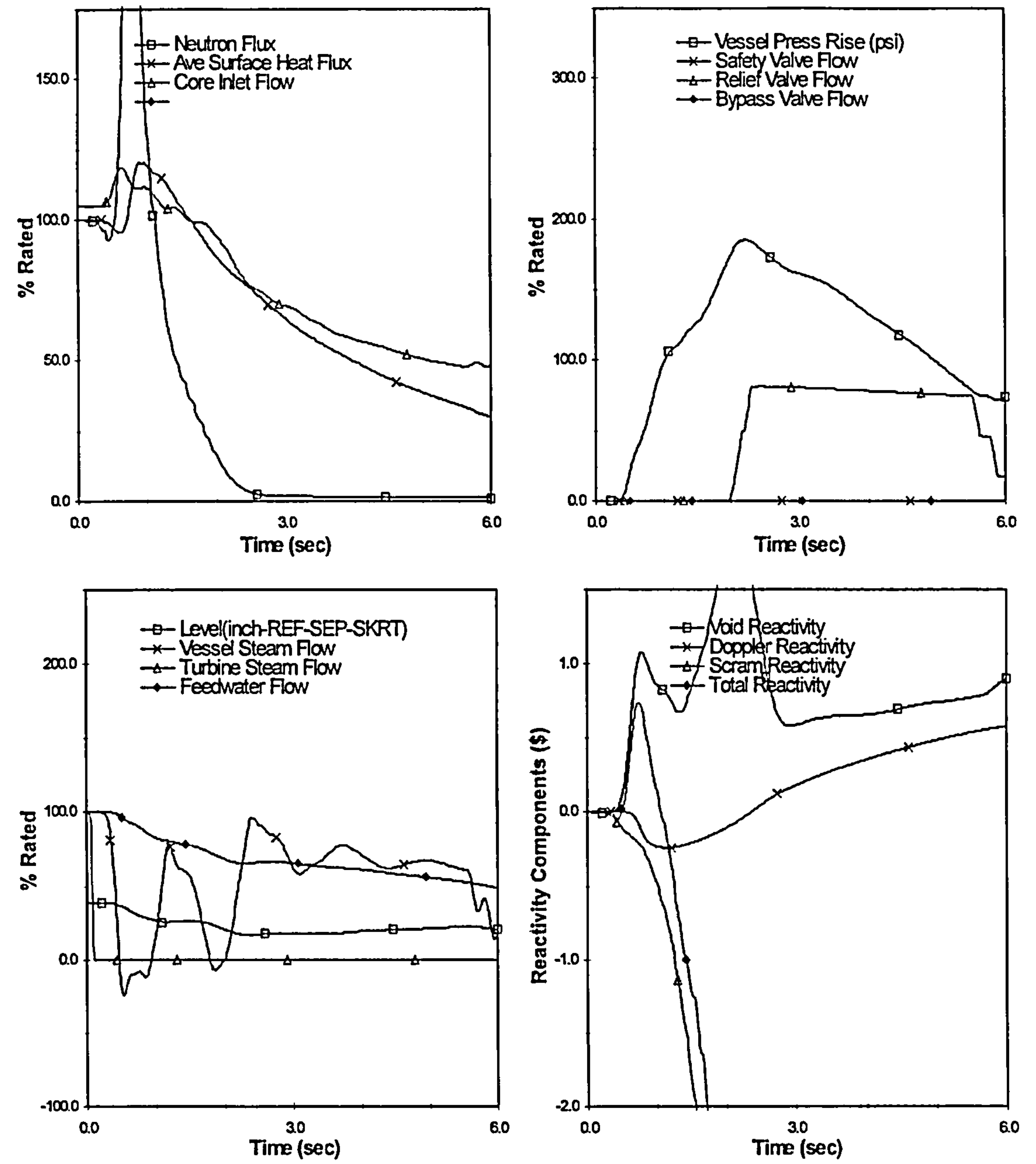

Figure 27 Plant Response to Turbine Trip w/o Bypass (BOC13 to EOR13-3245 MWd/MT (2944 MWd/ST) ICF with RPTOOS (HBB))

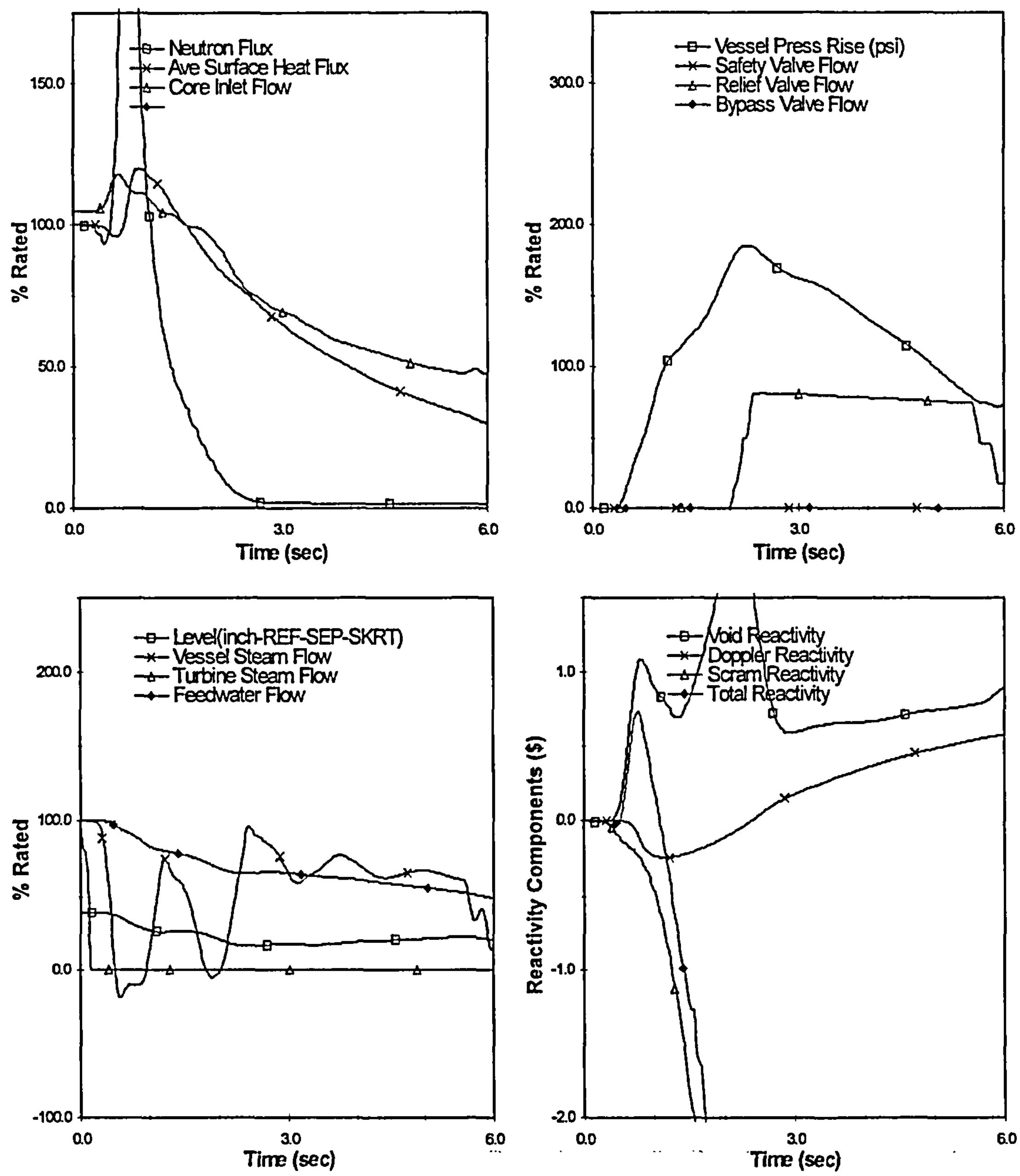

Figure 28 Plant Response to Load Reject w/o Bypass (BOC13 to EOR13-3245 MWd/MT (2944 MWd/ST) ICF with RPTOOS (HBB))

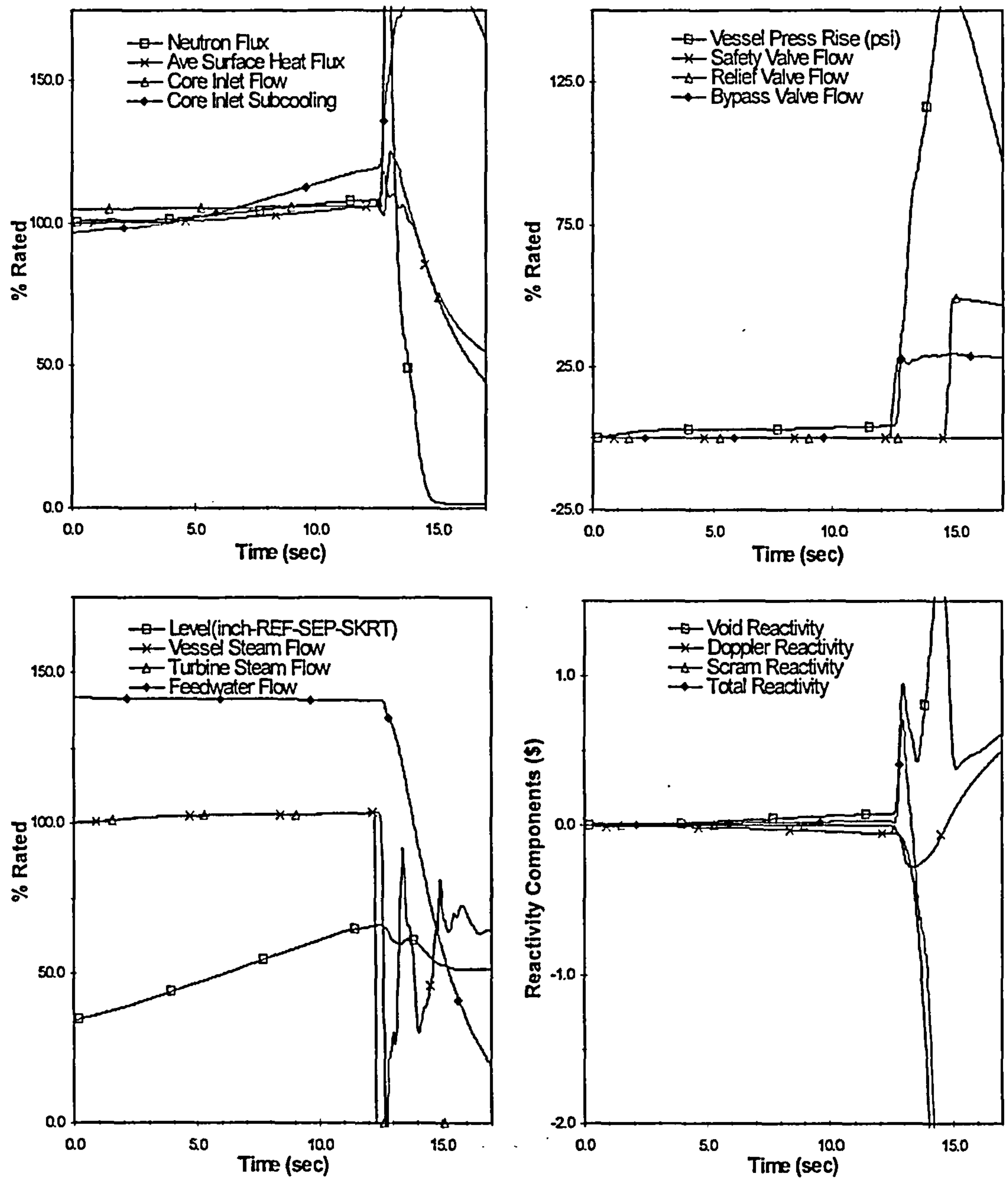

Figure 29 Plant Response to FW Controller Failure
(EOR13-3245 MWd/MT (2944 MWd/ST) to EOC13 ICF with RPTOOS (HBB))

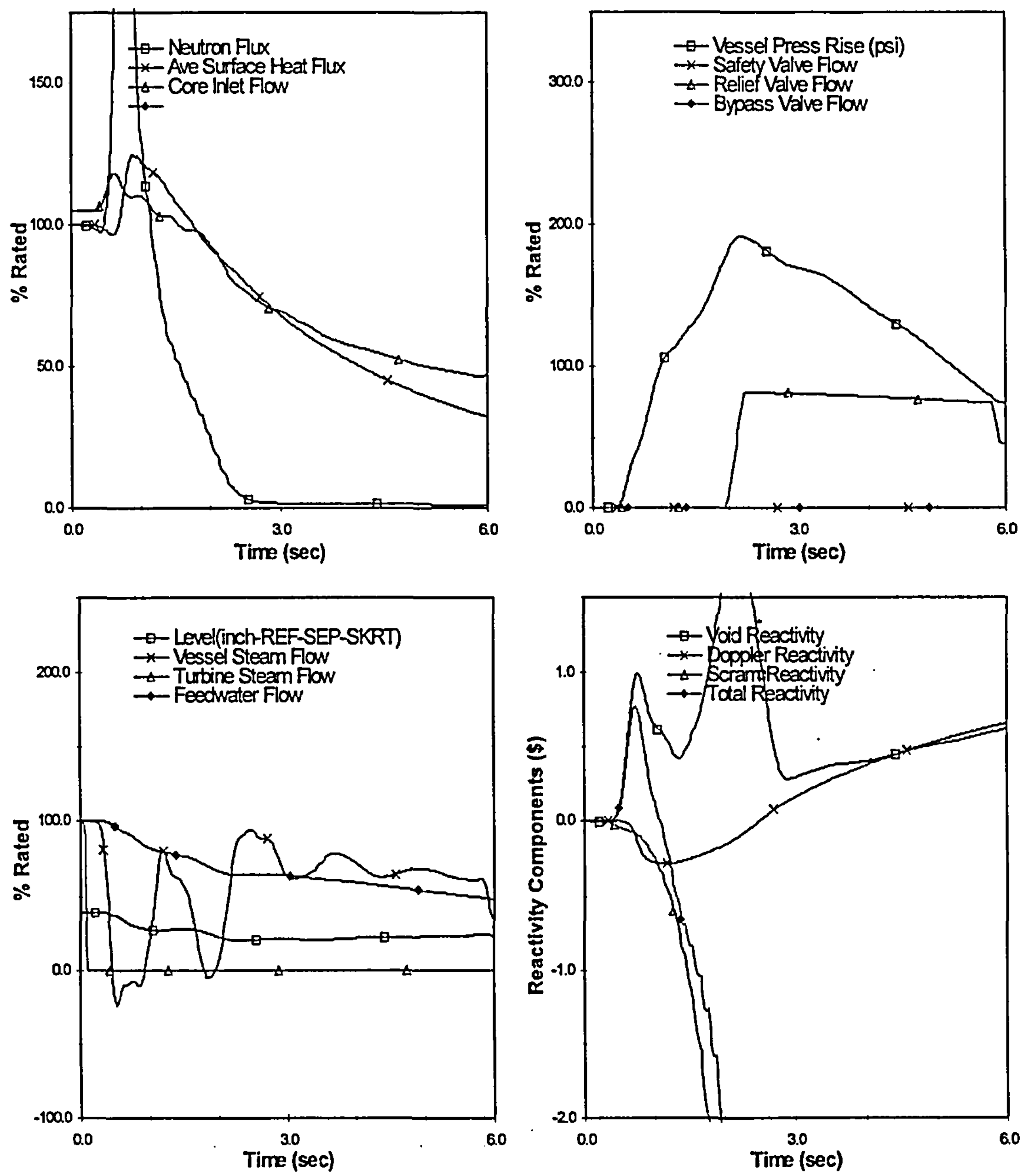

Figure 30 Plant Response to Turbine Trip w/o Bypass (EOR13-3245 MWd/MT (2944 MWd/ST) to EOC13 ICF with RPTOOS (HBB))

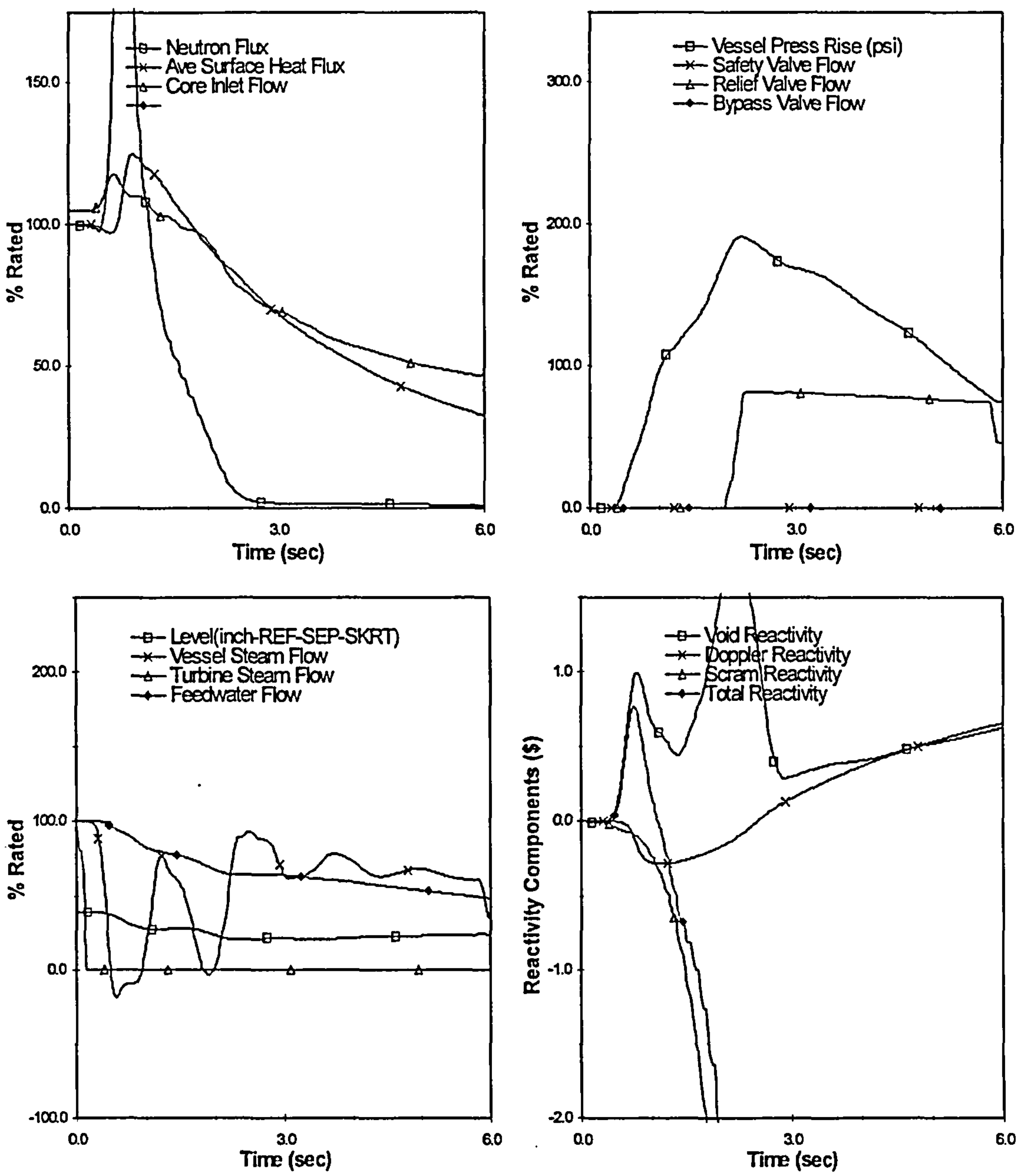

Figure 31 Plant Response to Load Reject w/o Bypass (EOR13-3245 MWd/MT (2944 MWd/ST) to EOC13 ICF with RPTOOS (HBB))

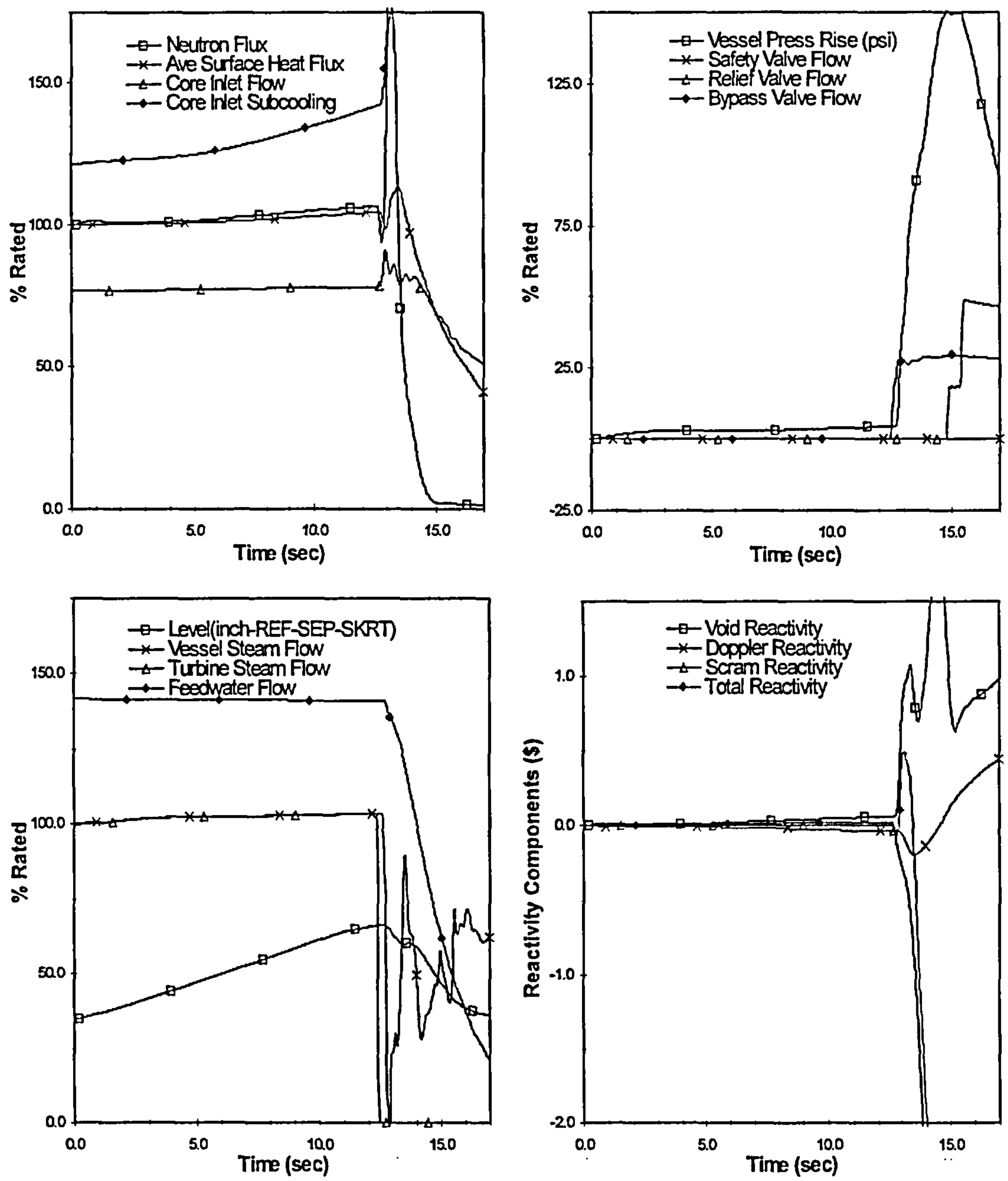

Figure 32 Plant Response to FW Controller Failure
(BOC13 to EOR13-3245 MWd/MT (2944 MWd/ST) MELLLA with RPTOOS (HBB))

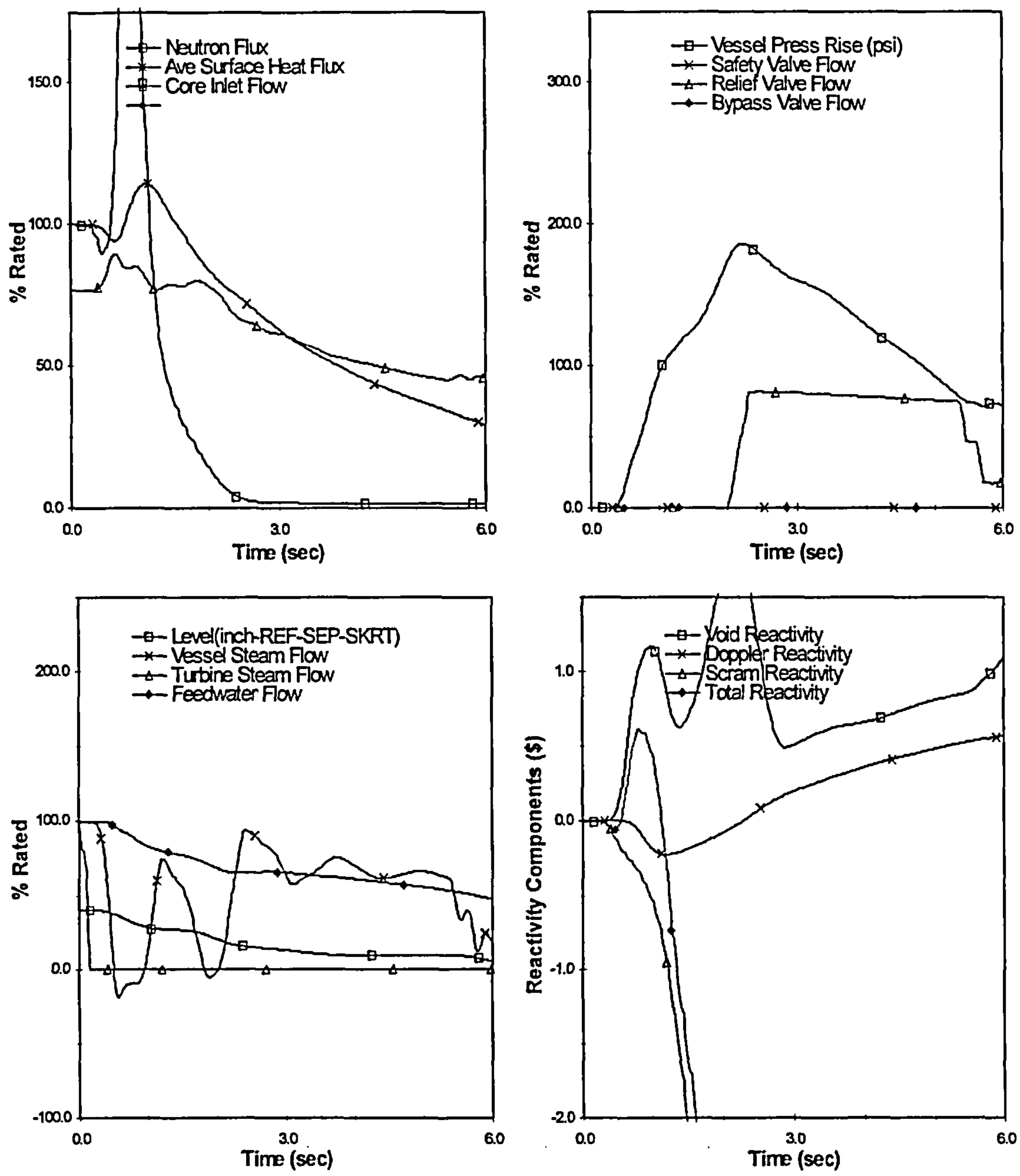

Figure 33 Plant Response to Load Reject w/o Bypass
(BOC13 to EOR13-3245 MWd/MT (2944 MWd/ST) MELLLA with RPTOOS (HBB))

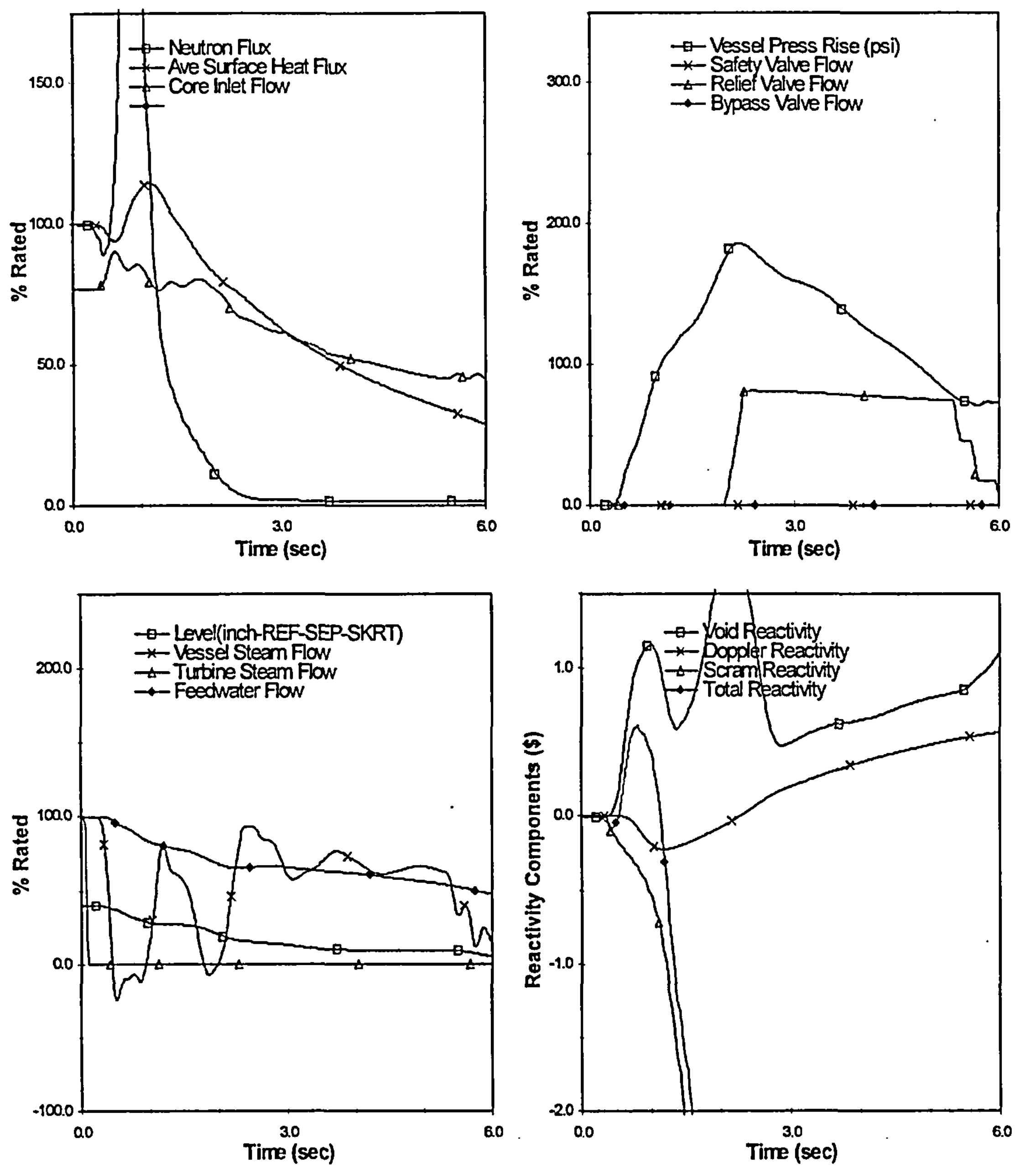

Figure 34 Plant Response to Turbine Trip w/o Bypass
(BOC13 to EOR13-3245 MWd/MT (2944 MWd/ST) MELLLA with RPTOOS (HBB))

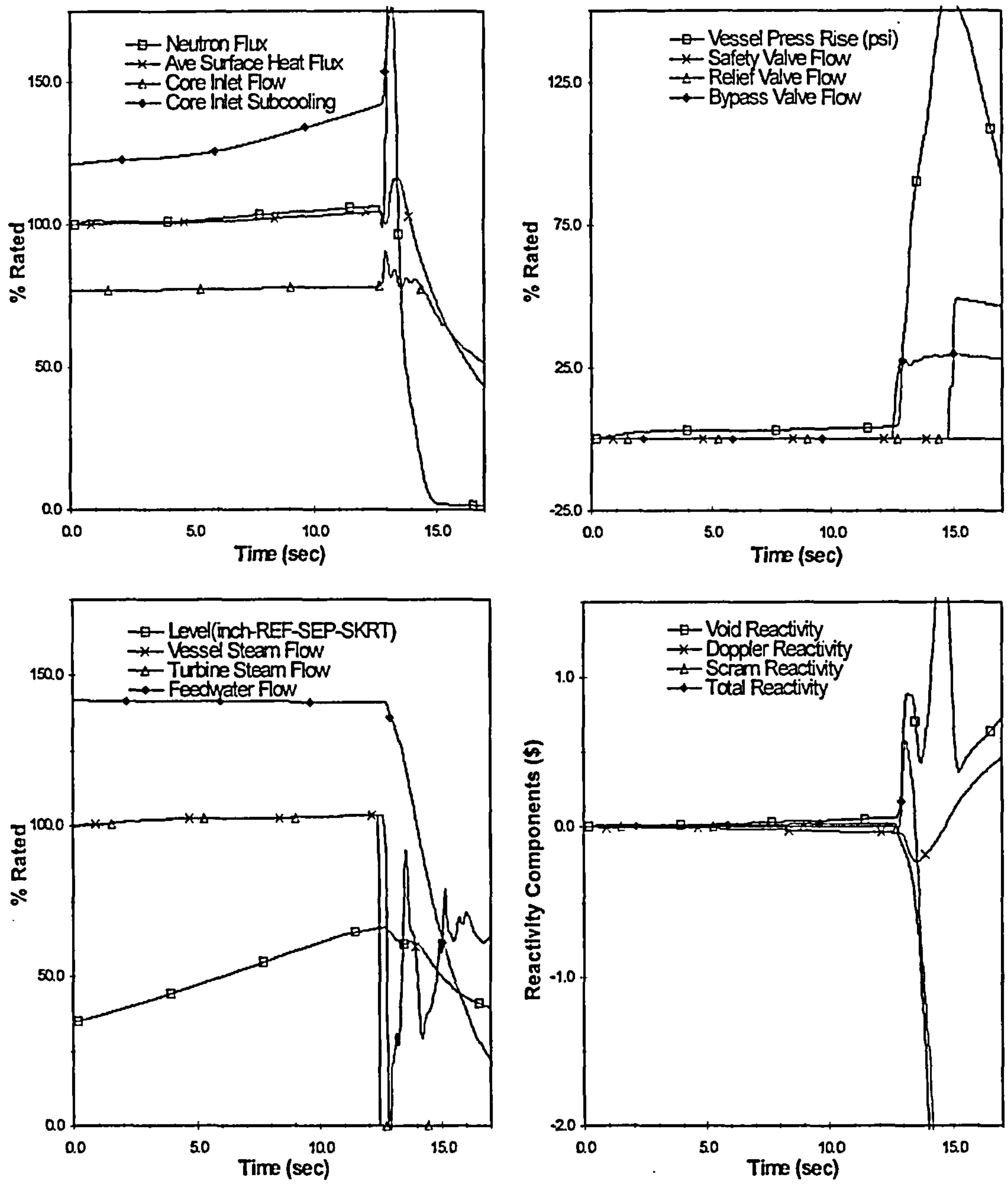

Figure 35 Plant Response to FW Controller Failure (EOR13-3245 MWd/MT (2944 MWd/ST) to EOC13 MELLLA with RPTOOS (HBB))

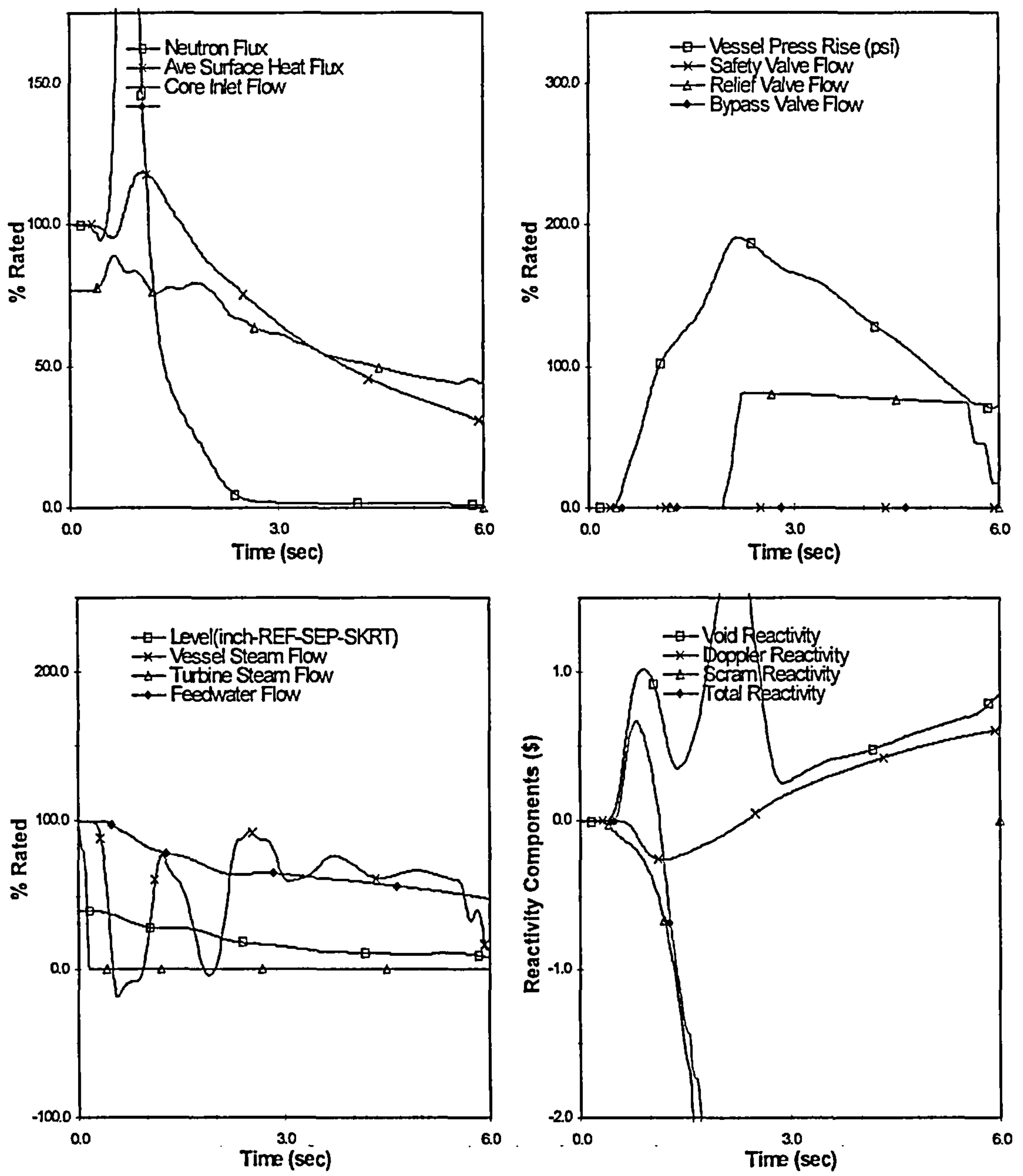

Figure 36 Plant Response to Load Reject w/o Bypass (EOR13-3245 MWd/MT (2944 MWd/ST) to EOC13 MELLLA with RPTOOS (HBB))

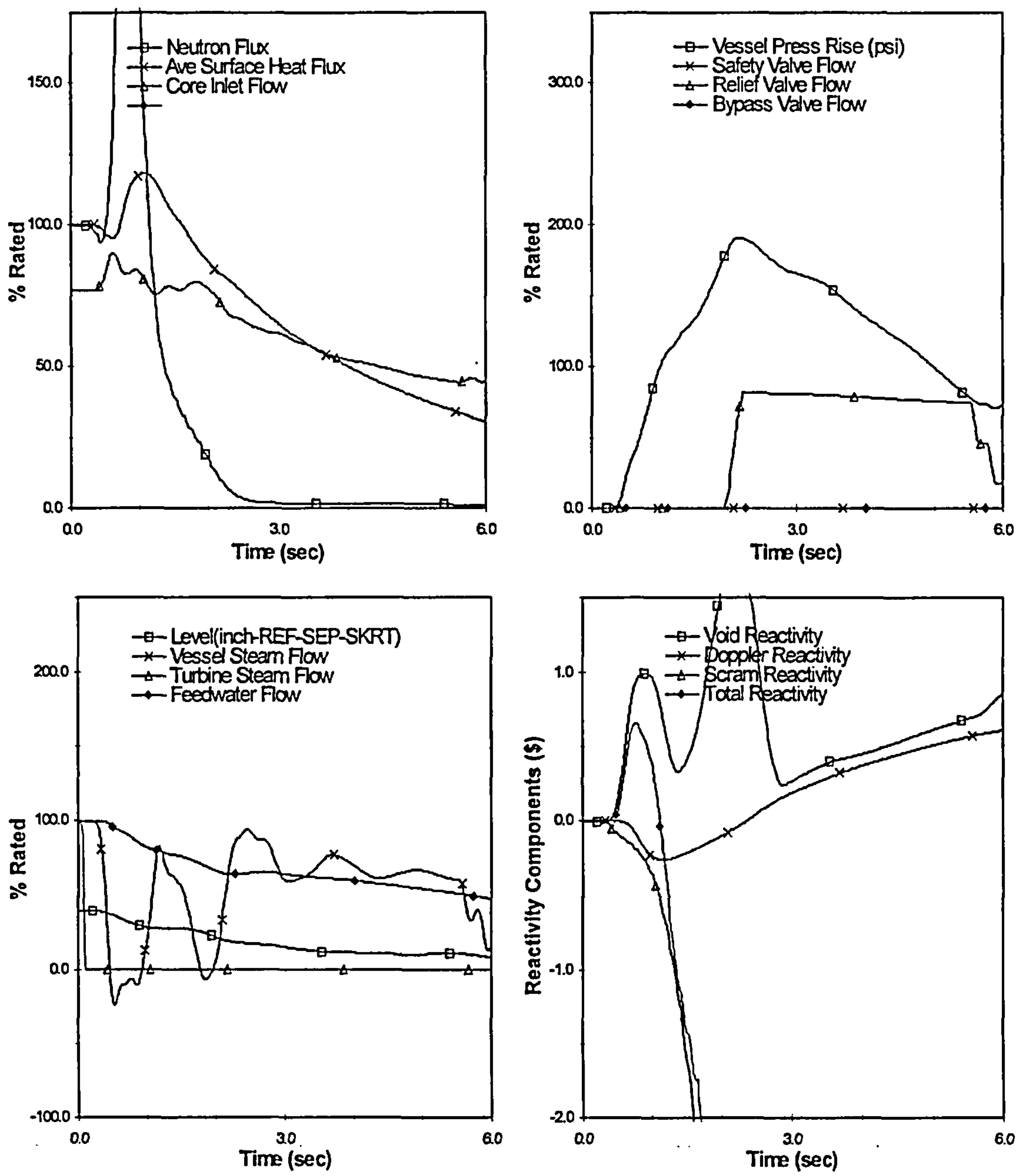

Figure 37 Plant Response to Turbine Trip w/o Bypass (EOR13-3245 MWd/MT (2944 MWd/ST) to EOC13 MELLLA with RPTOOS (HBB))

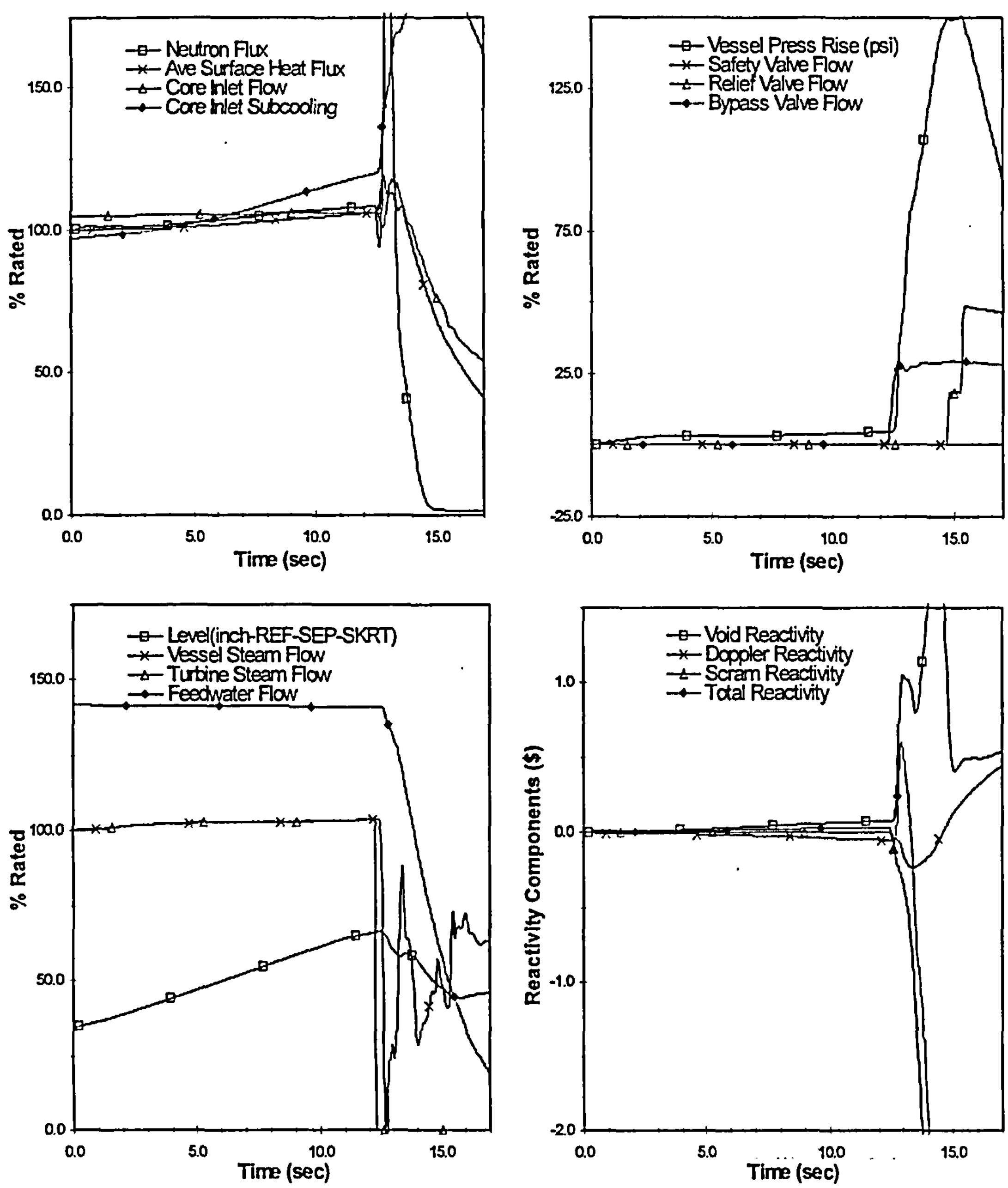

**Figure 38 Plant Response to FW Controller Failure
(EOR13-3245 MWd/MT (2944 MWd/ST) to EOC13 ICF with RPTOOS (UB))**

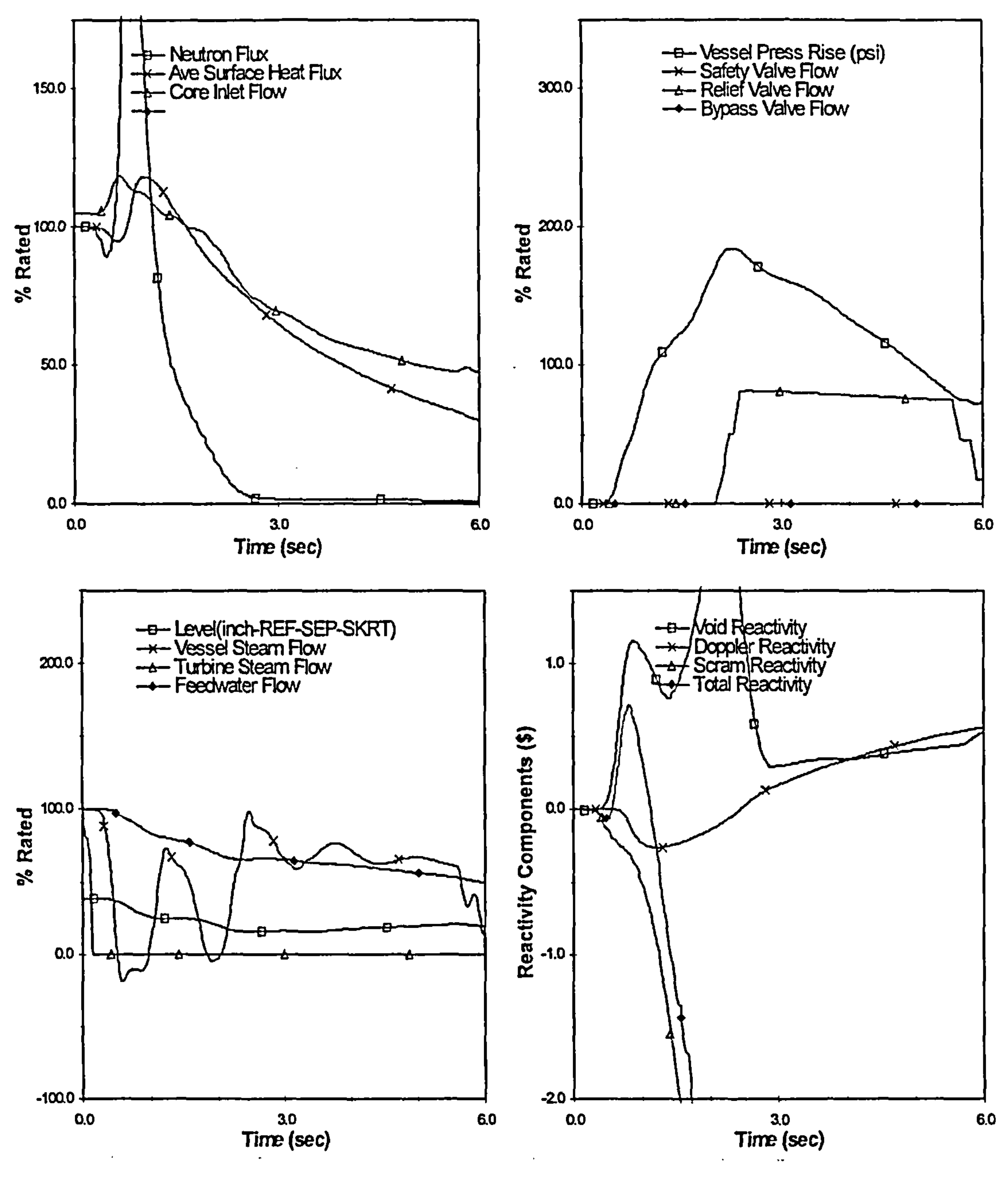

Figure 39 Plant Response to Load Reject w/o Bypass (EOR13-3245 MWd/MT (2944 MWd/ST) to EOC13 ICF with RPTOOS (UB))

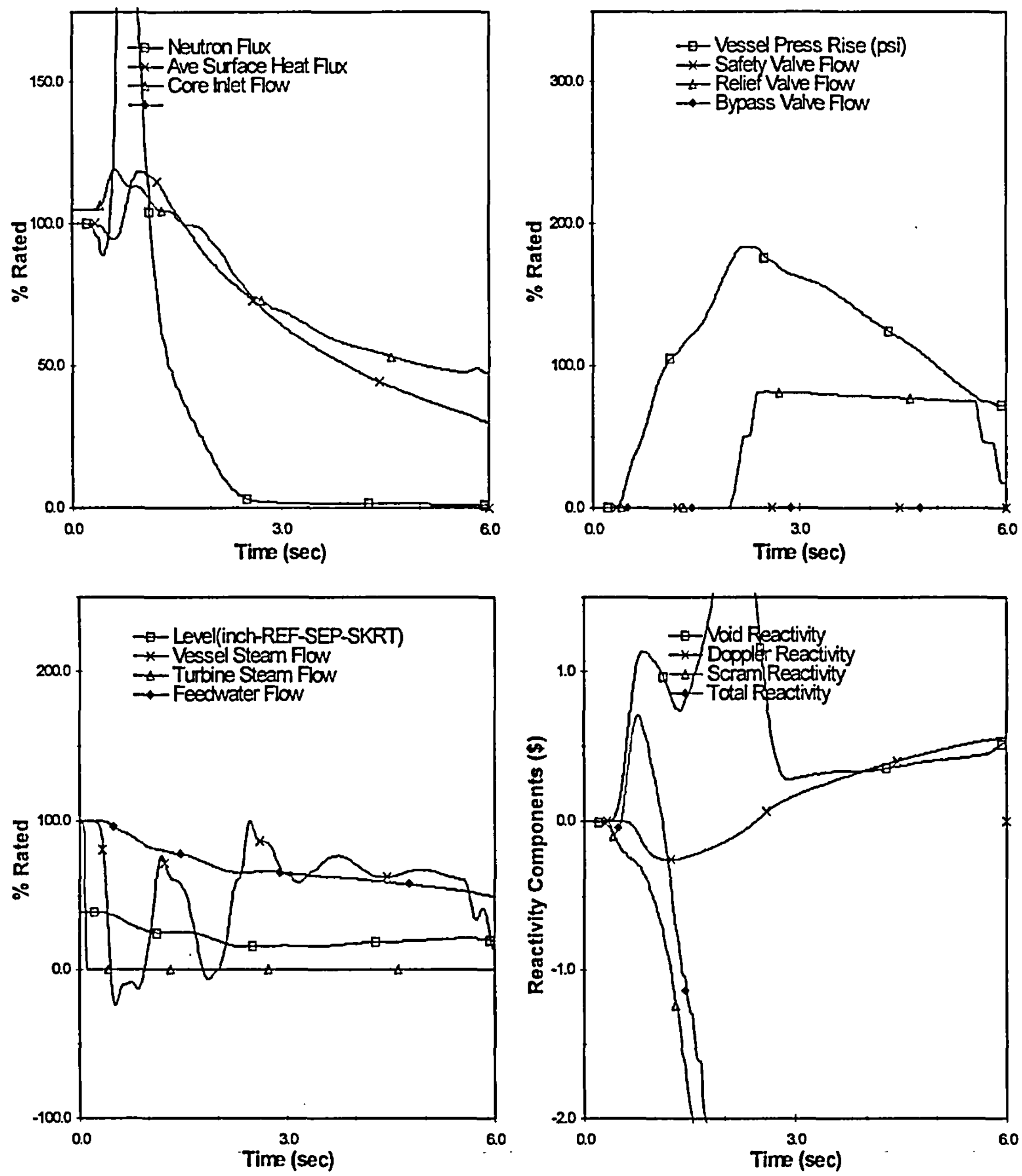

Figure 40 Plant Response to Turbine Trip w/o Bypass (EOR13-3245 MWd/MT (2944 MWd/ST) to EOC13 ICF with RPTOOS (UB))

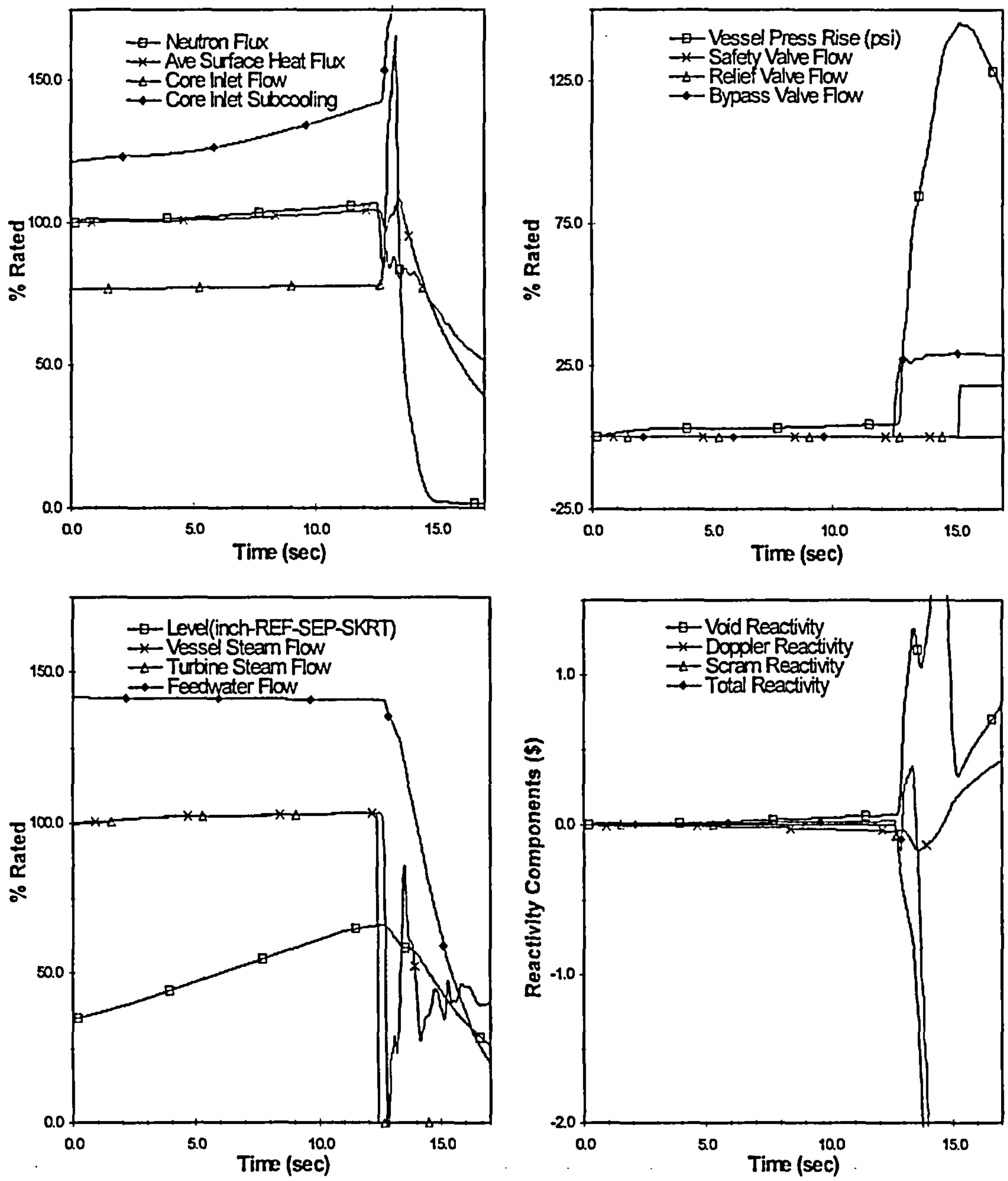

Figure 41 Plant Response to FW Controller Failure
(EOR13-3245 MWd/MT (2944 MWd/ST) to EOC13 MELLLA with RPTOOS (UB))

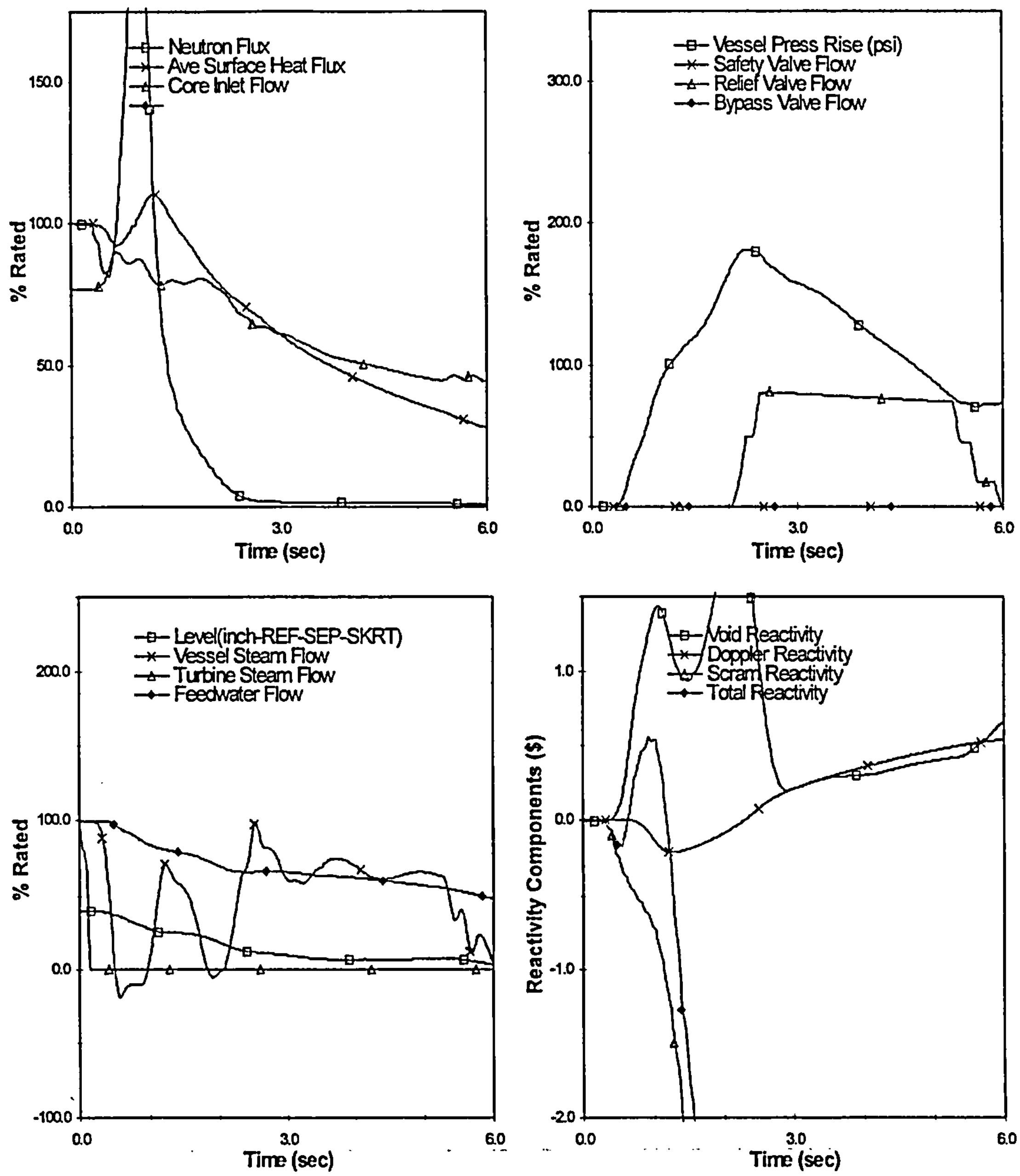

Figure 42 Plant Response to Load Reject w/o Bypass
(EOR13-3245 MWd/MT (2944 MWd/ST) to EOC13 MELLLA with RPTOOS (UB))

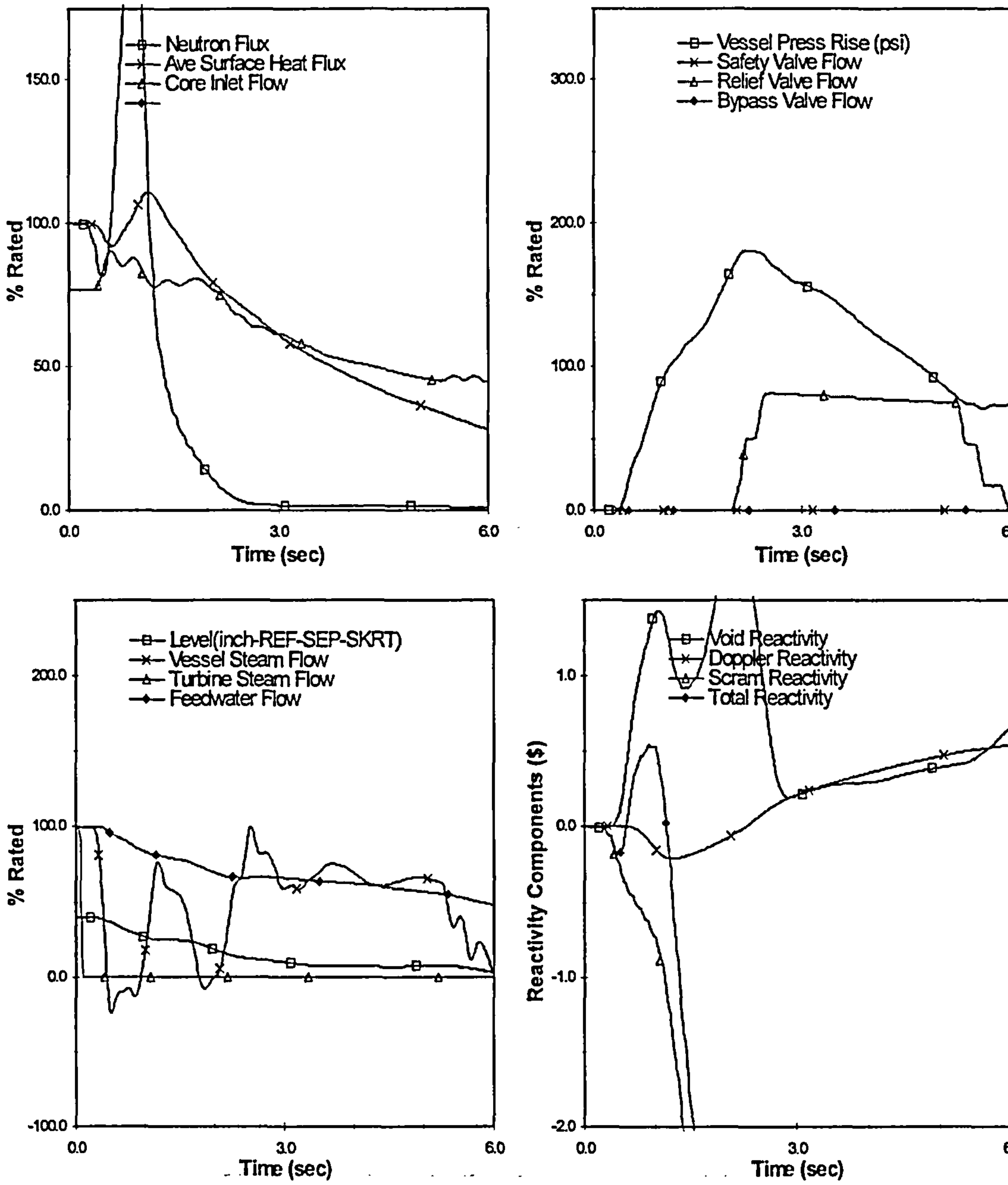

Figure 43 Plant Response to Turbine Trip w/o Bypass (EOR13-3245 MWd/MT (2944 MWd/ST) to EOC13 MELLLA with RPTOOS (UB))

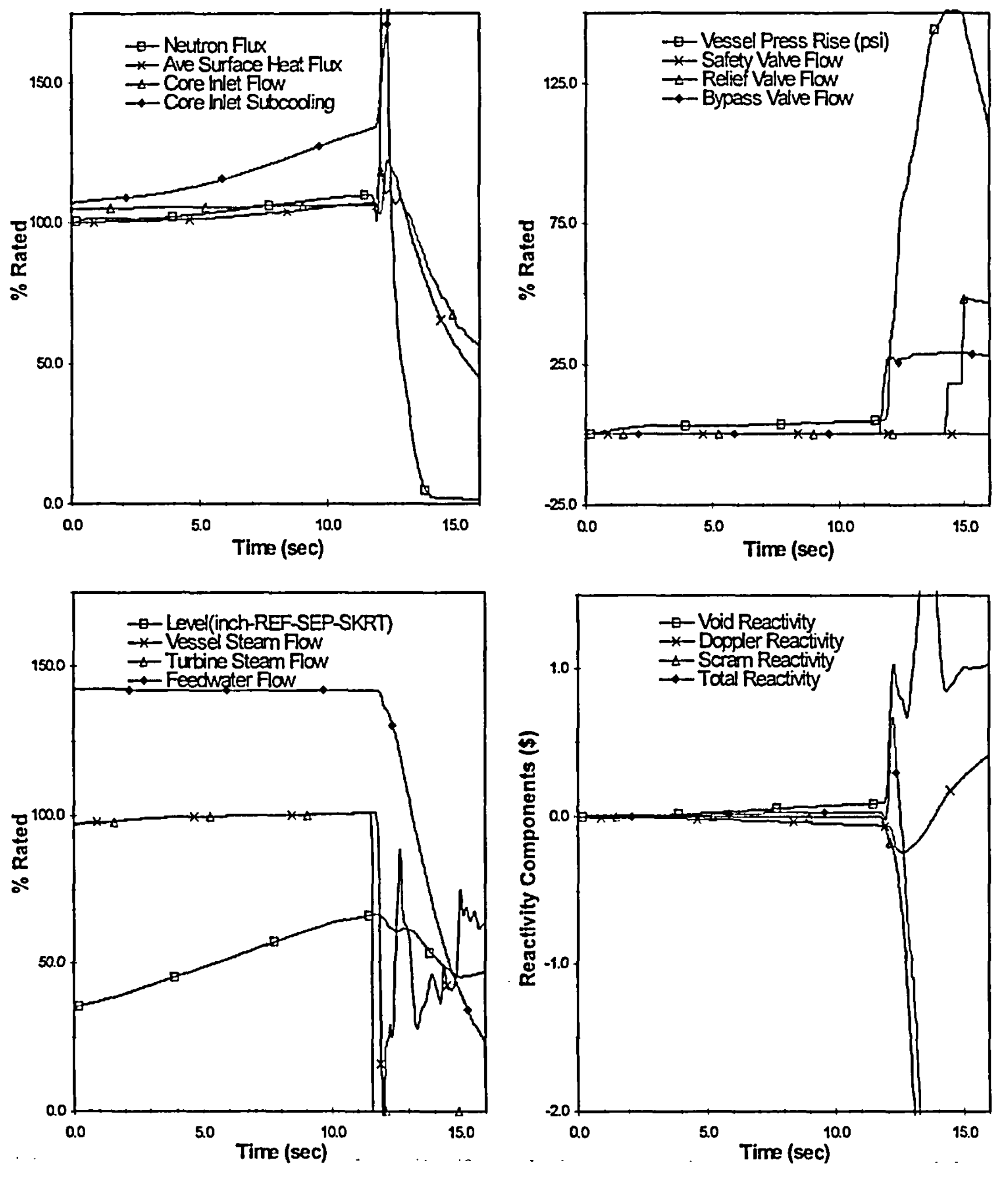

Figure 44 Plant Response to FW Controller Failure
(BOC13 to EOR13-3245 MWd/MT (2944 MWd/ST) ICF & MFWT with RPTOOS (HBB))

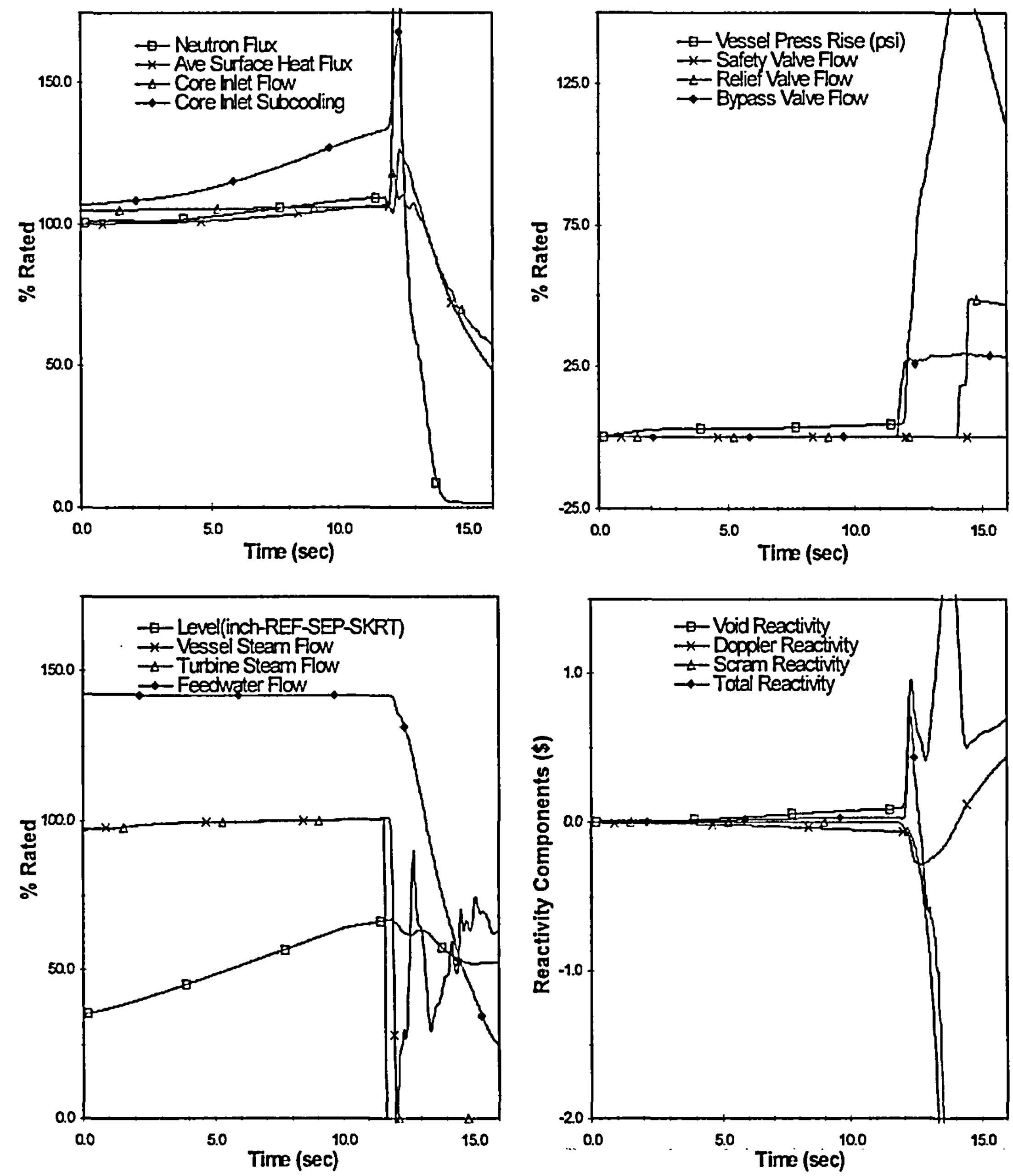

Figure 45 Plant Response to FW Controller Failure
(EOR13-3245 MWd/MT (2944 MWd/ST) to EOC13 ICF & MFWT with RPTOOS (HBB))

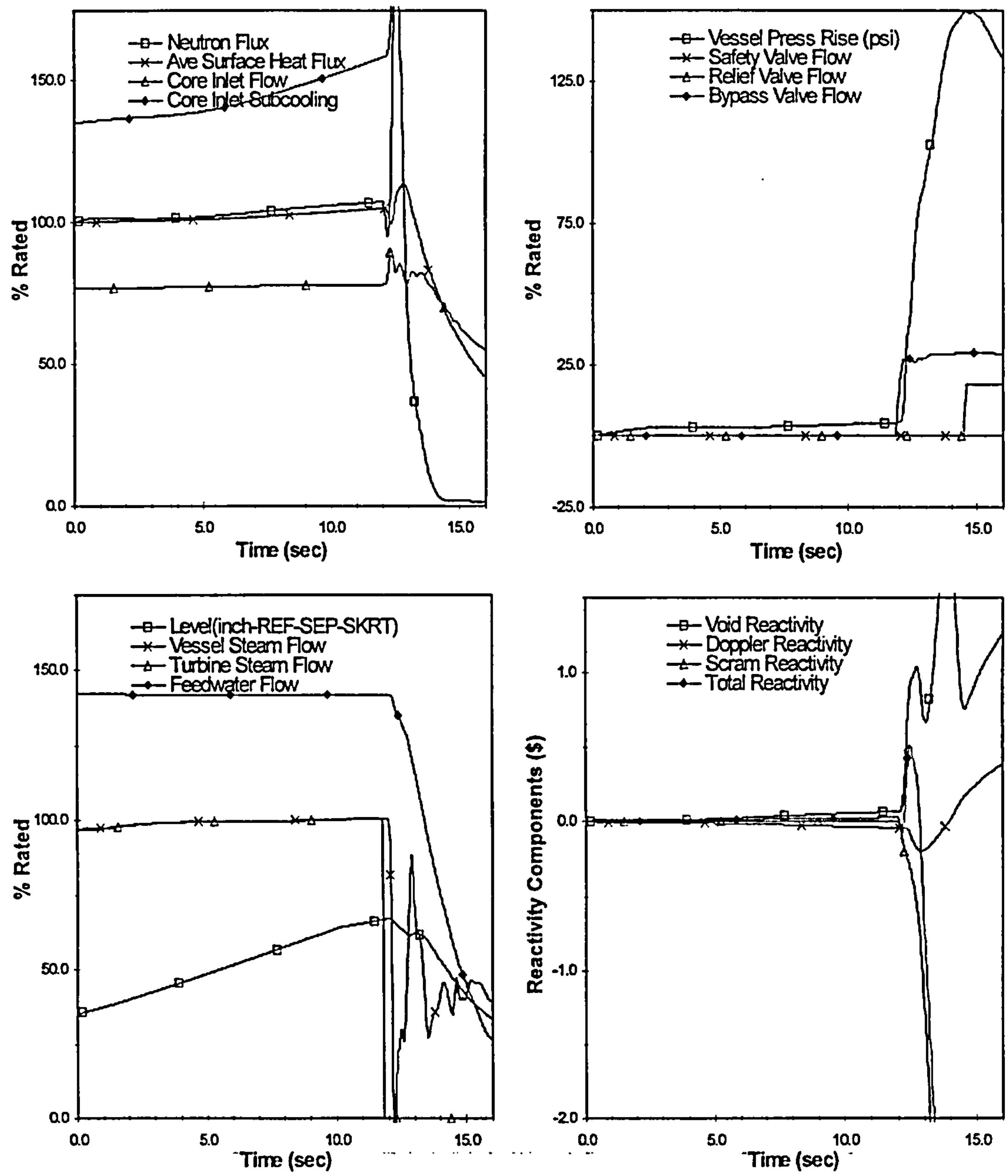

Figure 46 Plant Response to FW Controller Failure
(BOC13 to EOR13-3245 MWd/MT (2944 MWd/ST) MELLLA & MFWT with RPTOOS (HBB))

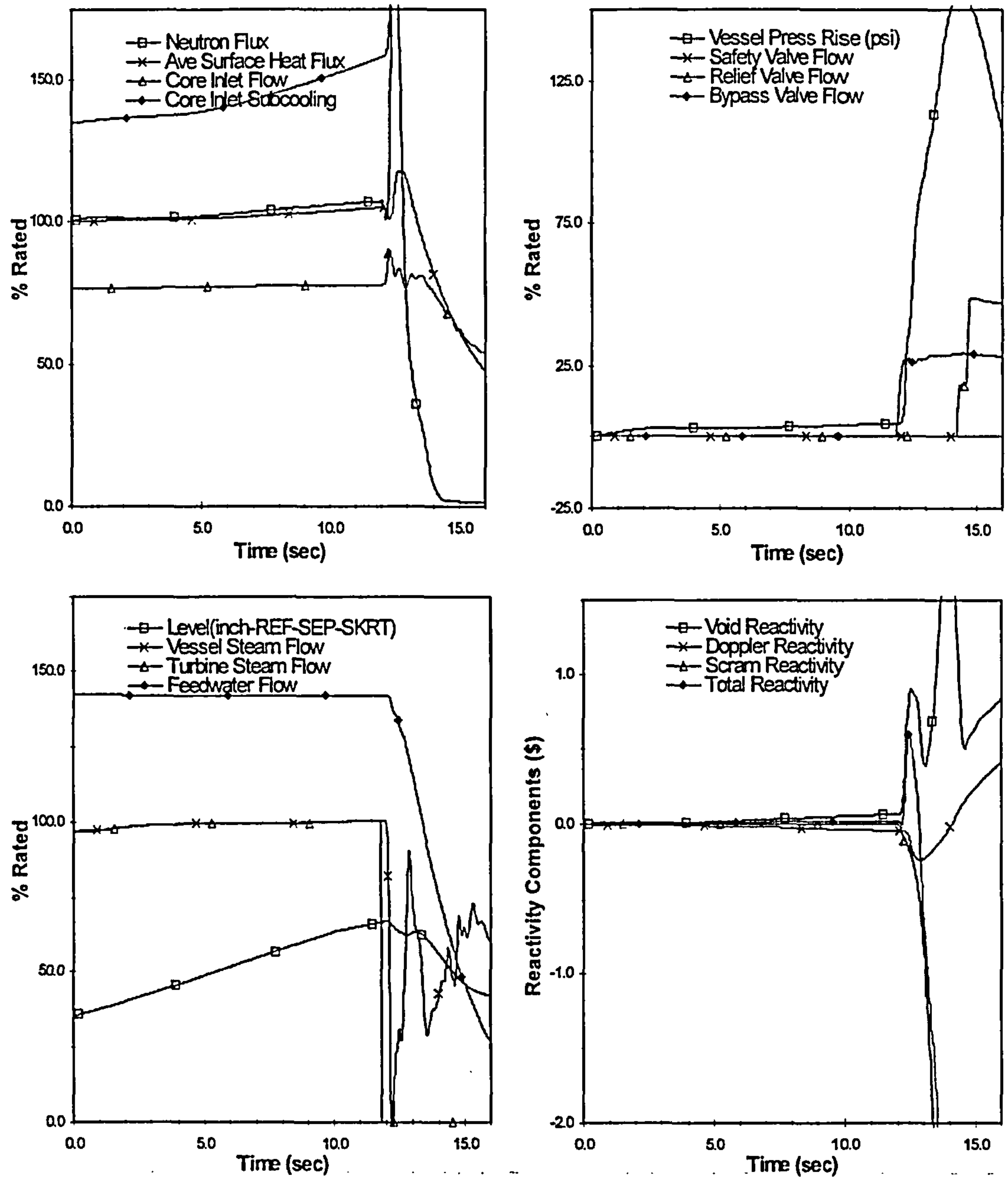

Figure 47 Plant Response to FW Controller Failure
(EOR13-3245 MWd/MT (2944 MWd/ST) to EOC13 MELLLA & MFWT with RPTOOS (HBB))

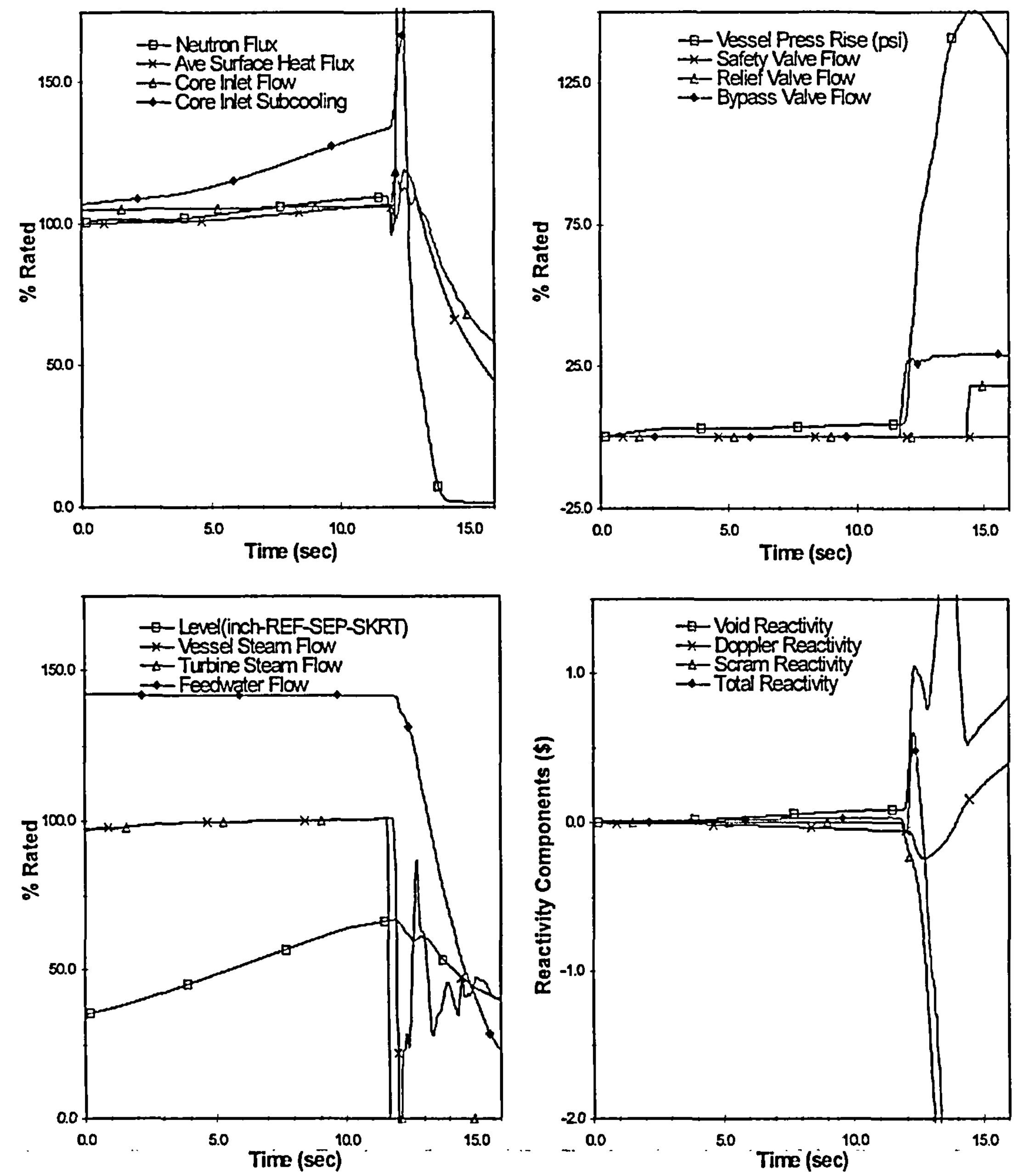

Figure 48 Plant Response to FW Controller Failure
(EOR13-3245 MWd/MT (2944 MWd/ST) to EOC13 ICF & MFWT with RPTOOS (UB))

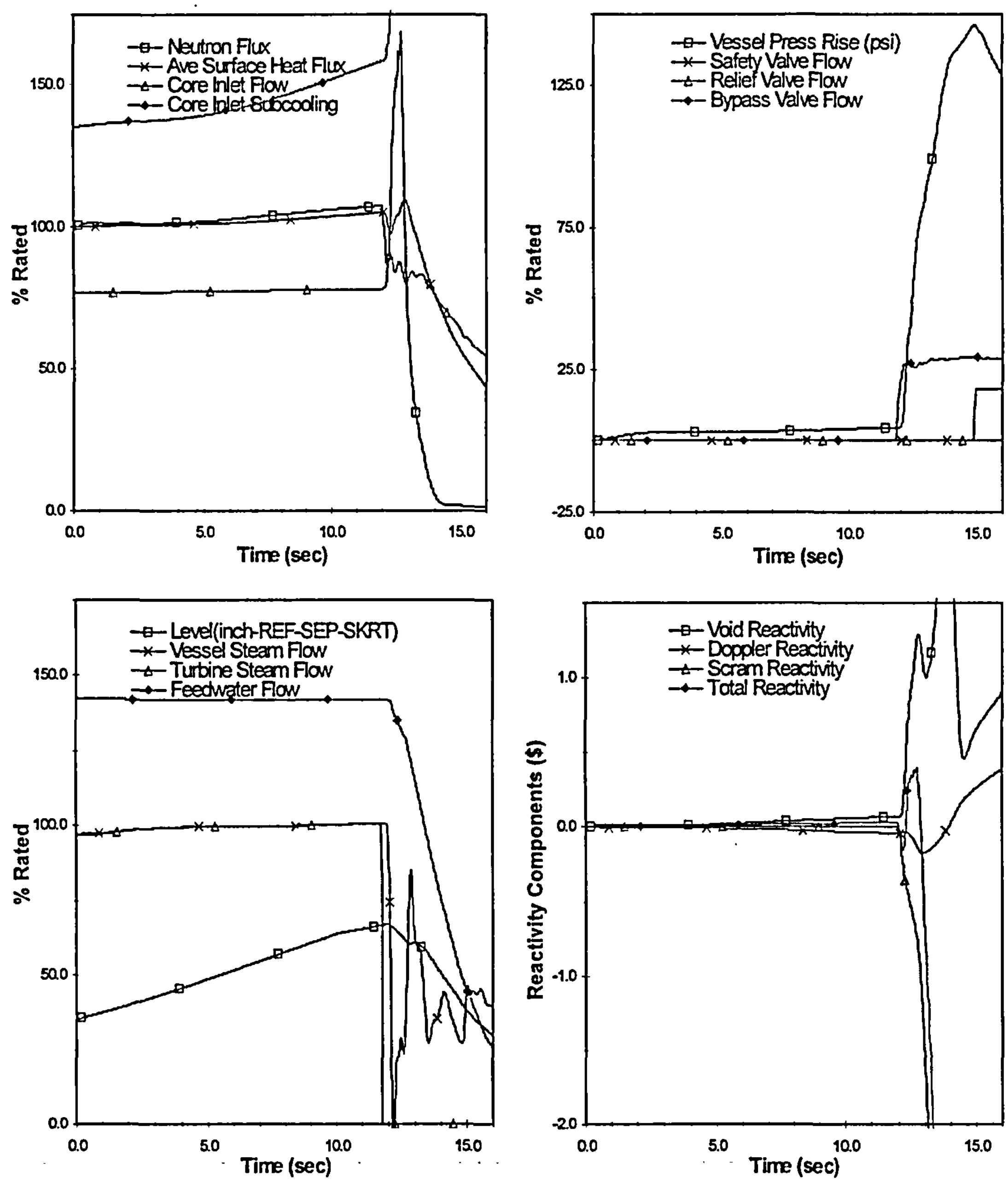

Figure 49 Plant Response to FW Controller Failure (EOR13-3245 MWd/MT (2944 MWd/ST) to EOC13 MELLLA & MFWT with RPTOOS (UB))

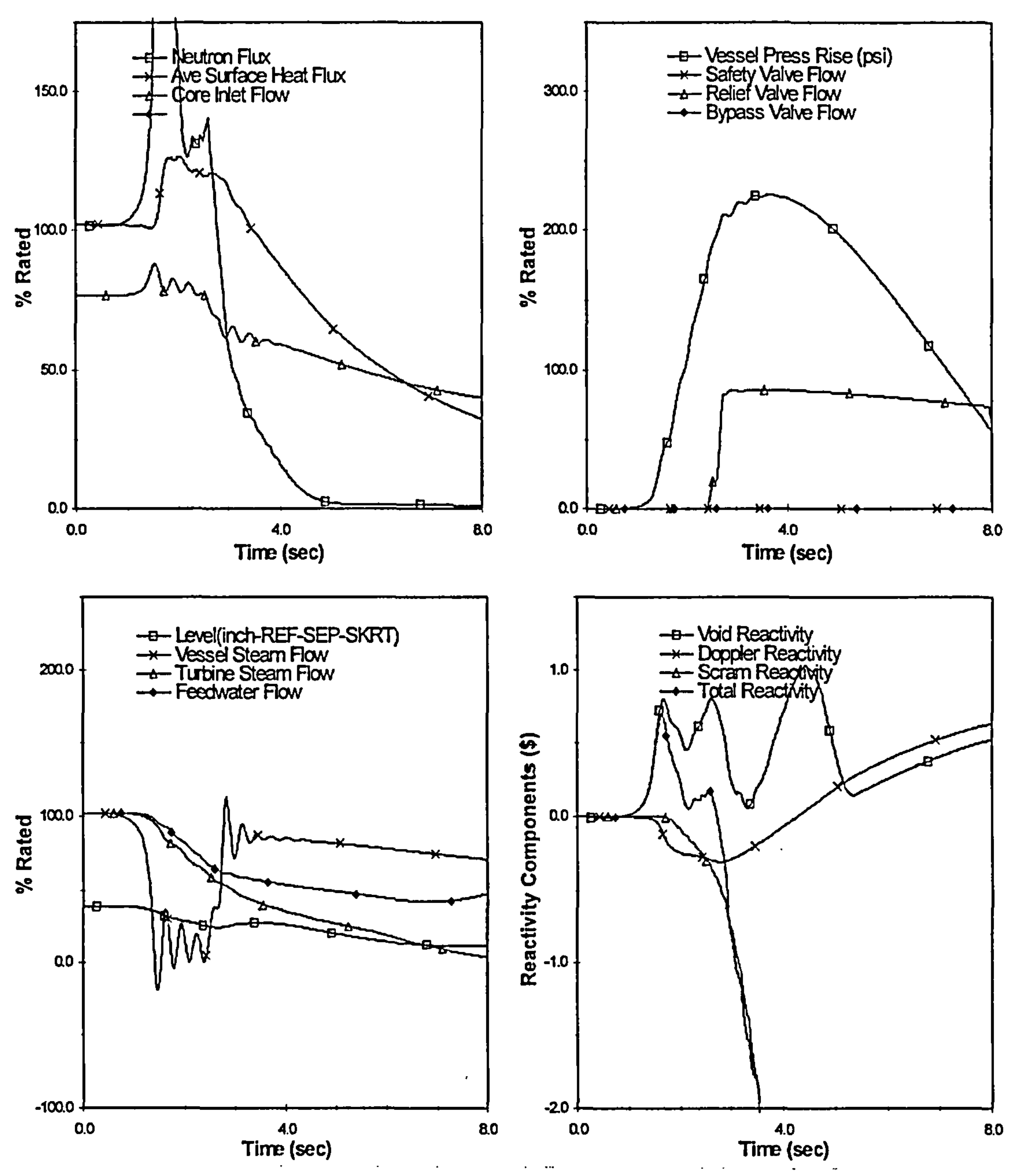

Figure 50 Plant Response to MSIV Closure (Flux Scram)

Appendix A
Analysis Conditions

To reflect actual plant parameters accurately, the values shown in Table A-1 were used this cycle.

Table A-1

	Analysis Value [12]			
Parameter	**ICF**	**ICF & MFWT**	**MELLLA**	**MELLLA & MFWT**
Thermal power, MWt	3339.0	3339.0	3339.0	3339.0
Core flow, Mlb/hr	105.0	105.0	76.6	76.6
Reactor pressure (core mid-plane), psia	1036.0	1031.5	1030.7	1026.4
Inlet enthalpy, BTU/lb	527.2	524.0	519.5	515.3
Non-fuel power fraction	0.036	0.036	0.036	0.036
Steam flow, Mlb/hr	14.43	13.99	14.39	13.96
Dome pressure, psig	1005.0	1000.7	1005.0	1000.7
Turbine pressure, psig	961.8	960.0	962.1	960.2
No. of Safety/Relief Valves[13]	14	14	14	14
Relief mode lowest setpoint, psig	1141.2	1141.2	1141.2	1141.2
Safety mode lowest setpoint, psig	-	-	-	-

[12] These analysis values were also applied for RPTOOS condition for ICF and MELLLA.
[13] One SRV is allowed to be out of service.

Appendix B
List of Acronyms

Acronym	Description
ΔCPR	Delta Critical Power Ratio
Δk	Delta k-effective
%NBR	Percent Nuclear Boiler Rated
2RPT	Two Recirculation Pump Trip
ADS	Automatic Depressurization System
ADSOOS	Automatic Depressurization System Out of Service
AOO	Anticipated Operational Occurrence
APRM	Average Power Range Monitor
ARTS	APRM, Rod Block and Technical Specification Improvement Program
BOC	Beginning of Cycle
BSP	Backup Stability Protection
BWROG	Boiling Water Reactor Owners Group
COLR	Core Operating Limits Report
CPR	Critical Power Ratio
DIVOM	Delta CPR over Initial MCPR vs. Oscillation Magnitude
DR	Decay Ratio
ECCS	Emergency Core Cooling System
EEOC	Extended End of Cycle
ELLLA	Extended Load Line Limit Analysis
EOC	End of Cycle
EOR	End of Rated (All Rods Out 100%Power / 100%Flow / NFWT)
ER	Exclusion Region
FFWTR	Final Feedwater Temperature Reduction
FMCPR	Final MCPR
FOM	Figure of Merit
FWCF	Feedwater Controller Failure
FWTR	Feedwater Temperature Reduction
GDC	General Design Criterion
GESTAR	General Electric Standard Application for Reactor Fuel
GETAB	General Electric Thermal Analysis Basis
GSF	General Shape Function
HAL	Haling Burn
HBB	Hard Bottom Burn
HBOM	Hot Bundle Oscillation Magnitude
HCOM	Hot Channel Oscillation Magnitude
HFCL	High Flow Control Line
HPCI	High Pressure Coolant Injection
ICA	Interim Corrective Action

Acronym	Description
ICF	Increased Core Flow
IMCPR	Initial MCPR
IVM	Initial Validation Matrix
LHGR	Linear Heat Generation Rate
LOCA	Loss of Coolant Accident
LPRM	Local Power Range Monitor
LRHBP	Load Rejection with Half Bypass
LRNBP	Load Rejection without Bypass
LTR	Licensing Topical Report
MAPLHGR	Maximum Average Planar Linear Heat Generation Rate
MCPR	Minimum Critical Power Ratio
MELLLA	Maximum Extended Load Line Limit Analysis
MELLLA+	MELLLA Plus
MFWT	Minimum Feedwater Temperature
MOC	Middle of Cycle
MRB	Maximal Region Boundaries
MSIV	Main Steam Isolation Valve
MSIVOOS	Main Steam Isolation Valve Out of Service
MTU	Metric Ton Uranium
MWd	Megawatt day
MWd/ST	Megawatt days per Standard Ton
MWd/MT	Megawatt days per Metric Ton
MWt	Megawatt Thermal
NBP	No Bypass
NCL	Natural Circulation Line
NFWT	Normal Feedwater Temperature
NOM	Nominal Burn
NTR	Normal Trip Reference
OLMCPR	Operating Limit MCPR
OOS	Out of Service
OPRM	Oscillation Power Range Monitor
Pdome	Peak Dome Pressure
Psl	Peak Steam Line Pressure
Pv	Peak Vessel Pressure
PCT	Peak Clad Temperature
PHE	Peak Hot Excess
PLHGR	Peak Linear Heat Generation Rate
PLUOOS	Power Load Unbalance Out of Service
PRFDS	Pressure Regulator Failure Downscale
PROOS	Pressure Regulator Out of Service
Q/A	Heat Flux
RBM	Rod Block Monitor
RC	Reference Cycle
RFWT	Reduced Feedwater Temperature
RPS	Reactor Protection System

Acronym	Description
RPT	Recirculation Pump Trip
RPTOOS	Recirculation Pump Trip Out of Service
RVM	Reload Validation Matrix
RWE	Rod Withdrawal Error
SC	Standard Cycle
SL	Safety Limit
SLMCPR	Safety Limit Minimum Critical Power Ratio
SLO	Single Loop Operation
SRLR	Supplemental Reload Licensing Report
SRV	Safety/Relief Valve
SRVOOS	Safety/Relief Valve(s) Out of Service
SS	Steady State
STU	Short Tons (or Standard Tons) of Uranium
TBV	Turbine Bypass Valve
TBVOOS	Turbine Bypass Valves Out of Service
TCV	Turbine Control Valve
TCVOOS	Turbine Control Valve Out of Service
TCVSC	Turbine Control Valve Slow Closure
TLO	Two Loop Operation
TRF	Trip Reference Function
TTHBP	Turbine Trip with Half Bypass
TTNBP	Turbine Trip without Bypass
UB	Under Burn

Appendix C

Decrease In Core Coolant Temperature Events

The Loss-of-Feedwater event was analyzed at 100% rated power using the BWR Simulator Code. The use of this code is permitted in GESTAR II. The transient plots, neutron flux and heat flux values normally reported in Section 9 are not an output of the BWR Simulator Code; therefore, those items are not included in this document. The OLMCPR result is shown in Section 11.

In addition, the Inadvertent HPCI start-up event without a Level 8 turbine trip was shown to be bounded by the LFWH event in accordance with *Determination of Limiting Cold Water Event*, NEDC-32538P-A.

The Rev. 0 SRLR (Reference C-1) indicated the Inadvertent HPCI with a Level 8 turbine trip is non-limiting.

References:

C-1. 0000-0031-0596-SRLR, *Supplemental Reload Licensing Report for Hope Creek Unit 1 Reload 12/Cycle 13*, Rev. 0, September 2004.

APPENDIX D

Basis for K_f Curve

A K_f curve for two-loop operation was provided for Cycle 9 in Reference D-1. The curve was updated for Cycle 13 application regarding core flow less than 40%. The updated curve is provided in Figure D-1 based on a maximum core flow runout of 109.0% and remains valid for Cycle 13.

References:

D-1. J11–03372SRLR, *Supplemental Reload Licensing Report for Hope Creek Generating Station Reload 8 Cycle 9*, Revision 0, December 1998.

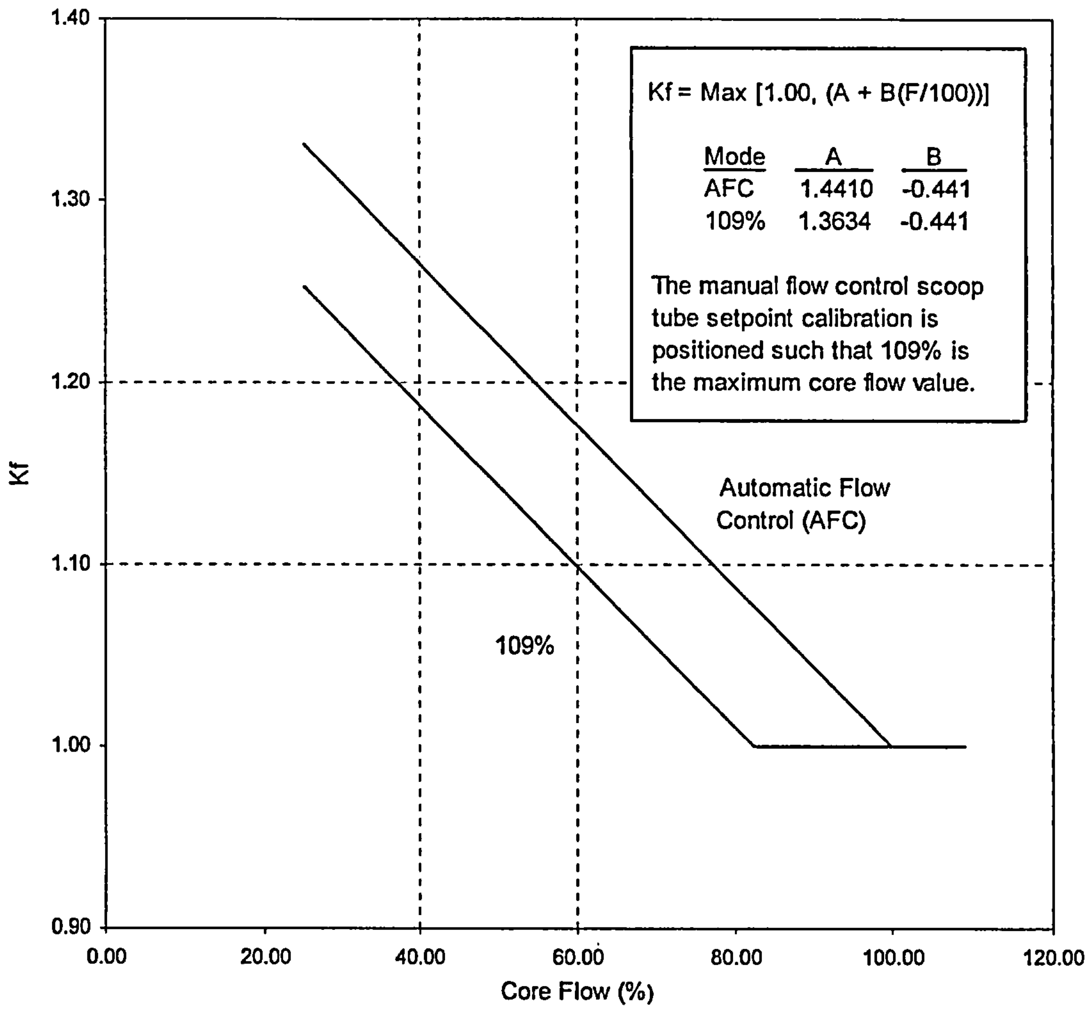

Figure D-1 Flow Dependent MCPR Multiplier for Hope Creek

APPENDIX E
Option B Licensing Basis

The NRC has concluded that a statistical approach (Option B) may be used for pressurization events analyzed with ODYN (References E-1 and E-2). The GEMINI statistical scram speed is provided in Table E-1.

Table E-1 GEMINI Methods: CRD Control Fraction vs. Time in BWR/2-5

	0%	5%	20%	50%	90%	100%
$\bar{X}$ (sec)	0.200	.324	.694	1.459	2.535	2.804
σ (sec)	- -	.014	.016	.031	.070	- -

The NRC Staff requires that, "in order to take credit for conservatism in the scram speed performance, it must be demonstrated that there is insufficient reason to reject the plant-specific scram speed as being within the distribution assumed in the statistical analysis".

General Electric presents the following procedure as one that satisfies the Staff's objectives for scram conformance. It should be noted that some utilities using ODYN Option B might desire to establish their own conformance procedures.

The procedure consists of testing, at the 5 percent significance level, the scram surveillance data at the 20 percent insertion position which is generated several times each cycle as required in the Reactivity Control System Technical Specification (20 percent insertion is representative of that portion of the scram most affecting the pressurization transient). The unique rod notch position closest to 20 percent (and the appropriately adjusted time of insertion) is expected to be utilized in actual plant application of this generic concept. For most plants, the surveillance requirements are as follows:

(1) all control rods are measured at beginning of cycle (BOC), and

(2) X% of control rods are measured every 120 days during cycle (X is plant-dependent and ranges from 10 to 50).

At the completion of each surveillance test performed in compliance with the technical specifications surveillance requirements, the average value of all surveillance data at the 20 percent insertion position generated in the cycle to date is to be tested at the 5 percent significance level against the distribution assumed in the ODYN analyses. The surveillance information which each plant, using this procedure, will have to retain throughout the fuel cycle is the number of active control rods measured for each surveillance test (the first test is at the BOC and is denoted N_1; the i^{th} test denoted N_i and the average scram time to the 20 percent insertion position for the active rods measured in test i denoted τ_i.

The equation used to calculate the overall average of all the scram data generated to date in the cycle is:

$$\tau_{ave} = \frac{\sum_{i=1}^{n} N_i \tau_i}{\sum_{i=1}^{n} N_i} \qquad (1)$$

where:

$n=$ number of surveillance tests performed to date in the cycle;

$\sum_{i=1}^{n} N_i =$ total number of active rods measured to date in the cycle; and

$\sum_{i=1}^{n} N_i \tau_i =$ sum of the scram time to the 20 percent insertion position of all active rods measured to date in the cycle to comply with the Technical Specification surveillance requirements.

The average scram time, τ_{ave}, is tested against the analysis mean using the following equation:

$$\tau_{ave} \le \tau_B \qquad (2)$$

where:

$$\tau_B = \mu + 1.65 \sqrt{\left(\frac{N_1}{\sum_{i=1}^{n} N_i} \right)} \sigma \qquad (3)$$

The parameters μ and σ are the mean and standard deviation of the distribution for average scram insertion time to the 20 percent position used in the ODYN Option B analysis.

If the cycle average scram time satisfies the Equation 2 criterion, continued plant operation under the ODYN Option B operating limit minimum critical power ratio (OLMCPR) for pressurization events is permitted. If not, the OLMCPR for pressurization events must be re-established, based on a linear interpolation between the Option B and Option A OLMCPRs.

The equation to establish the new operating limit for pressurization events is given below:

$$OLMCPR_{New} = OLMCPR_{Option\,B} + \frac{\tau_{ave} - \tau_B}{\tau_A - \tau_B} \Delta OLMCPR \qquad (4)$$

where: τ_{ave} and τ_B are defined in Equations 1 and 3, respectively;

τ_A = the technical specification limit on core average scram time to the 20 percent insertion position.

ΔOLMCPR = the difference between the OLMCPR calculated using Option A and that using Option B for pressurization events.

The control fractions presented in Table E-1 are based on a ratio of distance inserted to control rod stroke. Alternatively, scram times are expressed as a function of notch position. Table E-2 provides notch positions that correspond to approximately 20% control fraction. These notch positions and times can be used in equations 1 through 4.

Table E-2 GEMINI Methods: CRD Notch Positions for τ_B Determination

Notch Position	μ (pickup)	μ (dropout)	σ (pickup)	σ (dropout)
39	0.655	0.672	0.016	0.016
38	0.706	0.724	0.016	0.017
37	0.759	0.777	0.017	0.018
36	0.813	0.830	0.018	0.019

References:

E-1. NEDO-24154 and NEDE-24154-P, *Safety Evaluation for the General Electric Topical Report – Qualification of the One-Dimensional Core Transient Model for Boiling Water Reactors*, Volumes I, II, and III, USNRC, June 1980.

E-2. Letter, J. S. Charnley (GE) to H. N. Berkow (NRC), *Revised Supplementary Information Regarding Amendment 11 to GE Licensing Topical Report NEDE-24011-P-A*, January 16, 1986.

Appendix F
Reactor Recirculation Pump Seizure Event

The reactor recirculation pump seizure event is analyzed for Single Loop Operation (SLO) at HCGS (Reference F-1). This analysis was performed for the HCGS Cycle 13 transition cycle with GE14 and SVEA-96+ fuel in the core and transient analysis inputs that are consistent with the Reload 12/Cycle 13 analyses.

The SLO OLMCPR of 1.51 is required so that the reference SLO SLMCPR of 1.12 is protected in the event of a seizure of the recirculation pump in the active loop. If the cycle-specific Safety Limit Minimum Critical Power Ratio (SLMCPR) changes then the SLO OLMCPR may be adjusted by the following factor:

(Cycle Specific SLMCPR / 1.12)

Thus, for HCGS Cycle 13 with a SLO SLMCPR of 1.08 the SLO OLMCPR required is:

1.51 * (1.08/1.12) = 1.46

In order to protect the required SLO OLMCPR of 1.46 (based on a SLO SLMCPR of 1.08) the following TLO limits must be maintained:

Pre ARTS implementation:

- As long as the TLO full power OLMCPR is 1.33 or greater, the current Hope Creek K_f curves bound operation in SLO. If the full power OLMCPR is lower than 1.33 and is not bounded by the cycle specific off-rated limits, then the condition specific SLO OLMCPR of 1.46 should be applied for GE14 fuel and SVEA-96+ fuel.

Post ARTS implementation:

- As long as the TLO full power OLMCPR is 1.31 or greater, the proposed Hope Creek K(p) curve bounds operation in SLO. If the full power OLMCPR is lower than 1.31 and is not bounded by the cycle specific off-rated limits, then the condition specific SLO OLMCPR of 1.46 should be applied for GE14 fuel and SVEA-96+ fuel.

References:

F-1. NEDC-33158P, *Fuel Transition Report for Hope Creek Generating Station*, Revision 2, November 2004.